NATIONAL ADVISORY COMMITTEE FOR AERONAUTICS

TECHNICAL NOTE

No. 1264

STRESSES IN AND GENERAL INSTABILITY OF MONOCOQUE CYLINDERS WITH CUTOUTS

IV - PURE BENDING TESTS OF CYLINDERS WITH SIDE CUTOUT

By N. J. Hoff, Bruno A. Boley, and
Louis R. Viggiano

Polytechnic Institute of Brooklyn

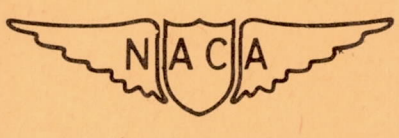

Washington
February 1948

NATIONAL ADVISORY COMMITTEE FOR AERONAUTICS

TECHNICAL NOTE NO. 1264

STRESSES IN AND GENERAL INSTABILITY OF MONOCOQUE CYLINDERS WITH CUTOUTS

IV – PURE BENDING TESTS OF CYLINDERS WITH SIDE CUTOUT

By N. J. Hoff, Bruno A. Boley, and
Louis R. Viggiano

SUMMARY

Nine 24–ST Alclad cylinders of 20–inch diameter, 39–inch to 90–inch length, and 0.012–inch wall thickness, reinforced with 24–ST aluminum–alloy stringers and rings, were tested in pure bending. On one side of the cylinder, situated symmetrically with respect to its horizontal plane of symmetry, there was a cutout extending over 12.9 inches or 19.3 inches in the longitudinal direction and over an angle of 45°, 90°, or 135° in the circumferential direction. The strain in the stringers and in the sheet covering was measured with metalectric strain gages.

The stress distribution on the complete side of the cylinders deviated little from the linear law valid for cylinders without a cutout. On the cutout side, however, the stresses were considerably reduced in the stringers over the middle portion of which the cutout extended. In the edge stringers, that is, stringers bordering the cutouts, the stress increased in the middle of the cylinder. The maximum value of the stress was about 10 percent higher than the value calculated from the conventional bending formula Mc/I when I was taken as the moment of inertia of the cross section of the portion of the cylinder where the cutout was situated. The only exception was the maximum stress in one cylinder with a large cutout, which stress amounted to 195 percent of that given by the formula Mc/I when the load was 80 percent of the buckling load. In the calculation of the moment of inertia, the effective width of sheet was used.

All the nine cylinders tested failed in general instability. The crest of the main bulge was located at the edge stringer on the compression side and secondary bulges appeared usually near the lowermost stringer in the cylinder. The buckling loads of the cylinders having cutouts extending over 45°, 90°, and 135° were 80.5, 59.7, and 58.7 (68.6, 65.5, and 60.8) percent, respectively, of the buckling load of the cylinder without a cutout. The values in parentheses refer to cylinders having 8 stringers, the other values to cylinders having 16 stringers.

The cylinders carried large loads even after buckling. In general the size of the bulge and the number of the bulges increased when the loading was continued after the first buckling.

INTRODUCTION

The problems of the distribution of the stresses in and the general instability of reinforced monocoque cylinders having cutouts were discussed in three earlier reports (references 1 to 3). These investigations dealt with cylinders in which the cutout was situated on the compression side. In the present report, results of experiments are presented that were obtained with cylinders in which there was on one side of the cylinder a cutout symmetric to the neutral axis of the cylinder.

Two major effects of cutouts in monocoques are to be noted. One is the redistribution of stress near the opening. The present report gives results of strain measurements which were obtained at the Polytechnic Institute of Brooklyn Aeronautical Laboratories with nine circular cylinders tested in pure bending. A later report will contain theoretical calculations and a comparison of the theory with experiment. It may be mentioned here, however, that good agreement has been obtained between the theoretical and the experimental axial stresses. The second item investigated is the effect of the cutout on the failure of the cylinder. This effect is included in the one first mentioned if failure occurs in the form of material failure, local buckling of a thin-walled element, or buckling of a stringer between two adjacent frames.

An entirely new problem arises, however, when failure is caused by general instability. General instability is defined as the simultaneous buckling of the longitudinal and circumferential reinforcing elements of a monocoque cylinder together with the sheet attached to them. This type of buckling of reinforced circular monocoque cylinders, each having a symmetric cutout and subjected to pure bending, was recently investigated at Polytechnic Institute of Brooklyn Aeronautical Laboratories and is described in references 1 and 3. An experimental report of the general instability of reinforced monocoque cylinders having no cutout is available in reference 4. It is rather obvious that a cutout in a monocoque cylinder makes general instability possible under a load smaller than the buckling load of a complete cylinder.

The second purpose of the investigations described in the present report was to collect data regarding the buckled shape and the buckling load of cylinders having side cutouts of different sizes. In a later report an attempt will be made to develop a strain-energy theory of the general instability of reinforced monocoque cylinders with side cutout.

The investigations described were conducted under the sponsorship and with the financial aid of the National Advisory Committee for Aeronautics. Mr. Harold Liebowitz' contribution to the construction, testing, and evaluation of the test results is acknowledged.

SYMBOLS

c	distance from neutral axis
d	stringer spacing measured along circumference
E	Young's modulus
I	moment of inertia of cylinder cross section with respect to neutral axis
I_c	moment of inertia with respect to neutral axis of cross section of portion of cylinder where cutout is situated
M	applied bending moment
M_{cr}	critical bending moment (at general instability)
y_c	distance from neutral axis of cylinder cross section with cutout
$2w$	effective width of flat panel
$2w'$	effective width of curved panel
γ	shear strain
ϵ_c	normal strain in sheet in circumferential direction
ϵ_{calc}	calculated normal strain in axial direction
ϵ_{curved}	buckling strain of nonreinforced circular cylinder under uniform axial compression
ϵ_{exp}	experimental normal strain in axial direction
ϵ_{flat}	buckling strain of flat panel under uniform compression
ϵ_{str}	axial strain in stringer
ϵ_x	normal strain in sheet covering in axial direction

TEST SPECIMENS, RIG, AND PROCEDURE

The test cylinders are shown in the schematic drawings of figures 1(a) and 1(b). They were numbered consecutively from 35 to 43. They consist of a 24-ST Alclad sheet covering of 0.012-inch thickness, eight or sixteen 24-ST aluminum-alloy stringers of $\frac{3}{8}$-inch square section, and a number of 24-ST aluminum-alloy rings of $\frac{1}{8}$- by $\frac{3}{8}$-inch rectangular section. The diameter of the cylinders is 20 inches and their length varies from 39 to 90 inches. Except for the length of the cylinder and the location of the cutout, the cylinders were constructed in exactly the same manner as those described in reference 1. In the test series of the present report, each cylinder had a cutout on one side extending over two or three ring fields and one to six stringer fields.

The test rig and the attachment of the cylinders to the rig were very much the same as those used in the tests described in reference 1. Figure 2 is a photograph of the test setup and figure 3 a close-up of the swiveling parallel-linkage mechanism inserted between the loading head and the loading arm. The upper joint of this mechanism is attached to the loading head by means of ball thrust bearings, while at the lower joint a ball bearing constitutes a roller which can transmit to the loading head compressive forces only. The rest of the mechanism is a simple parallel linkage. The swiveling arrangement was provided in order to permit twisting of the monocoque cylinder at buckling. In the experiments, however, no such twisting could be observed.

As in the earlier tests, the load was applied by means of a mechanical jack and its magnitude was measured by Baldwin-Southwark SR-4 metalectric strain gages type A-1 cemented to a calibrated load link. The strain in the test cylinders was measured in every stringer in two end bands $5\frac{1}{2}$ inches from the edge of the end rings, except in Cylinder 41 in which the end band was $3\frac{1}{4}$ inches from the end rings. The strain was also measured in the middle band in the plane of symmetry of the cylinder and with some cylinders in as many as three additional bands between the ends and the middle of the cylinder. The measurements were made with pairs of SR-4 type A-1 strain gages cemented to opposite sides of the stringer and connected in series, in order to obtain the average normal strain in the stringer. In Cylinder 40 the axial strain was measured also in the sheet covering on the tension side around the cutout in the middle of eight panels by pairs of SR-4 type R-4 equilateral strain rosettes cemented to each side of the sheet covering. In addition, the rosette readings were used to determine the shear strain in these panels.

In reference 1 it was mentioned that a systematic decrease in the normal strain was observed from the loading head in the direction of the end stand. Since the observation was made in the evaluation stage of the work after completion of all the experiments, the reason for this

increase could not be investigated at that time. At the beginning of the present test series, an investigation disclosed that the load in the cable that had one end attached to the loading head and the other to the counterweight varied during the loading. The variations were attributed to friction in the sheaves, particularly when the direction of the cable became inclined because of the deformations of the test specimen. For this reason, for Cylinders 36 to 43 all the experiments were carried out with a calibrated load link inserted in the cable between the loading head and the first sheave, and the force in the cable was measured at the beginning of each stage of loading. If this force deviated from the known weight of the loading head, weights were added or taken off until the required load reading was obtained. In this manner the systematic error discussed in reference 1 was eliminated. The accuracy of the measurements was the same as in the experiments described in reference 1. The maximum error of the strain measurements was found to be $\pm 10 \times 10^{-6}$ inch per inch. The applied load was measured with an error of less than ± 50 pounds.

ANALYSIS AND DISCUSSION

Presentation of Test Results

Results of the strain measurements in the stringers are presented for one or both end bands, for the middle band, and in some cases for intermediate bands of the cylinders. The presentation is in the form of diagrams in which the strain is plotted against the distance of the stringer from the horizontal diameter of the cylinder. These basic data are contained in figures 4 to 30. The shear strain measured in the panels of Cylinder 40 is indicated in figure 31.

The effect of the size of the cutout upon the strain is shown in figures 32 to 42. Figures 32 to 35 contain comparisons of the strain diagrams corresponding to cutouts of small, medium, and large size in the circumferential direction. Figures 36 to 39 present the variation of the axial strain along the edge stringer and the stringer next to the edge at different values of the applied bending moment. Figures 40 to 42 are strain trajectories.

The variation of the strain with applied bending moment is plotted in figures 43 to 46 for a few stringers of three representative cylinders.

The final results of the experimental investigation are presented in figures 47 to 49. Figures 47 and 48 show the strain factors for various percentages of the buckling load. The strain factor is defined as the maximum strain measured in the cylinder at a given load divided by the maximum strain corresponding to the same load as calculated from the formula Mc/I_c in which I_c is the effective moment of inertia of the

cross section (calculated with consideration of the effective width of sheet) of the cylinder at the location of the cutout. The value of the bending moment at buckling is shown in figure 49 as a function of the size of the cutout and the number of stringers contained in the cylinder.

Some of the experimental data are contained in the two tables. In table I the applied bending moments are compared with those calculated from the strain values measured in the various bands. In table II data related to the buckling of the cylinder are given. The buckled shape of the cylinder can be seen from the photographs presented as figures 50 and 51.

Nonlinearity of Normal Strain Distribution

It is customary in airplane stress analysis, and entirely justified, to assume that the normal stress is distributed according to a linear law and that the neutral axis is the horizontal diameter of the cylinder, when a pure bending moment is applied in a vertical plane to a reinforced monocoque cylinder. The linearity of the stress distribution is a consequence of the assumption that plane sections perpendicular to the axis of the unloaded cylinder remain plane and perpendicular to the axis when the cylinder is distorted by the applied moment. The stress distribution remains linear even when the sheet covering buckles on the compression side of the cylinder but the neutral axis shifts toward the tension side. The normal stress can still be calculated by the simple formula Mc/I provided that in all those panels where the sheet is in a buckled state the effective width of the sheet rather than the total width is considered when the centroid and the moment of inertia of the section are determined. These conclusions were borne out by the experiments described in reference 4.

The situation is entirely different, however, when there is a cutout in the monocoque cylinder. Stringers from which portions have been cut out offer little resistance to axial displacement, so that the stress distribution in the cylinder is not linear when the end sections of the cylinder remain plane during the distortions. Conversely, if the stress is applied to the end sections of the cylinder corresponding to the linear pattern assumed in bending theory, then during the ensuing distortions of the cylinder the end sections do not remain plane.

In the experiments presented herein as well as in those of references 1 and 4 the end sections of the cylinder were forced to remain plane during the tests. In the tests of reference 4 some shimming was necessary in order to achieve linearity of the displacements, and this linearity could be checked with the aid of the strain-gage readings. In the present tests, as well as in those of reference 1, no direct check of the linearity of the displacements was possible, since a plane

end section did not correspond to a linear strain distribution. Nevertheless the rigidity of the end rings and loading head is believed to have been sufficient to keep the end sections plane, because these elements were materially heavier than those used in the tests described in reference 4 whereas the maximum applied moments were smaller.

An indirect proof of the plane distortion pattern at the end rings was obtained analytically. The stresses in the stringers were calculated on the basis of the assumption that the end rings remain plane, and the strain distribution obtained was in good agreement with that measured. Details of these calculations and comparisons are given in Part V of the present investigation (reference 5).

If there is a cutout in a reinforced monocoque cylinder, at some distance from the cutout in the axial direction both the displacements and the stresses will be distributed linearly within the accuracy required in engineering calculations. It appears, however, that this distance is considerable. Deviations from the linear law for the stress distribution were observed on the cutout side of each cylinder in the end bands, except in Cylinder 43, which was 90 inches long and had a cutout extending over 90° in the circumferential direction and 12.86 inches in the axial direction. Figures 29, 28, and 30 corresponding to the middle band, the intermediate band, and the end band, respectively, of Cylinder 43 show how the deviations from linearity decrease with distance from the cutout. Bands G and H are in the middle of the cylinder, band D at a distance equal to 80 percent of the diameter from the edge of the cutout, and band N at a distance equal to 166 percent of the diameter from the edge of the cutout.

In the present tests linearity of the displacements was enforced at the end sections since this condition is considered to be in better agreement with reality than linearity of the stress distribution. Moreover, this end condition is more convenient for experimental work.

As in references 1 and 4, the fundamental strain data obtained in the tests are presented in a number of diagrams. In figures 4 to 30 the ordinate is the distance of any individual stringer from the horizontal diameter of the cylinder, and the abscissa is the strain measured in the stringer. An individual curve is drawn for each stage of loading, and three individual diagrams, related to either the middle band and the two end bands, or to the middle band, one end band, and one intermediate band, are presented for each test cylinder. The following observations may be made in connection with these diagrams:

1. The stress distribution is sensibly linear on the side opposite to the cutout.

2. In the intermediate and end bands on the cutout side of the cylinder the stresses are considerably reduced in the stringers having the middle portions cut out.

3. The deviations from linearity in the intermediate and end bands on the cutout side of the cylinder are slight in the case of the 45° cutout, greater in the case of the 90° cutout, and very large in the case of the 135° cutout. The effect of the circumferential size of the cutout upon the linearity of the stress distribution in the end band can be best seen in figures 32 and 33 in which strain diagrams are presented for the cutouts of different sizes corresponding to the same applied bending moment.

4. In the middle of the cylinder on the cutout side there are in general slight or no deviations from linearity in the case of the 45° cutout. The deviations become more and more noticeable when the size of the cutout is increased to 90° and 135°. In most cases there is an increase in the stress in the edge stringer. In some cases there is also a marked increase in the stress in the stringer adjacent to the edge stringer. A comparison of the strain diagrams of the middle bands of cylinders having different-size cutouts is presented in figures 34 and 35.

5. The slight effect of a small-size cutout upon the stress distribution is in contrast with the comparatively large effect observed in the tests described in reference 1. This difference is easily understandable, however, if it is remembered that in the earlier tests the small-size cutout caused a discontinuity in the originally most highly stressed stringer, whereas in the present case the small cutout disturbs at most the stringer that is located at the original neutral axis of the cylinder and carries no load.

6. In the case of Cylinder 43 one stringer located at the neutral axis was removed over a length corresponding to two ring fields. The effect of this very slight disturbance became negligible only at a distance of 166 percent of the diameter from the edge of the cutout. The strain diagrams presented in figures 4 to 30 indicate that the effect of cutouts involving a greater number of stringers extends over far greater distances.

7. The agreement was found to be good between strain values measured in strain gages located symmetrically with respect to the vertical plane of symmetry of the cylinder.

Strain in Sheet Covering

The strains calculated from the rosette readings are recorded in figure 31 for four applied bending moments. The axial strains were used when plotting the strain trajectories of figure 42. They were found to be in good agreement with the strains measured in the stringers.

The circumferential strain was compressive in the panels where the axial strain was tensile. Its magnitude was between approximately one-third and one-fourth of that of the axial strain.

In the absence of an applied shear force the shear-strain distribution should be antisymmetric with respect to the vertical plane of symmetry of the cylinder. Consequently, shear strains located symmetrically to the middle of band E in figure 31 should be equal in magnitude and opposed in sign. In reality, the axis of antisymmetry appears to be shifted slightly to the left in this figure. The magnitude of the shear strain is between approximately one-seventh and one-ninth of the axial strain.

Equilibrium of Forces and Moments

The resultant force and the resultant moment were calculated from the strain measurements in each band. They are listed in table I together with the values of the applied moment. In the calculation it was assumed that on the tension side the entire sheet was fully carrying, whereas on the compression side the effective width of sheet was determined with the aid of the formulas

$$\left.\begin{aligned} 2w' &= 2w + \left(\epsilon_{curved}/\epsilon_{str}\right)(d - 2w) \\ 2w &= \left[\epsilon_{flat}/\left(\epsilon_{str} - \epsilon_{curved}\right)\right]^{1/3} d \end{aligned}\right\} \qquad (1)$$

The critical values of the strain were taken as

$$\left.\begin{aligned} \epsilon_{flat} &= 0.5 \times 10^{-4} \qquad \text{(16 stringers)} \\ \epsilon_{flat} &= 0.174 \times 10^{-4} \qquad \text{(8 stringers)} \\ \epsilon_{curved} &= 3 \times 10^{-4} \end{aligned}\right\} \qquad (2)$$

The agreement between the moments applied and those calculated was found to be reasonably good. The axial force resultant was also small as compared with the total tensile force on the tension side and the total compressive force on the compression side of the cylinder, the difference of which is the force resultant. In general the bending moment calculated from the strain readings in the end band was found to be greater than that in the middle band. The reason for this phenomenon is the fact that in the end bands the sheet carried little stress because it was not attached to the end rings. On the other hand, in the middle of the cylinder the sheet is fully carrying on the tension side since the stress distribution there corresponds closely to that obtainable in an infinitely long cylinder. Because in the calculation of the effective width no distinction was made between middle band and end bands, the same rules being used for all bands, exaggerated values were obtained for the bending-moment resultant at the end of the cylinder.

Strain Variation along Stringers

The variation of the strain in the edge stringers of Cylinders 41, 42, and 43 and the variation of the strain along the stringer next to the edge stringer in Cylinder 42 are presented in figures 36 to 39. At each stage of loading the stress in the middle of the stringer is higher than in any other place along the stringer. Since in these cylinders only the stringer at the neutral axis is discontinuous because of the cutout, the increase in the strain in the middle of the stringer is probably due to the fact that the edge stringer has to carry the load that would be carried in a complete cylinder by the sheet if it had not been removed. In some of the figures there is a slight increase in stringer strain at the ends of the cylinder. This may be attributed to the fact that the stringer has to carry the load that the sheet cannot carry because it is not attached to the end rings.

Strain Trajectories

Figures 40, 41, and 42 present the strain trajectories of Cylinders 35, 38, and 40, respectively. The cylinder is imagined to be cut along a stringer and developed into the plane of the drawing. The location of the stringers and the rings is shown. Points on the developed surface subjected to the same strain are connected with lines denoted as trajectories. Since each trajectory represents a constant value of strain, the trajectories had to be constructed by means of interpolation between the measured values of the strain.

The trajectories may be visualized as the contour lines of a topographic map of the strain surface. The characteristic feature of all the contour diagrams corresponding to the present series of tests as distinct from those of the diagrams corresponding to the symmetric cut-out series described in reference 1 is the prevalence of almost horizontal straight lines. This shows that the presence of a cutout near the neutral axis disturbs the strain distribution in the complete cylinder much less than does a cutout on the compression side.

Systematic deviations from the straight lines can be observed only near the cutout. They indicate an increase in the strain in the edge stringer in the middle of the cutout and a decrease in the strain near the cutout in the stringers that are interrupted by the cutout. In most figures this latter deviation could not be determined accurately because of the small number of strain readings. The curves are indicated, therefore, by dashed lines.

Variation of Strain with Applied Moment

In figures 43 to 46 the strain is plotted against the applied moment for a number of stringers. The curves are for Cylinders 35, 36, and 38. Similar curves were drawn for all the other cylinders of the

test series also, since they were needed in determining by extrapolation the strain at the moment of buckling. Figures 43 to 46 represent, therefore, typical examples of different series of curves.

All the curves begin as straight lines in good approximation. Near the buckling load some of them increase more rapidly, but the rate of increase of others becomes smaller or even negative. For instance, for the end band of Cylinder 35 (fig. 43) the slope of the strain curve of one of the edge stringers increases, but that of the other remains unchanged. A similar situation exists in the stringers adjacent to the edge stringer in which the absolute value of the strain is higher than that in the edge stringer. In the end bands of the edge stringers of Cylinder 36 (fig. 44) the strain becomes practically constant when the buckling load is approached. This condition is probably due to the fact that the edge stringers were bent considerably in the last stages of loading before buckling occurred. In the stringers next to the edge of this same cylinder the rate of increase of the strain becomes slightly greater in the last stages of loading, so that the maximum value of the strain in the stringer next to the edge is considerably higher than that in the edge stringer when buckling occurs. In the end bands of Cylinder 38 (fig. 45) the strain in the edge stringer increases slightly, that in the stringer next to the edge somewhat more rapidly, and that in the second stringer from the edge more and more slowly as the buckling load is approached. Thus at buckling the maximum strain is reached in the stringer next to the edge, but during the earlier stages of loading the second stringer from the edge carries the highest loads. The situation is shown to be quite similar in figure 46, which represents the strain in the middle band of Cylinder 38.

Strain Factors

The most important results of the strain measurements are presented in figures 47 and 48 in the form of strain factors. A strain factor is the ratio of the maximum value of the normal strain measured in the cylinder to the maximum theoretical strain calculated at the same load from the formula Mc/I_c. The value of I_c is calculated for the middle section of the cylinder where the cutout is located. The strain factors are given for each 10 percent of the moment measured at buckling in figure 47 and for each 20 percent in figure 48. Figure 47 presents the strain factors for the cylinders having 8 stringers, figure 48 for those having 16 stringers. The ordinate is the strain factor and the abscissa the circumferential length of the cutout in degrees.

The value of the strain factor does not differ materially from unity except for Cylinder 36, which had 16 stringers and a cutout extending over 135°. It appears, therefore, that the maximum strain, and consequently the maximum stress, can be calculated with reasonable accuracy from the formula Mc/I_c when cylinders of a construction similar to that of the test specimens are subjected to pure bending. The maximum stresses may be considerably higher, however, when the cutout is very large (near 135°).

General Instability

All nine cylinders tested failed in general instability. In all the tests the edge stringer on the compression side showed large deflections before buckling occurred. At the moment of buckling the edge stringer and one or two adjacent stringers, as well as the sheet covering between them, were suddenly displaced and this displacement was always accompanied by a sudden, though often not very large, decrease in the applied load. In a number of tests the loading was continued after buckling. In these cases it was always possible to increase the value of the load prevailing after the drop, but the load prevailing just before buckling was never again reached. After a steady increase in the load, a second sudden drop occurred at the moment when one or more additional stringers buckled. In such a manner three consecutive buckling loads were obtained with some cylinders. Of the three loads the first one was always the highest. The buckled shapes of the cylinders at the different stages of loading are shown in figures 50 and 51.

It was noticed that the tension side of the cylinder did not distort at all and the loading head was not rotated. Consequently, the use of the swiveling parallel linkage in place of the ordinary parallel linkage proved to be an unnecessary measure of precaution. In some cases the edge stringer buckled in the inward direction, in others in the outward direction. It was not possible to establish any systematic preference for the direction of buckling.

The buckling load decreased with increasing size of the cutout. The buckling loads are plotted in figure 49 against the size of the cutout. Cylinders 38, 35, and 36, having 45°, 90°, and 135° cutout, respectively, and 16 stringers show a comparatively rapid increase in the buckling load as the circumferential size of the cutout decreases. For comparison, the buckling load of Cylinder 11 is also plotted. This cylinder was tested in the series of complete cylinders described in reference 4. The dashed portion of the curve shows a sudden increment in the buckling load at 0°. The jump corresponds to the difference between the buckling load of a cylinder which is slotted along a generator (corresponding to a 0° cutout) and that of a complete cylinder.

Cylinders 39, 37, and 40 had eight stringers and cutouts of 45°, 90°, and 135°, respectively. The calculated buckling load of a complete cylinder having eight stringers is also shown in figure 49 for comparison. It was calculated by the method presented in reference 6.

The buckling loads of Cylinders 41, 42, and 43 constitute the third group of points in figure 49. These three cylinders had eight stringers each and a cutout extending over 90° in the circumferential direction. The length of the cutout in the axial direction was 12.9 inches, corresponding to two ring fields. The buckling loads of these three cylinders were very much alike and slightly higher than the buckling load of

Cylinder 37. Cylinder 37 differed from Cylinders 41 to 43 inasmuch as its cutout extended over three stringer fields. The purpose in testing Cylinders 41, 42, and 43 was to investigate the effect of the length of the cylinder upon the buckling load. The lengths of Cylinders 41, 42, and 43 were 39, 64, and 90 inches, respectively. The differences in the buckling load were small and they were not systematic.

Table II gives the maximum moments carried by the various cylinders together with data concerning the behavior of each cylinder after buckling. The average drop immediately after collapse was 11.6 percent of the original buckling load. Each cylinder was tested again after the final load had been left on overnight. The average maximum bending moment reached on the second day of loading of the cylinders was 83.8 percent of the original buckling load. After this new maximum was reached, the load was entirely removed and then the cylinders were loaded once again. The average maximum load reached in this last test was 78.2 percent of the original buckling load.

CONCLUSIONS

The following conclusions can be drawn on the basis of testing nine reinforced monocoque cylinders with side cutout in pure bending:

1. On the complete side of the cylinder the stress distribution is linear in very good approximation, both at the ends of the cylinder and in the middle where the cutout is located.

2. On the cutout side the stress is usually higher in the middle of the edge stringer than in the stringer located in a corresponding position on the complete side of the cylinder. In cylinders having large cutouts this stress is often the maximum stress in the entire cylinder. The stress in the cut stringers is always less than in corresponding stringers on the complete side of the cylinder.

3. The maximum value of the stress can be calculated in first approximation by means of the conventional bending formula Mc/I in which I is determined on the basis of the section of the cylinder in which the cutout is located. When calculating this moment of inertia, the effective width of sheet should be used. Deviations of the actual maximum stress from the values calculated can be estimated with the aid of the strain factors presented.

4. The buckling load of the cylinder decreases as the size of the cutout increases. In cylinders constructed similarly to those tested, values of the bending moment at buckling can be estimated with the aid of the data presented on the effect of size of cutout on critical moment.

5. The cylinders can carry large loads even after buckling. In general, the size of the bulge and the number of the bulges increase when the loading is continued after the first buckling.

Polytechnic Institute of Brooklyn
Brooklyn, N. Y., February 6, 1946

REFERENCES

1. Hoff, N. J., and Boley, Bruno A.: Stresses in and General Instability of Monocoque Cylinders with Cutouts. I - Experimental Investigation of Cylinders with a Symmetric Cutout Subjected to Pure Bending. NACA TN No. 1013, 1946.

2. Hoff, N. J., Boley, Bruno A., and Klein, Bertram: Stresses in and General Instability of Monocoque Cylinders with Cutouts. II - Calculation of the Stresses in a Cylinder with a Symmetric Cutout. NACA TN No. 1014, 1946.

3. Hoff, N. J., Boley, Bruno A., and Klein, Bertram: Stresses in and General Instability of Monocoque Cylinders with Cutouts. III - Calculation of the Buckling Load of Cylinders with Symmetric Cutout Subjected to Pure Bending. NACA TN No. 1263, 1947.

4. Hoff, N. J., Fuchs, S. J., and Cirillo, Adam J.: The Inward Bulge Type Buckling of Monocoque Cylinders. II - Experimental Investigation of the Buckling in Combined Bending and Compression. NACA TN No. 939, 1944.

5. Hoff, N. J., and Klein, Bertram: Stresses in and General Instability of Monocoque Cylinders with Cutouts. V - Calculation of the Stresses in Cylinders with Side Cutout. NACA TN No. 1435, 1948.

6. Hoff, N. J., and Klein, Bertram: The Inward Bulge Type Buckling of Monocoque Cylinders. III - Revised Theory Which Considers the Shear Strain Energy. NACA TN No. 968, 1945.

TABLE I.- FORCE AND MOMENT EQUILIBRIUM

Cylinder	Condition	Load			
		First		Second	
		Moment (in.-lb)	Force (lb)	Moment (in.-lb)	Force (lb)
35	Applied	36,200	0	64,800	0
	Band A	33,600	-37	55,800	-124
	Band E	33,800	-71	56,100	-16
	Band I	34,800	55	61,600	-179
36	Applied	27,200	0	42,200	0
	Band A	23,600	36	37,300	-32
	Band E	24,600	-133	38,700	-102
	Band I	24,500	81	40,200	-128
37	Applied	11,300	0	20,600	0
	Band A	10,400	25	19,800	10
	Band E	9,100	3	17,800	17
	Band I	10,900	10	21,400	3
38	Applied	14,300	0	33,900	0
	Band A	14,800	61	31,400	2
	Band E	13,900	-8	30,700	-49
	Band I	14,700	-37	32,600	-32
39	Applied	12,100	0	29,500	0
	Band A	11,600	-3	30,100	0
	Band E	10,200	-12	26,100	25
	Band G	11,000	10	27,800	22
	Band I	12,800	20	32,000	32
40	Applied	11,300	0	22,100	0
	Band A	12,400	47	25,300	79
	Band C	11,300	25	22,800	32
	Band E	10,700	0	21,600	-10
	Band I	12,700	-49	27,900	-331
41	Applied	13,400	0	29,300	0
	Band B	14,100	165	29,700	-81
	Band C	14,100	25	30,300	-86
	Band F	15,200	37	31,402	-25
42	Applied	18,000	0	30,100	0
	Band A	18,000	-116	31,000	-257
	Band C	16,600	-91	27,950	-180
	Band F	16,700	-59	30,400	-180
	Band G	18,300	-264	29,900	-353
43	Applied	16,500	0	29,300	0
	Band A	13,800	-44	27,500	-118
	Band D	13,700	-138	26,400	-242
	Bands G and H	14,600	-42	27,700	-81
	Band I	14,600	-64	27,600	-109
	Band L	14,700	-69	27,400	-123
	Band N	17,000	-200	31,200	-84

TABLE II.- BUCKLING DATA

Cylinder	Cutout (deg)	Number of stringers	Maximum moment (in.-lb)	Percent of maximum moment for 0° cutout	Deflection of compressive edge stringer	Behavior after collapse							
						Immediately after collapse		After overnight rest		Maximum moment after overnight rest			
										Before decrease to zero		After decrease to zero	
						Moment (in.-lb)	Percent of maximum moment	Moment (in.-lb)	Percent of maximum moment	Moment (in.-lb)	Percent of maximum moment	Moment (in.-lb)	Percent of maximum moment
35	90	16	172,600	59.7	Out	-------	----	-------	----	-------	----	164,700	95.4
36	135	16	169,900	58.7	Out	161,700	95.2	126,300	74.5	146,300	86.4	118,500	69.8
37	90	8	107,900	65.5	In	95,800	88.8	87,200	80.9	91,300	84.5	82,500	76.5
38	45	16	232,500	80.5	Out	213,700	91.8	-------	----	217,700	93.3	-------	----
39	45	8	113,000	68.6	Out	105,200	93.1	96,900	85.7	105,700	93.4	99,500	88.0
40	135	8	100,000	60.8	Out	81,000	81.0	71,200	71.2	76,100	76.1	75,300	75.3
41	90	8	126,300	76.9	In	121,600	96.2	101,800	80.5	105,200	83.3	100,500	79.6
42	90	8	115,700	70.3	In	95,900	82.9	-------	----	87,200	75.4	81,300	70.3
43	90	8	120,600	73.3	In	94,600	78.5	88,200	73.2	94,400	78.3	85,600	71.0
							[a]88.4		[a]77.7		[a]83.8		[a]78.2
[b]11	0	16	289,000	100.0									
[c]--	0	8	164,400	100.0									

[a]Average percentages.
[b]This cylinder is described in reference 4.
[c]Maximum moment calculated according to reference 6.

NACA

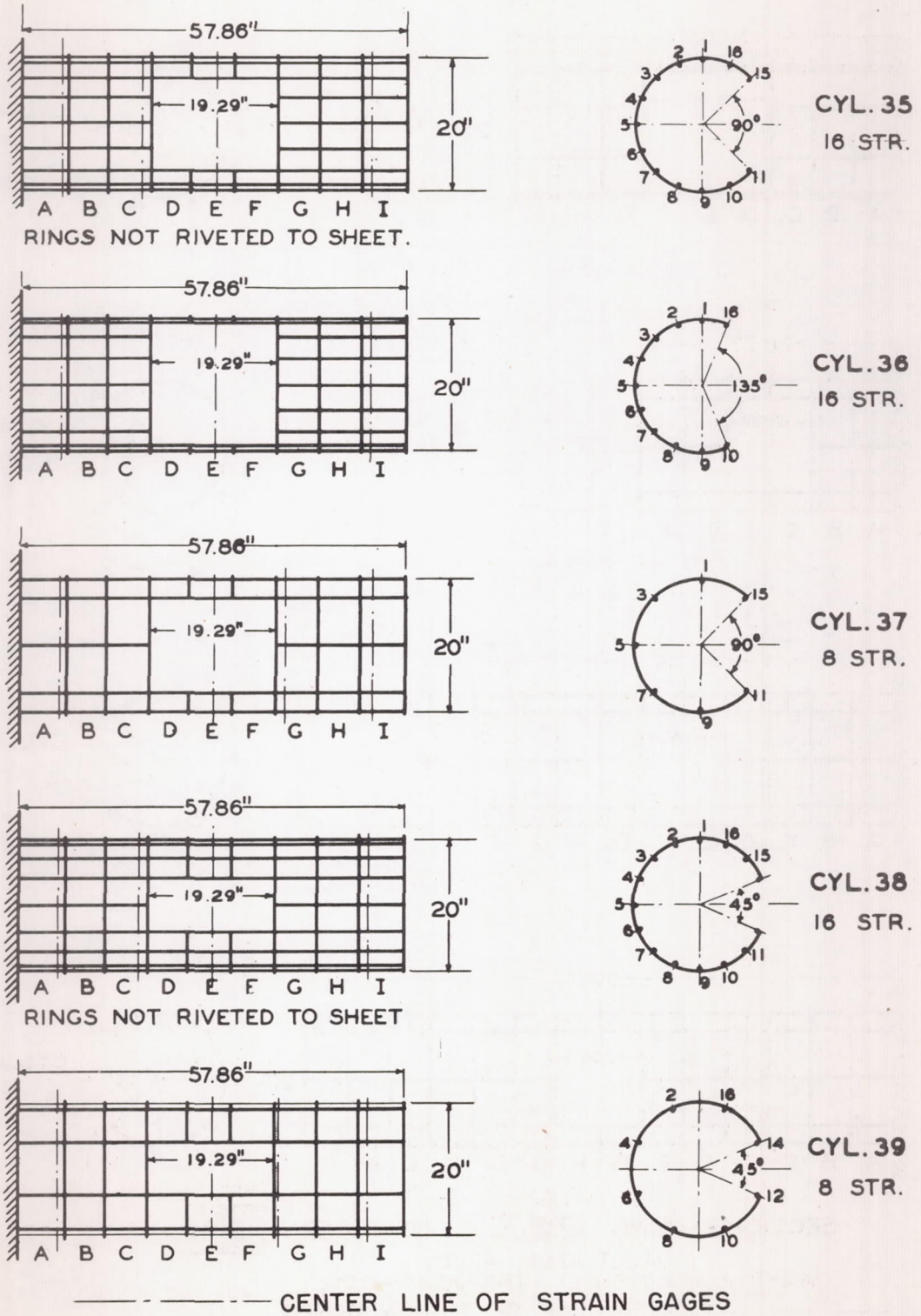

(a) Cylinders 35 to 39.

Figure 1.- Schematic drawings of test specimens.

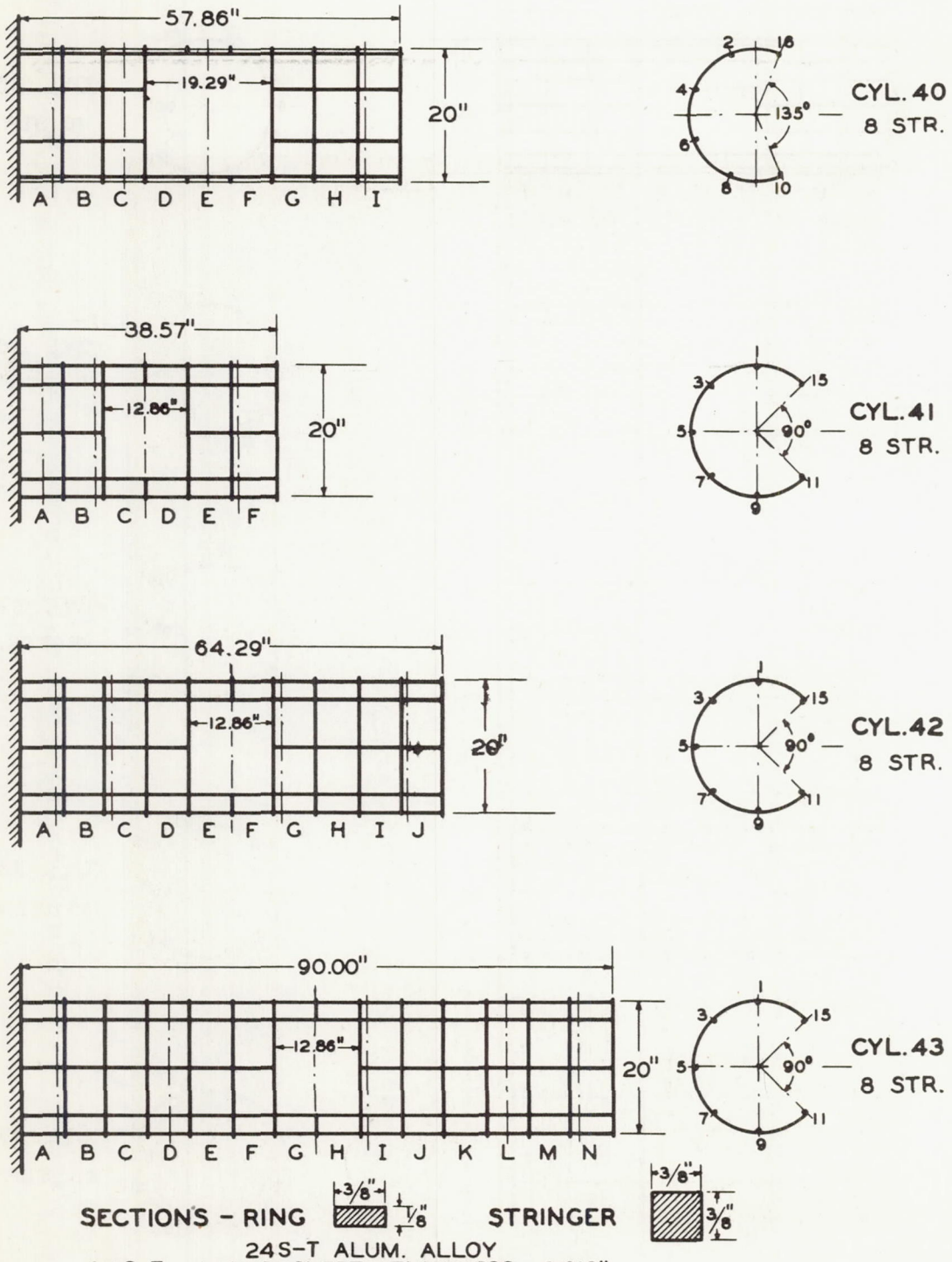

(b) Cylinders 40 to 43.

Figure 1.- Concluded.

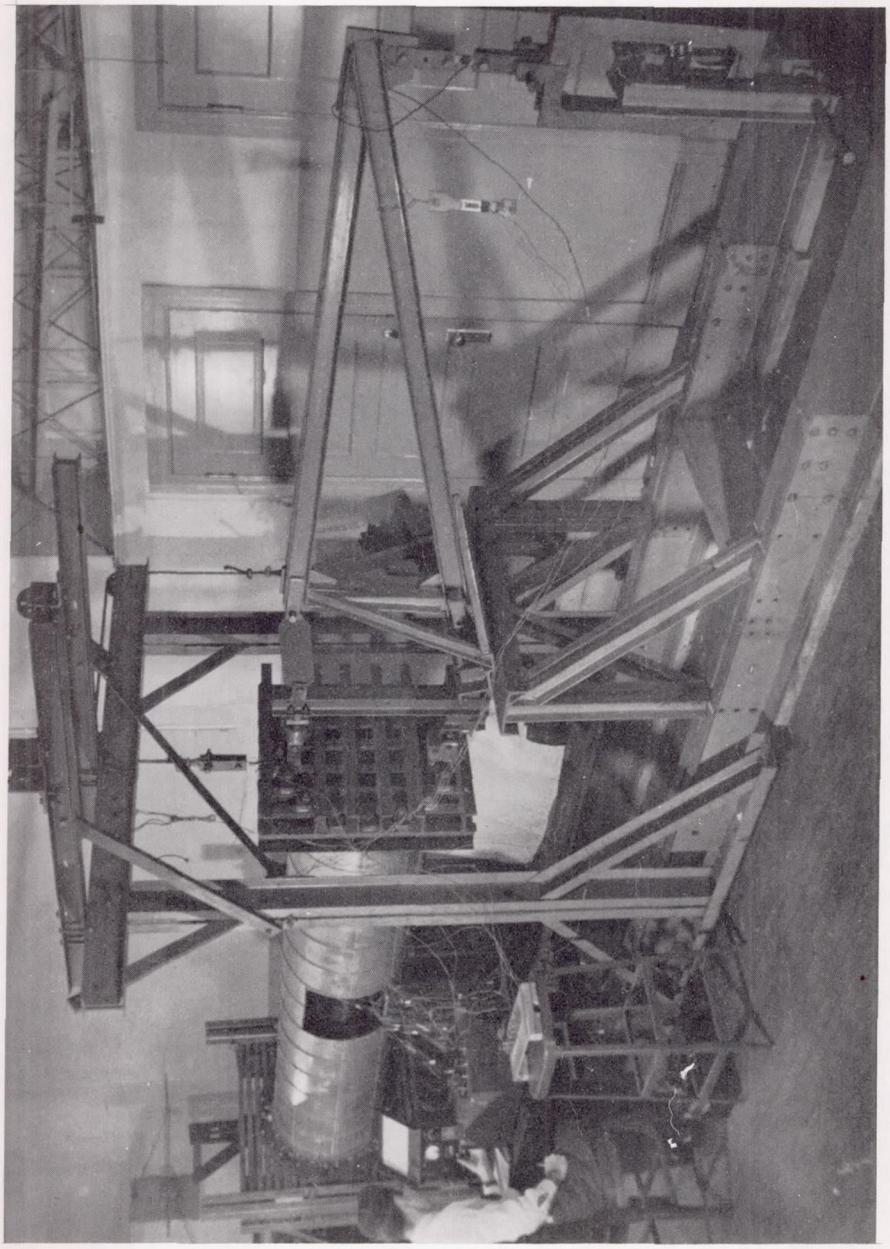

Figure 2.- Photograph of test setup.

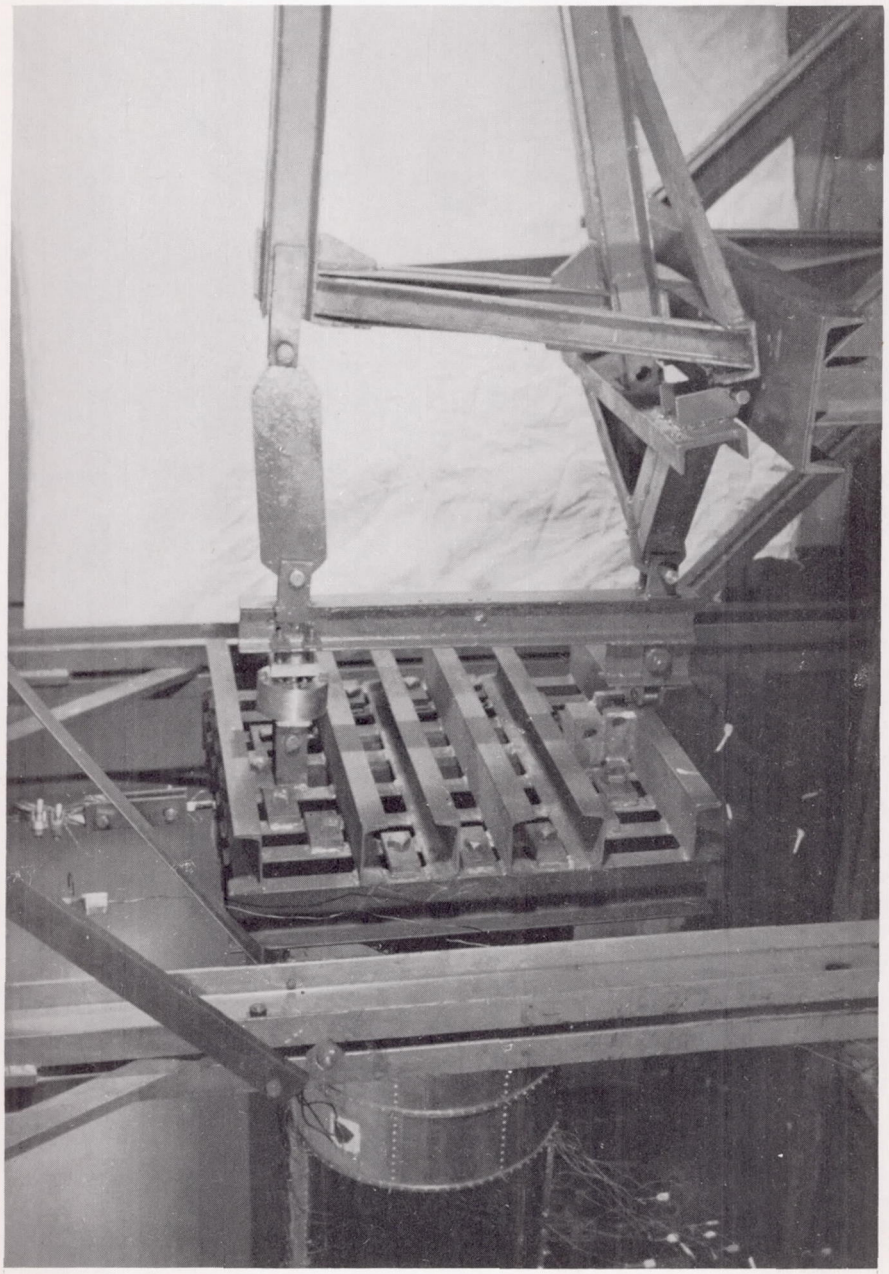

Figure 3.- Swiveling parallel-linkage mechanism.

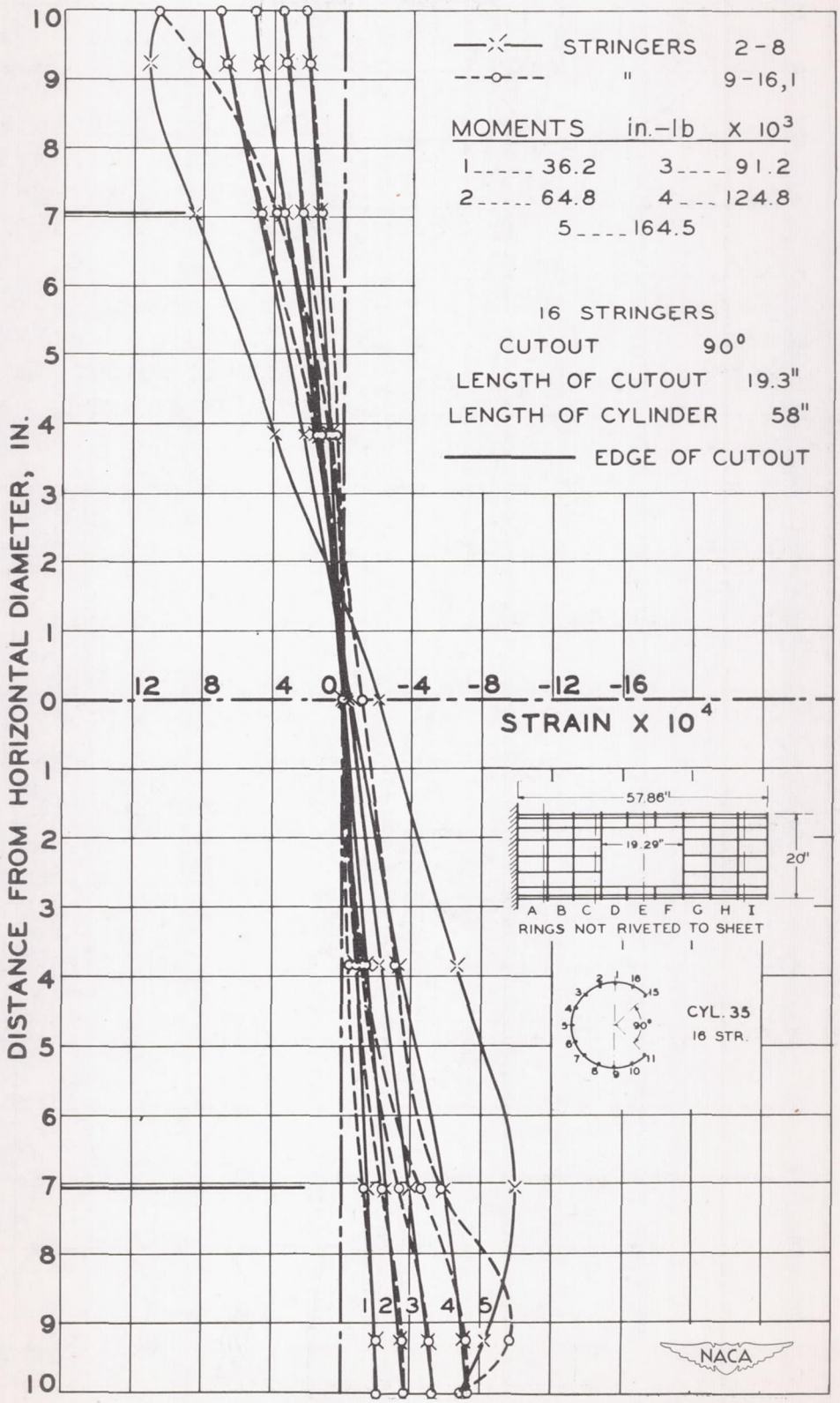

Figure 4.- Strain diagram of cylinder 35. Band A.

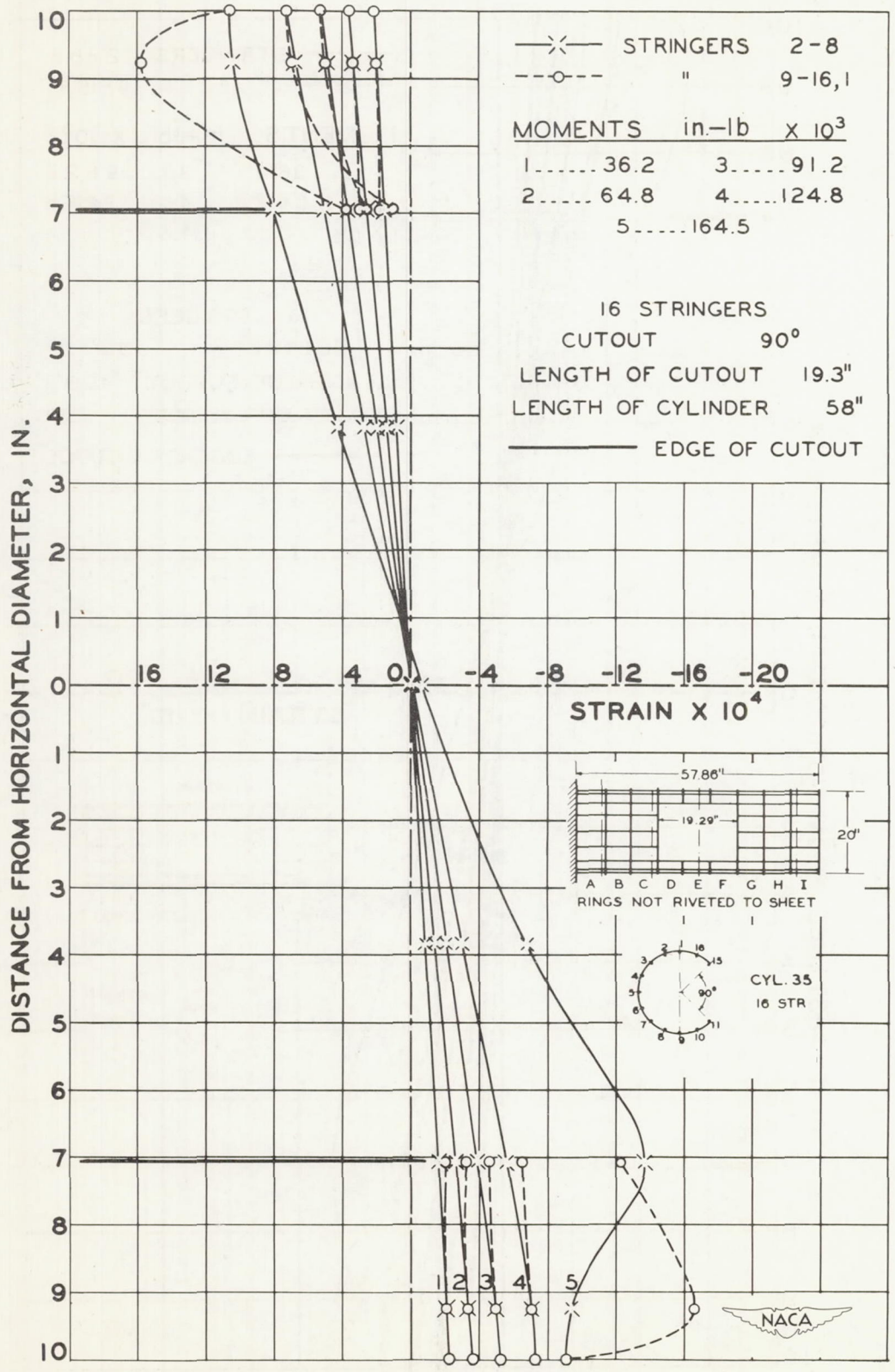

Figure 5.- Strain diagram of cylinder 35. Band E.

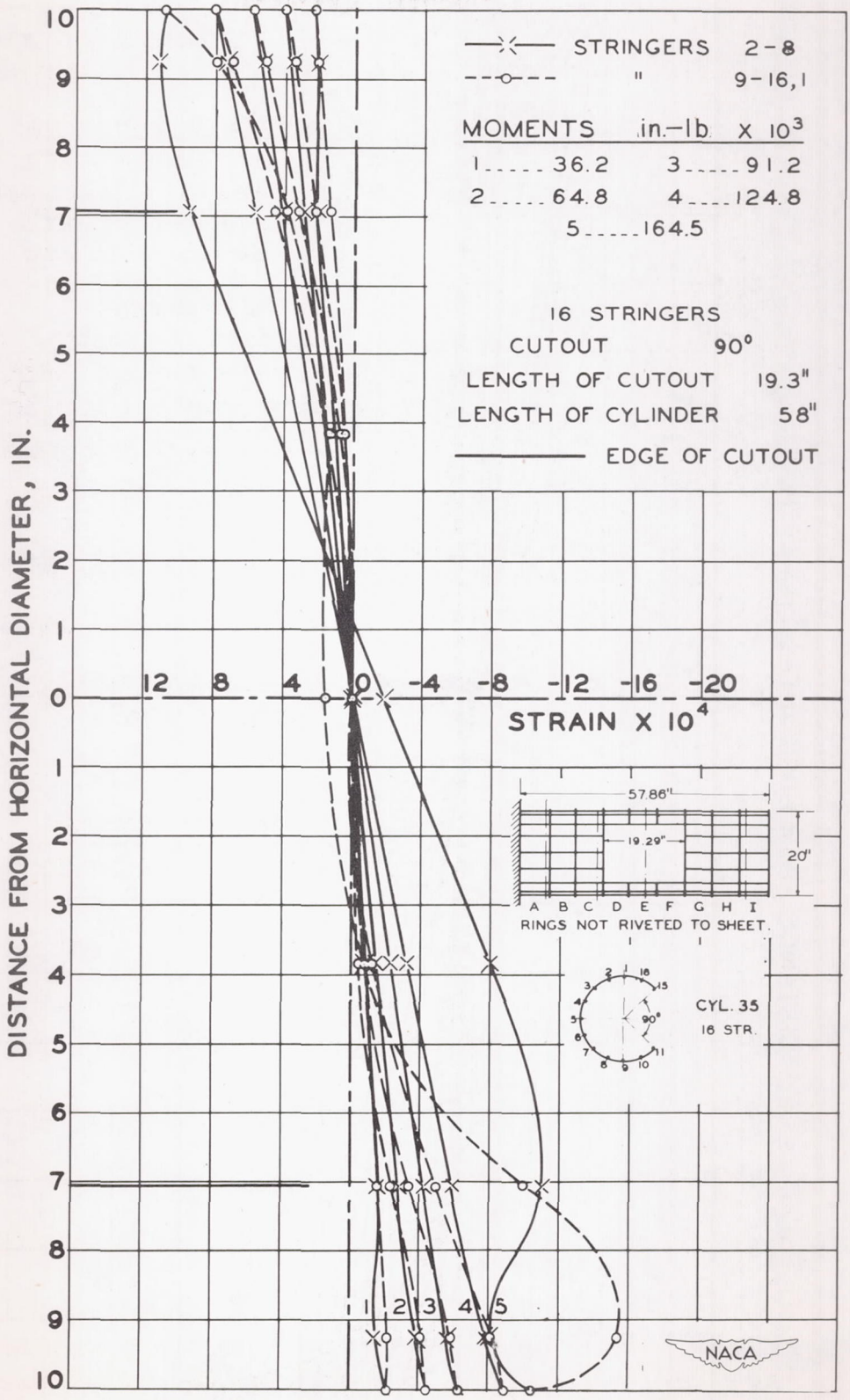

Figure 6.- Strain diagram of cylinder 35. Band I.

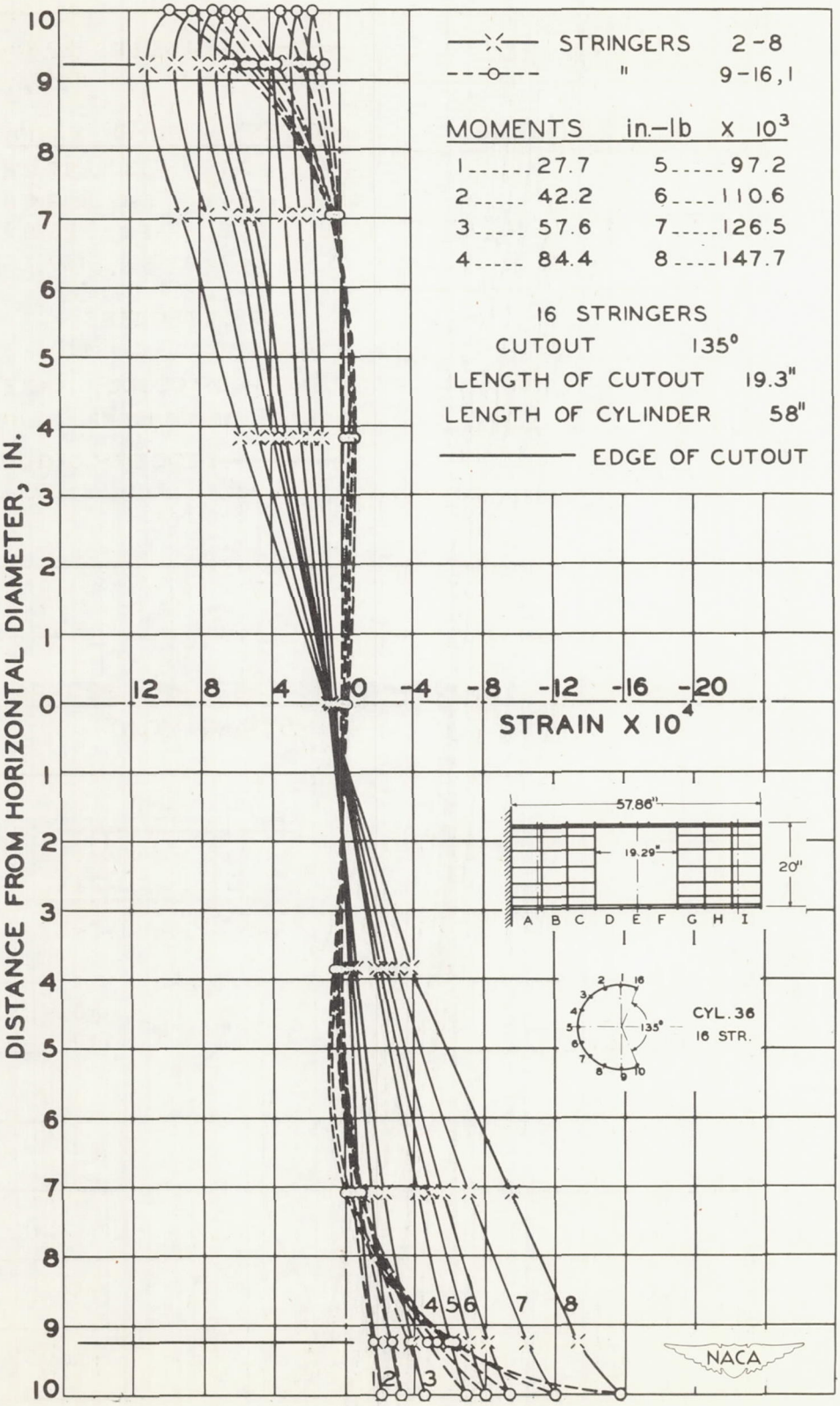

Figure 7.- Strain diagram of cylinder 36. Band A.

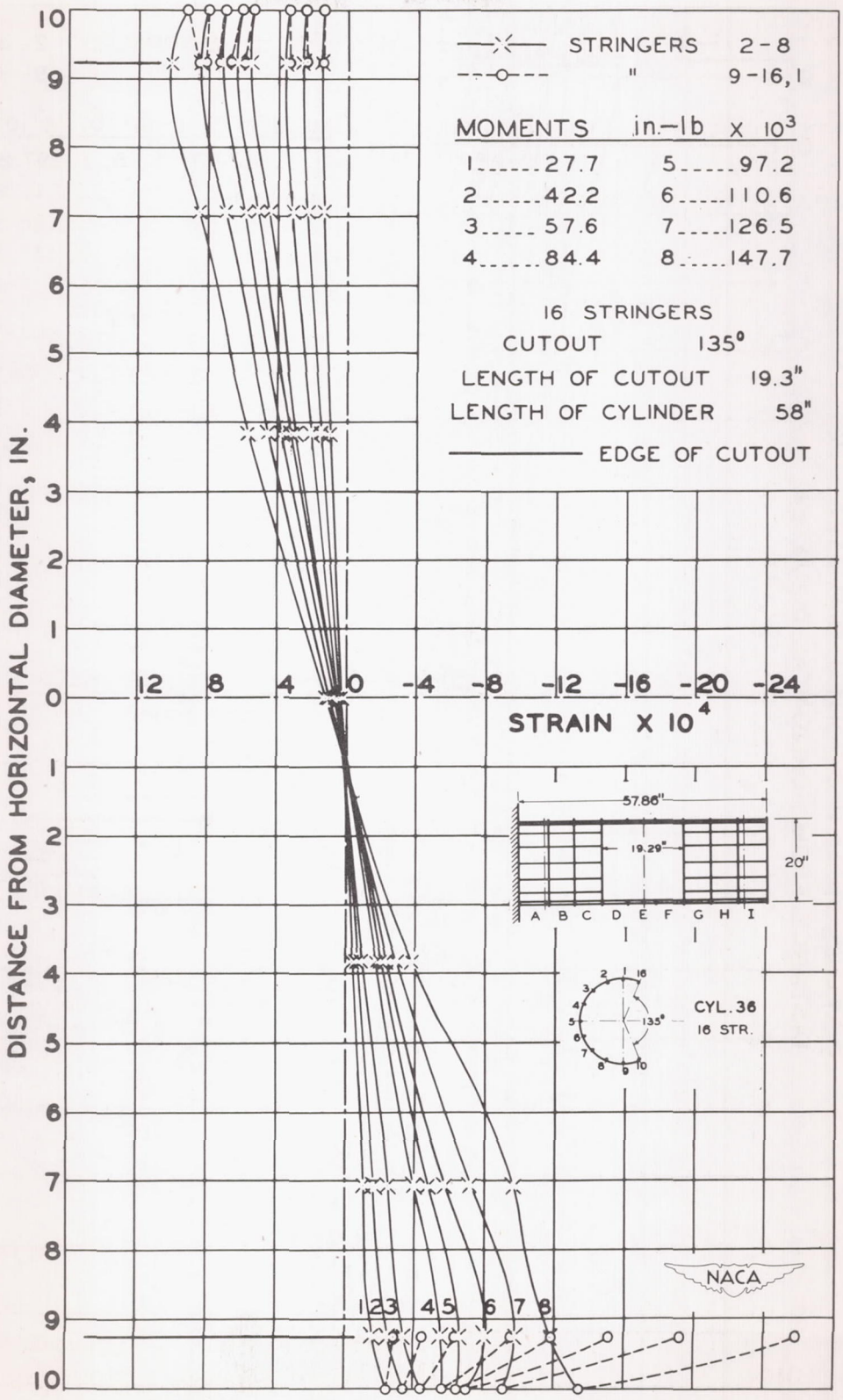

Figure 8.- Strain diagram of cylinder 36. Band E.

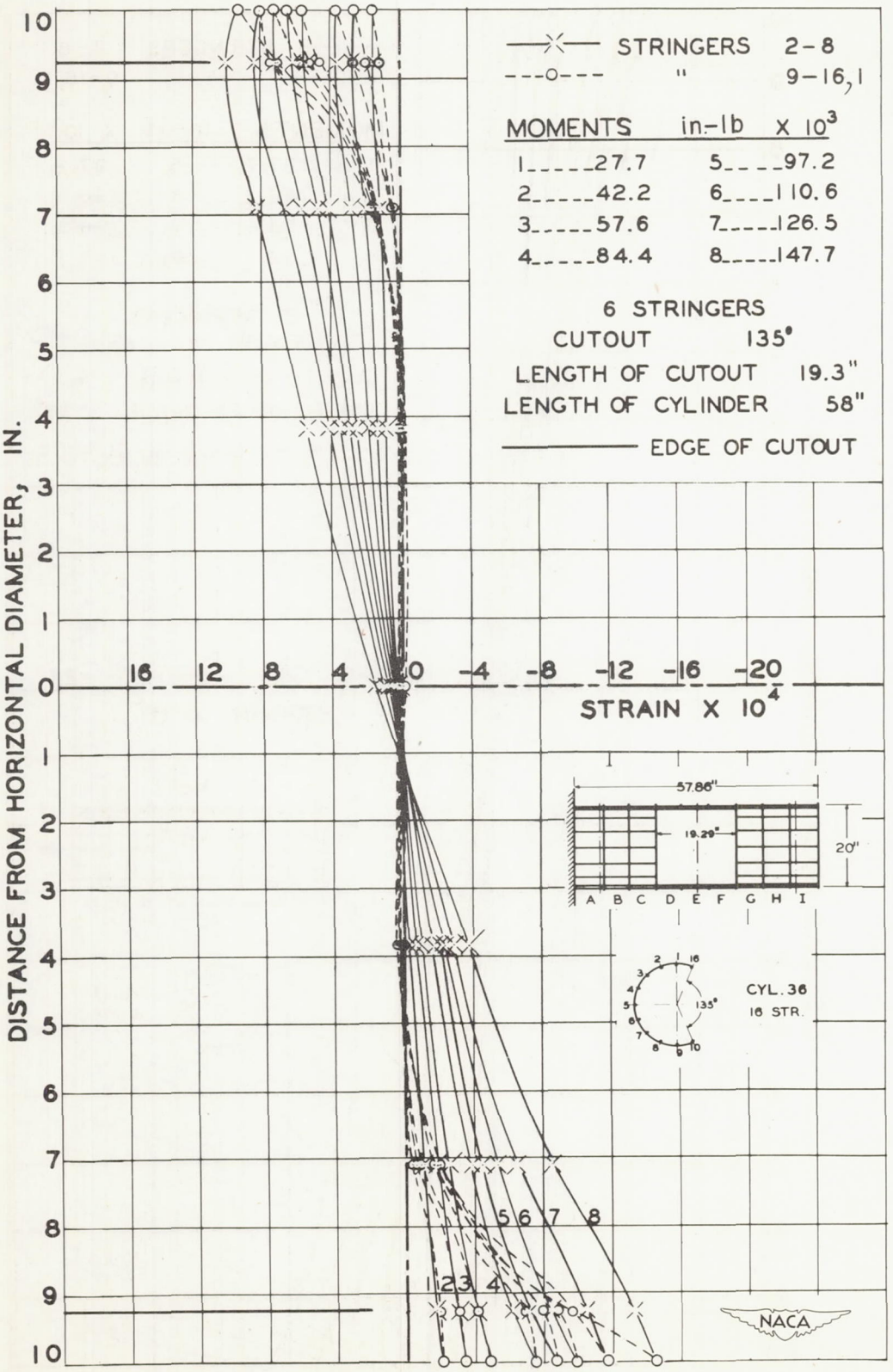

Figure 9.- Strain diagram of cylinder 36. Band I.

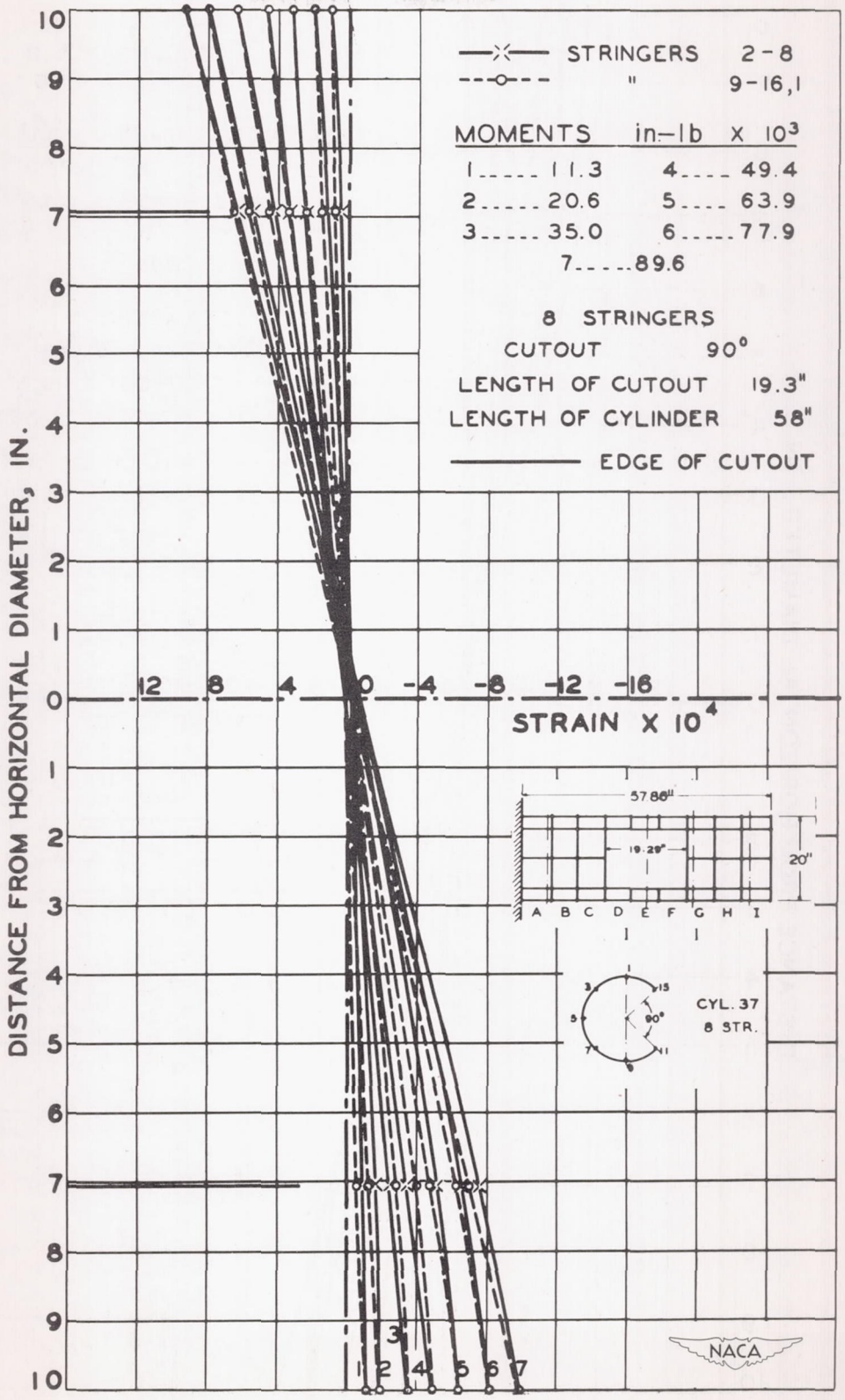

Figure 10.- Strain diagram of cylinder 37. Band A.

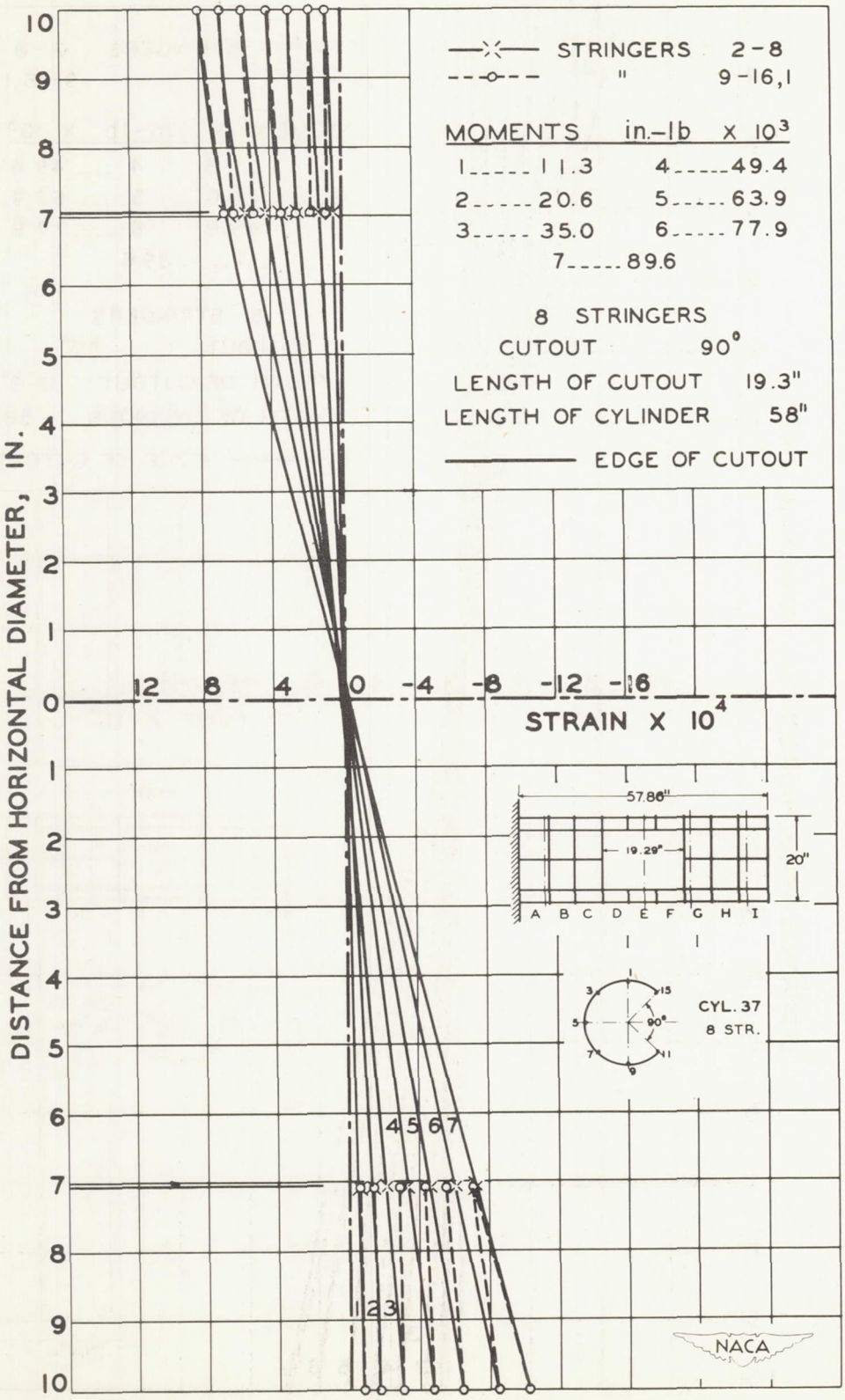

Figure 11.- Strain diagram of cylinder 37. Band E.

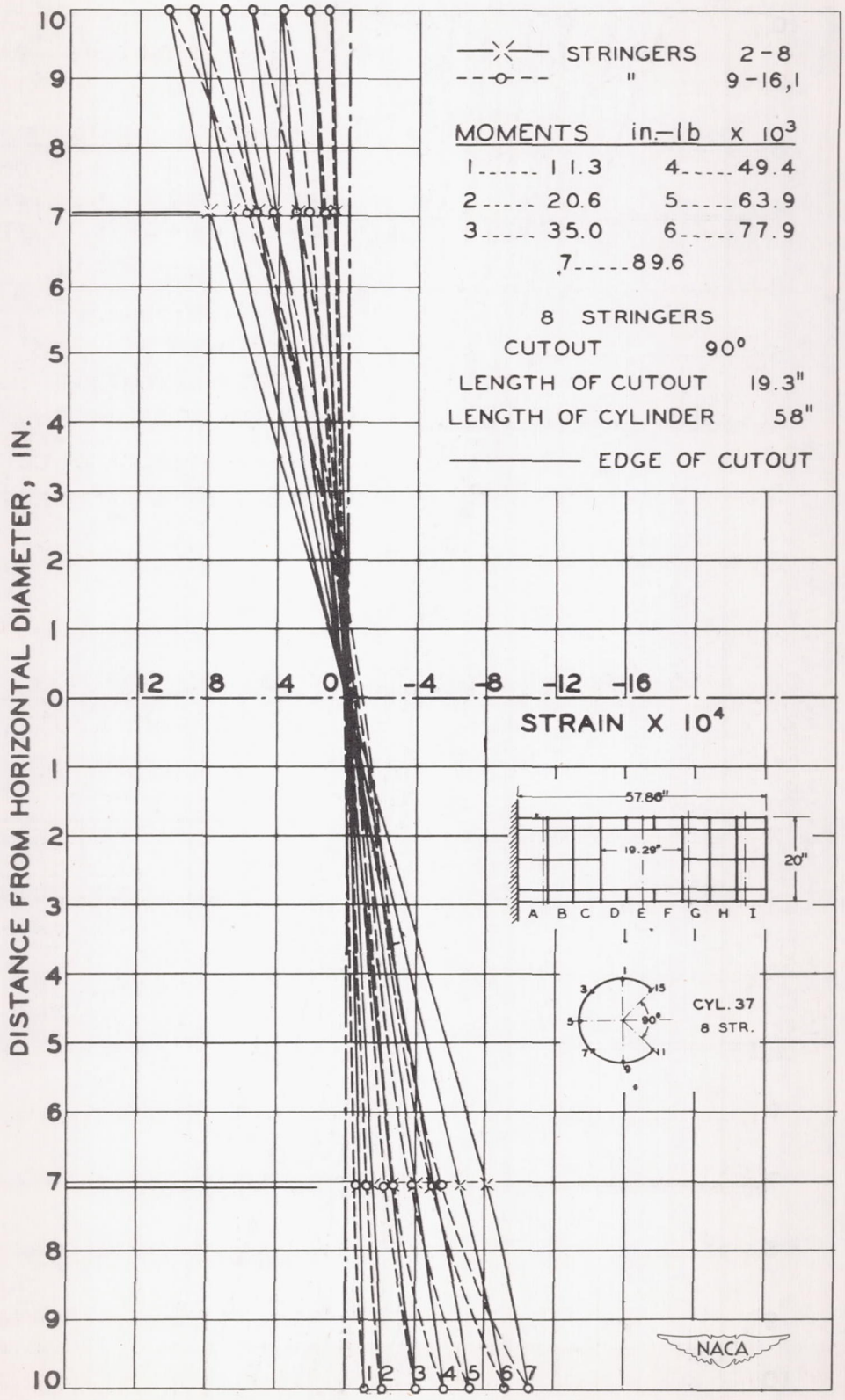

Figure 12.- Strain diagram of cylinder 37. Band I.

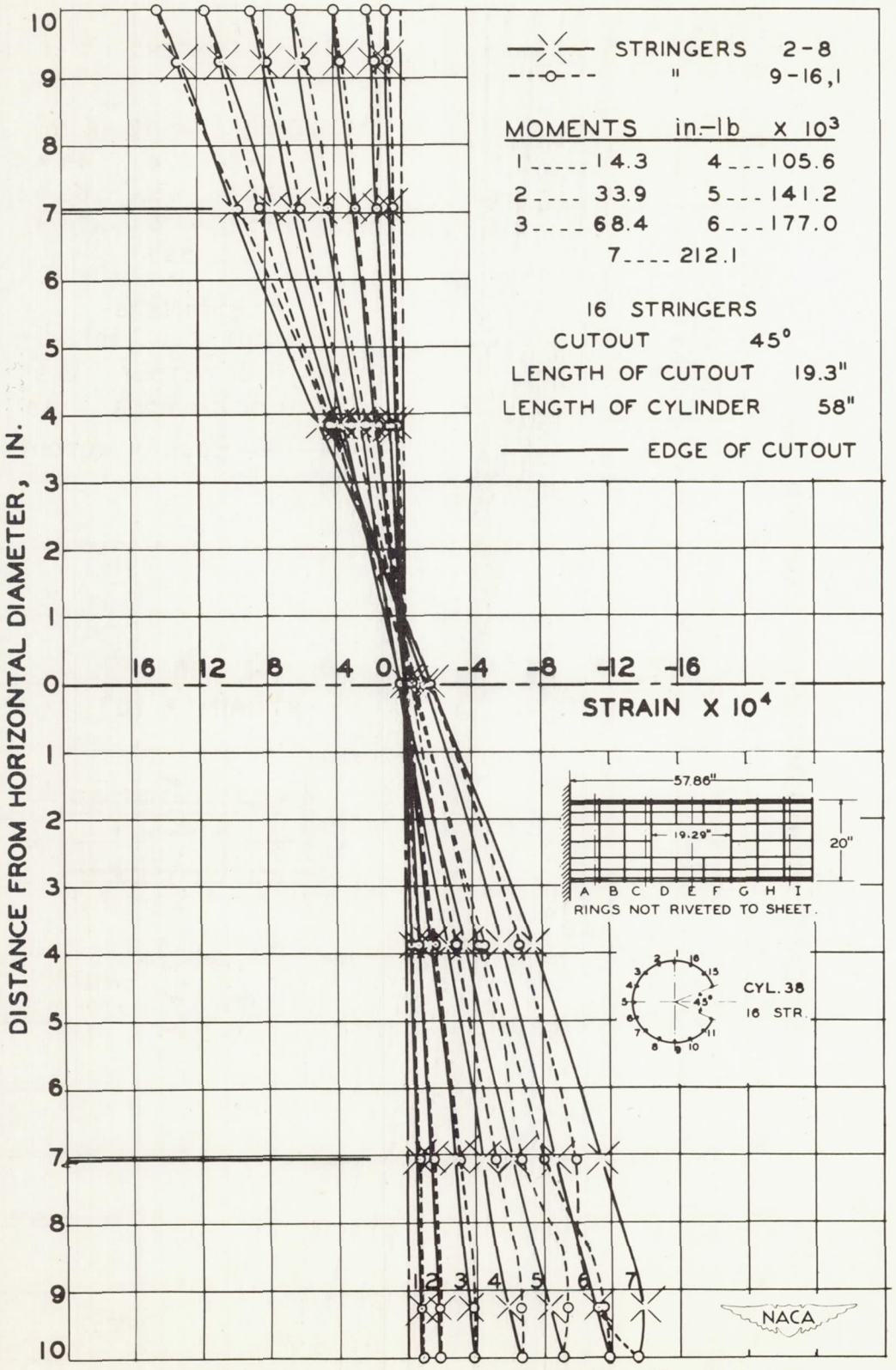

Figure 13.- Strain diagram of cylinder 38. Band A.

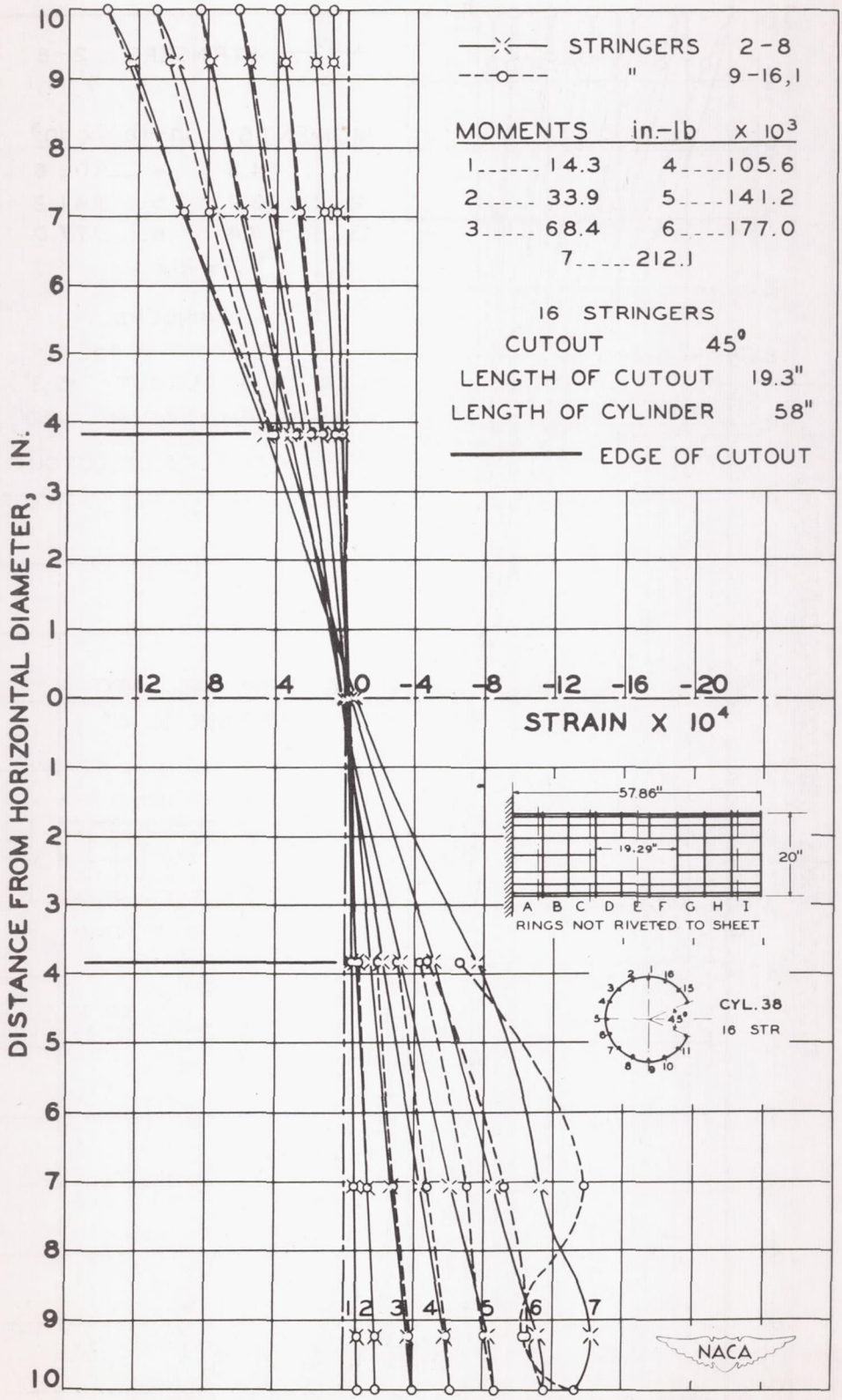

Figure 14.- Strain diagram of cylinder 38. Band E.

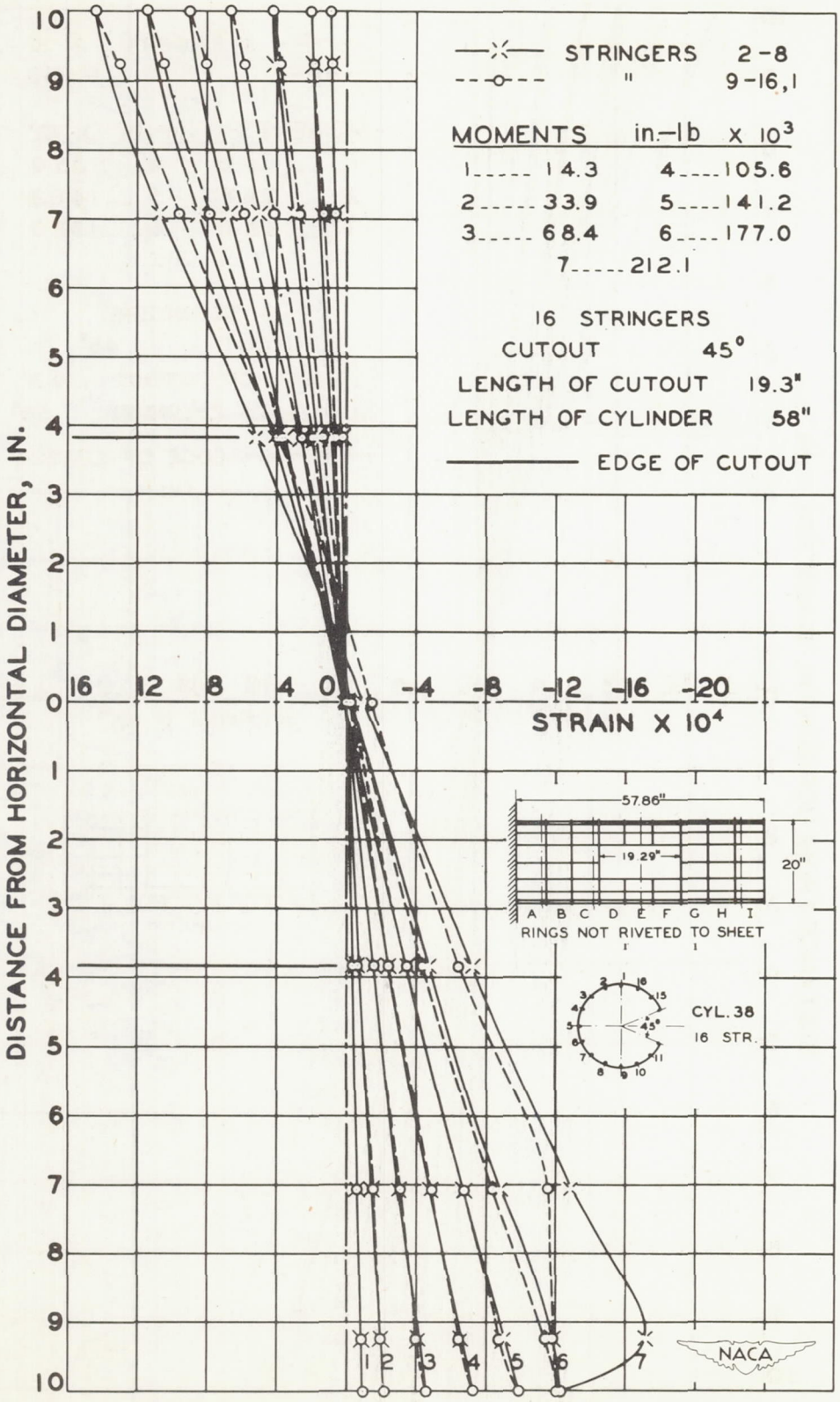

Figure 15.- Strain diagram of cylinder 38. Band I.

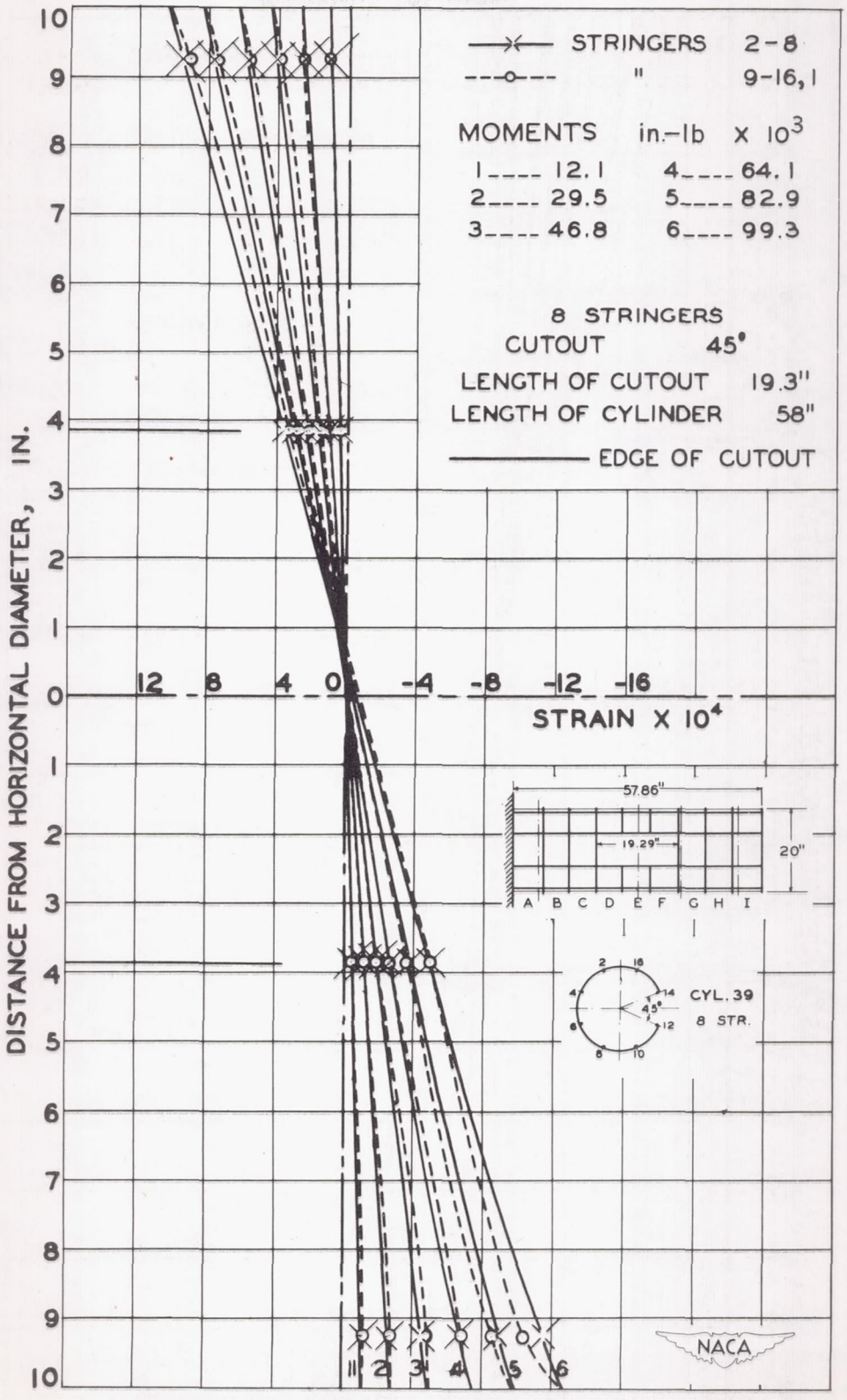

Figure 16.- Strain diagram of cylinder 39. Band G.

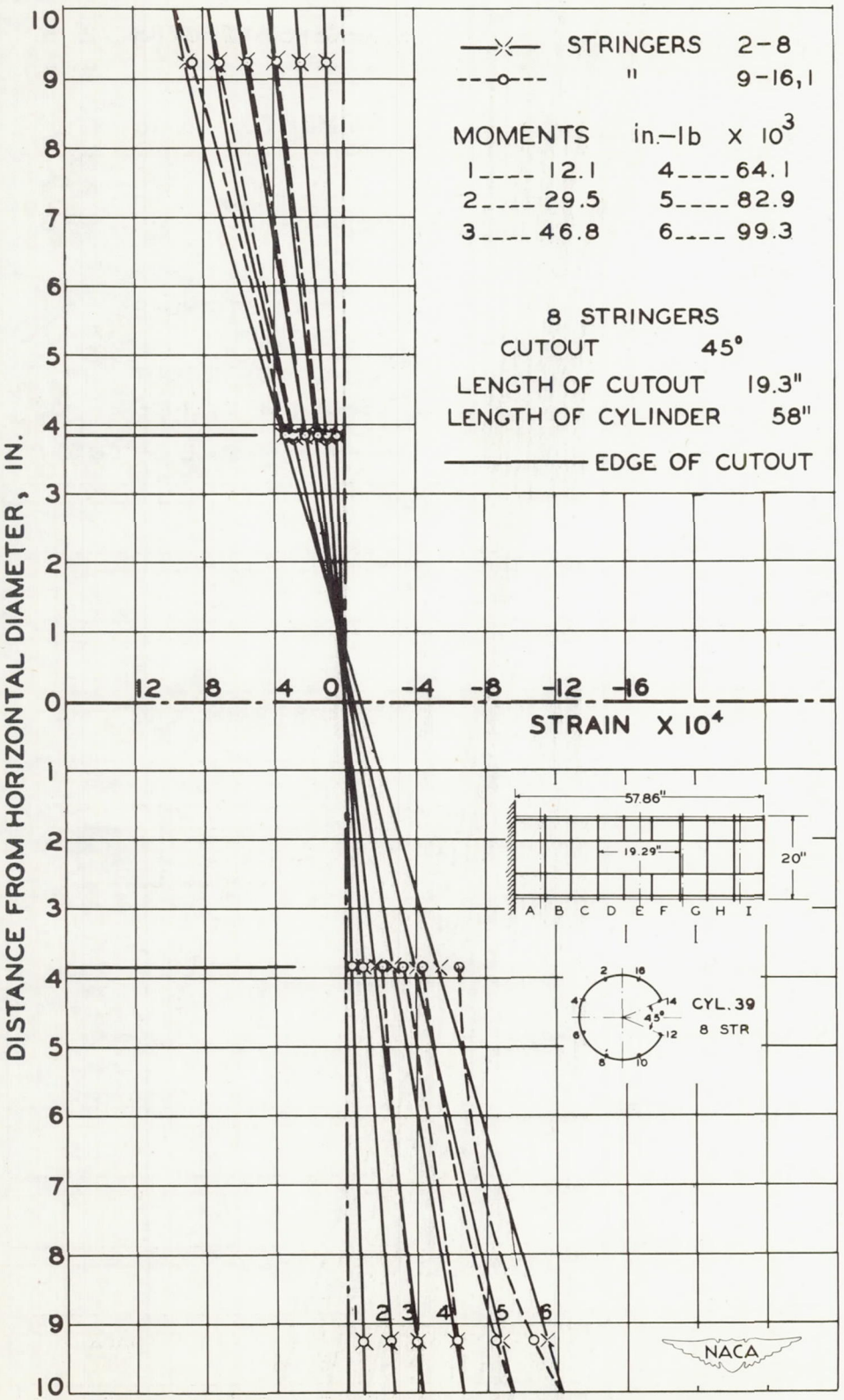

Figure 17.- Strain diagram of cylinder 39. Band E.

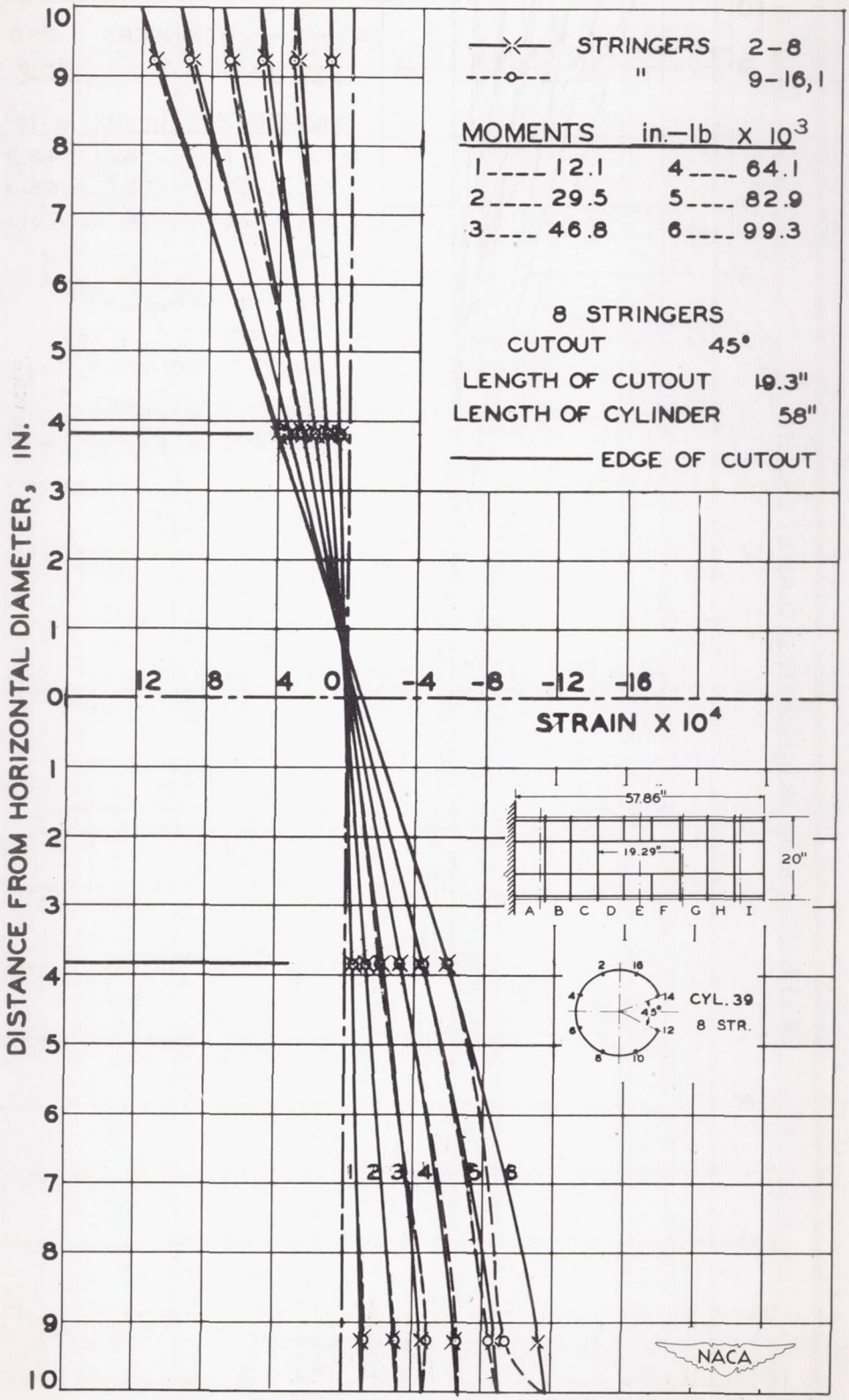

Figure 18.- Strain diagram of cylinder 39. Band I.

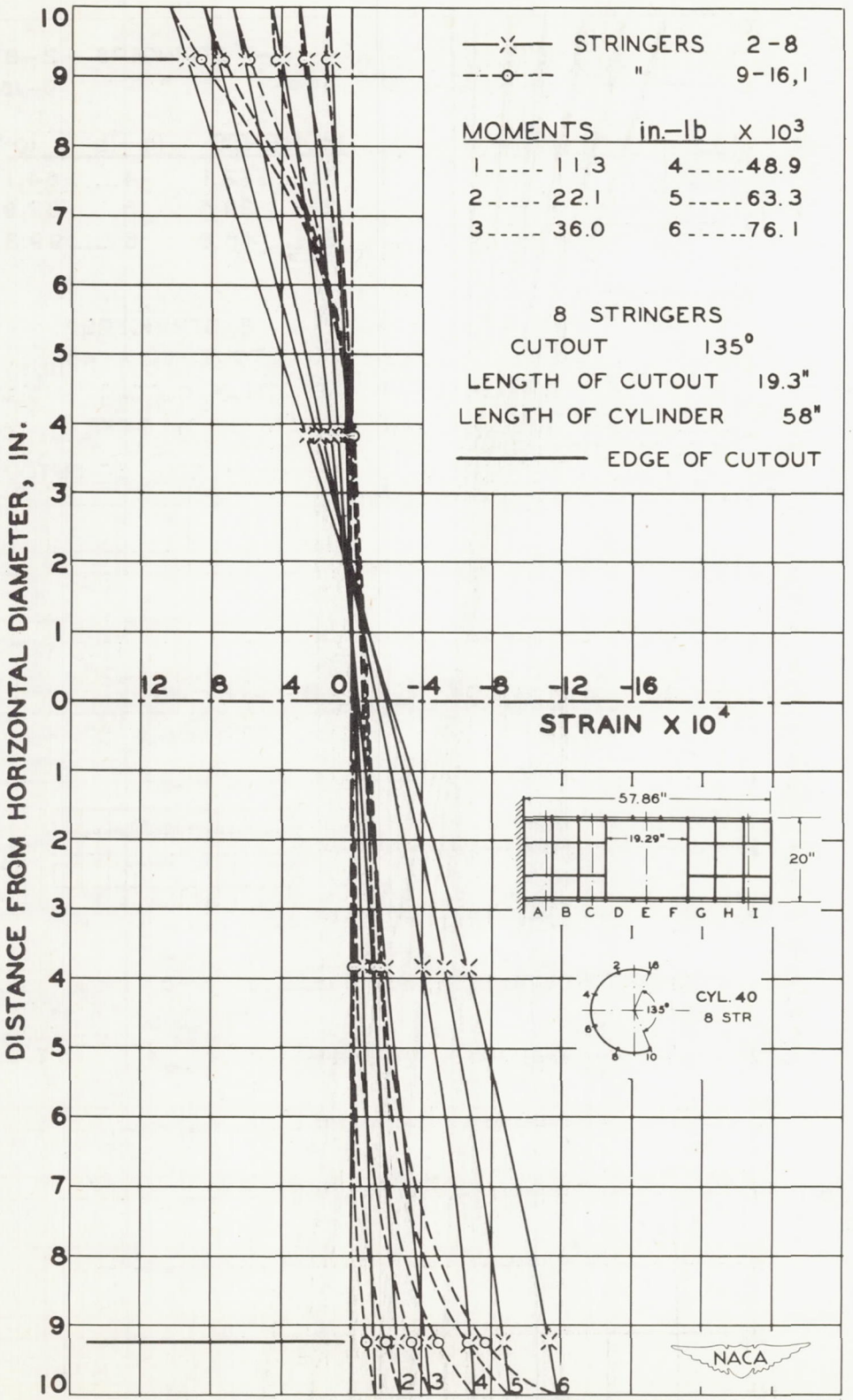

Figure 19.- Strain diagram of cylinder 40. Band A.

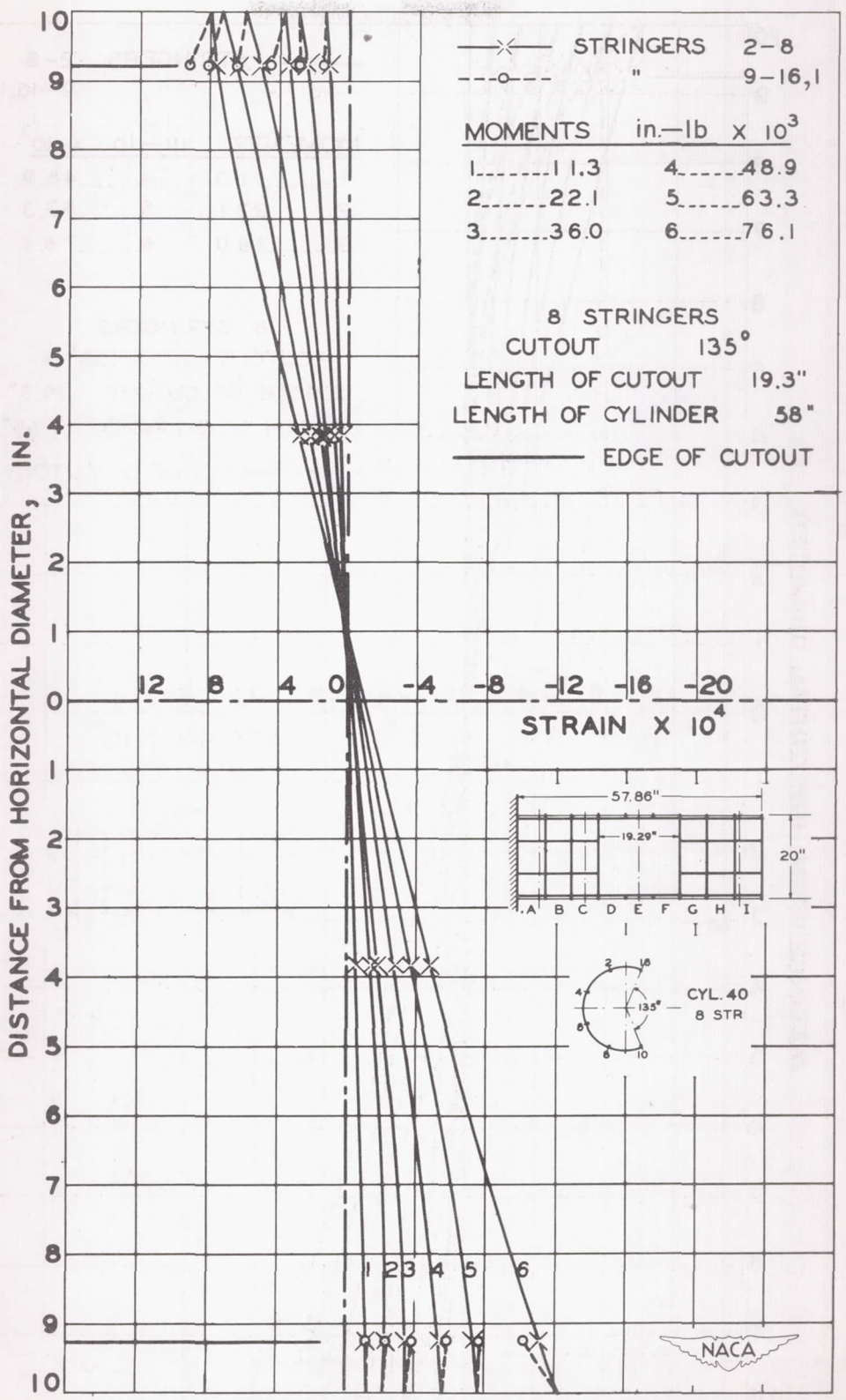

Figure 20.- Strain diagram of cylinder 40. Band E.

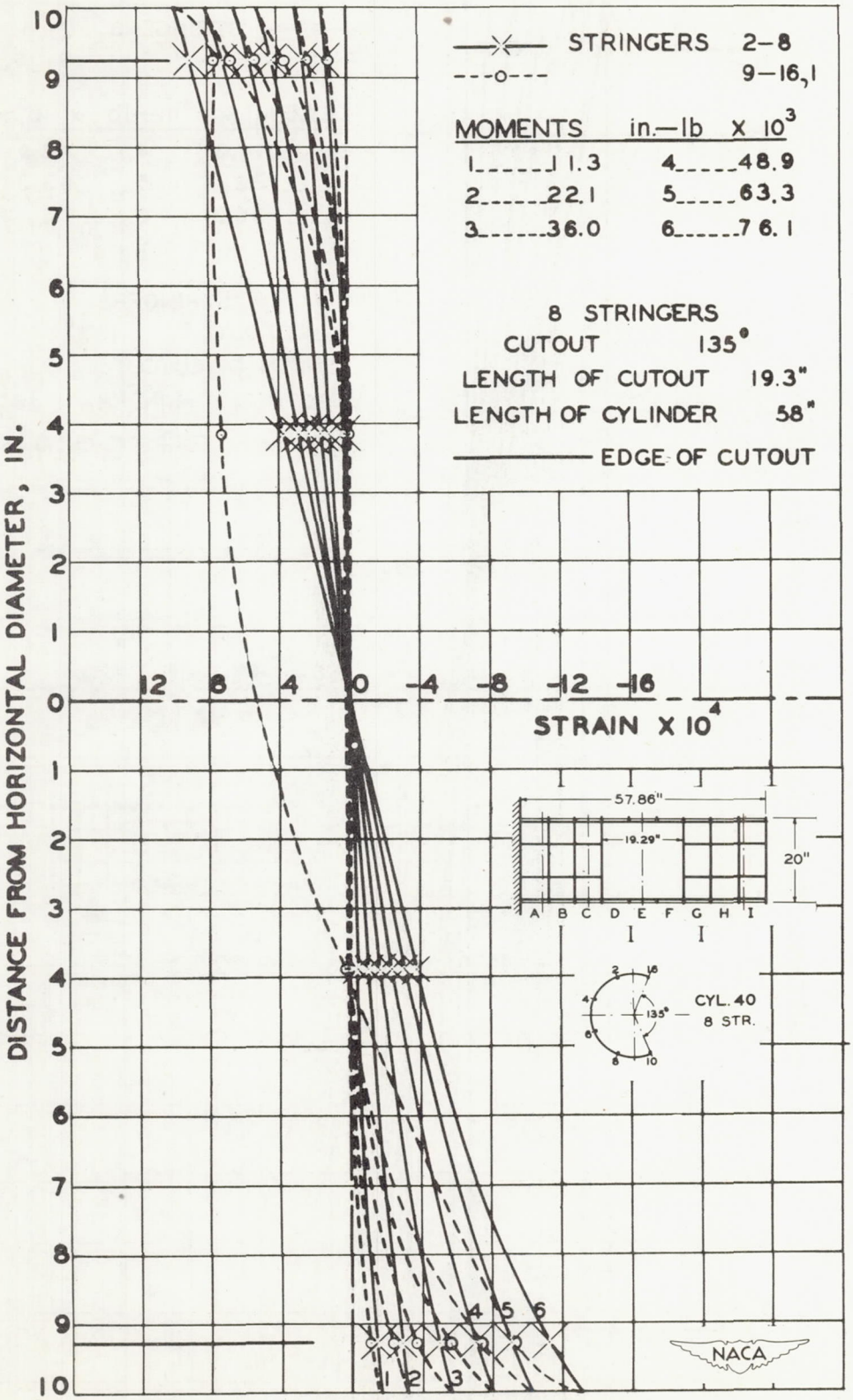

Figure 21.- Strain diagram of cylinder 40. Band I.

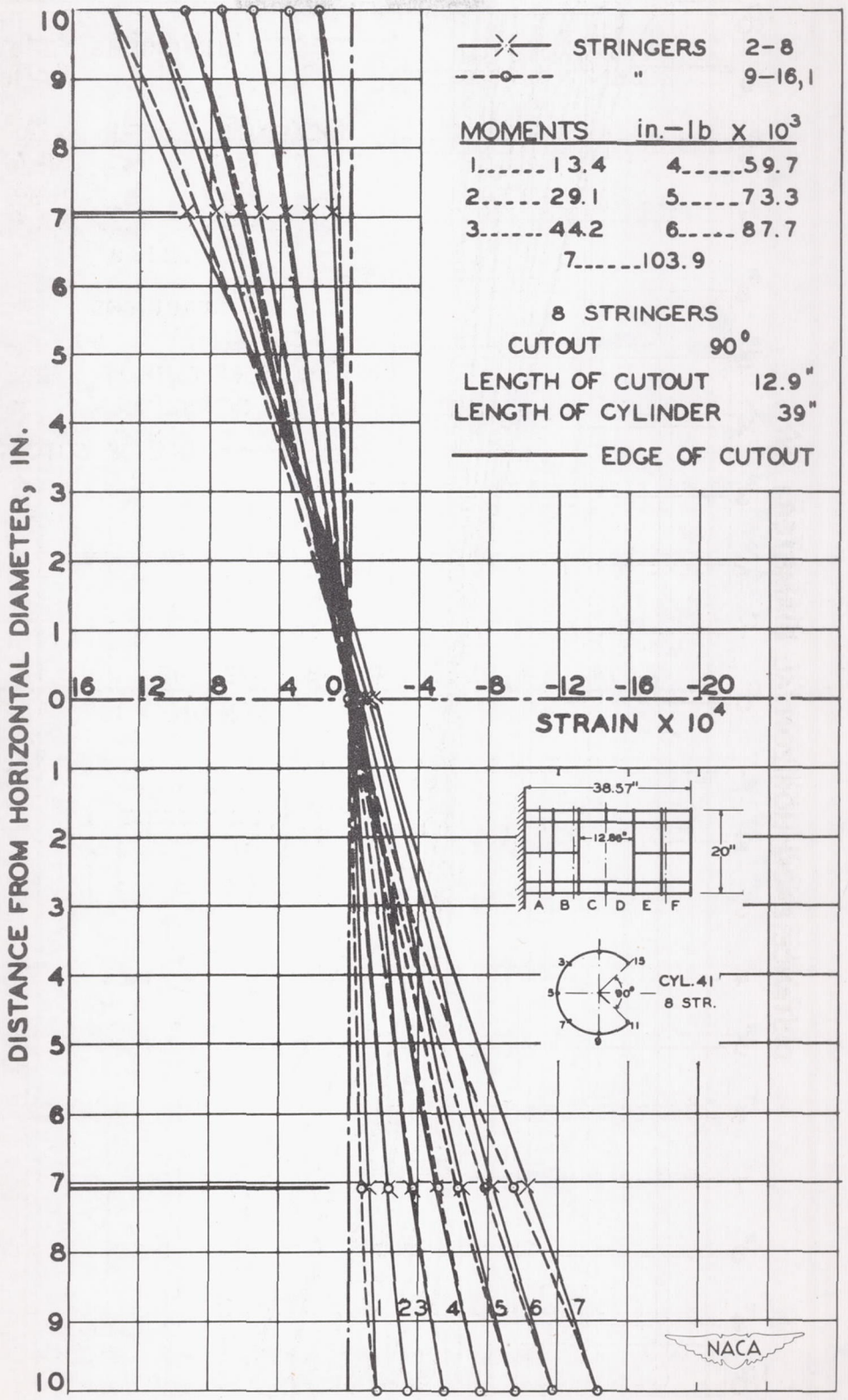

Figure 22.- Strain diagram of cylinder 41. Band A.

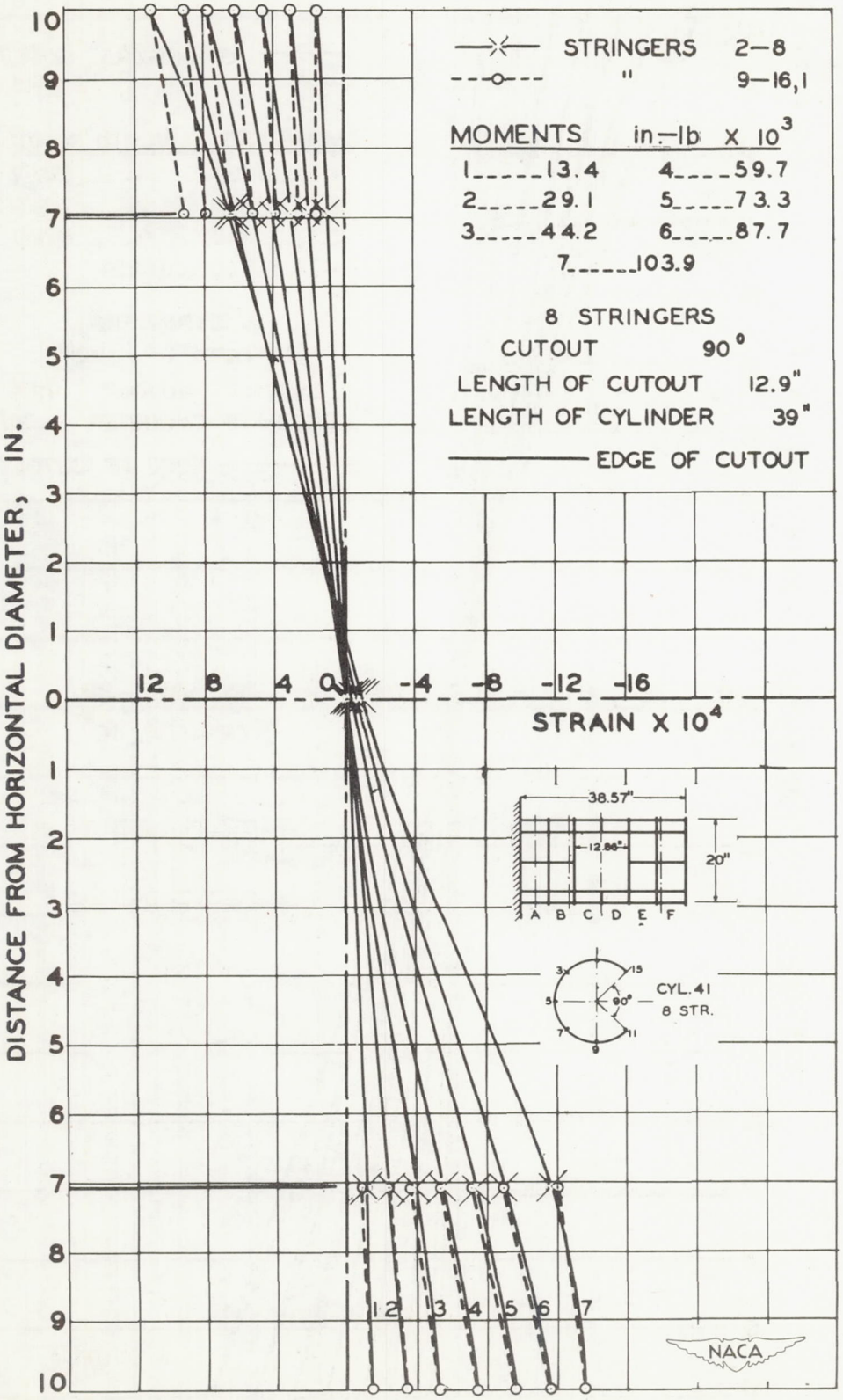

Figure 23.- Strain diagram of cylinder 41. Bands C and D.

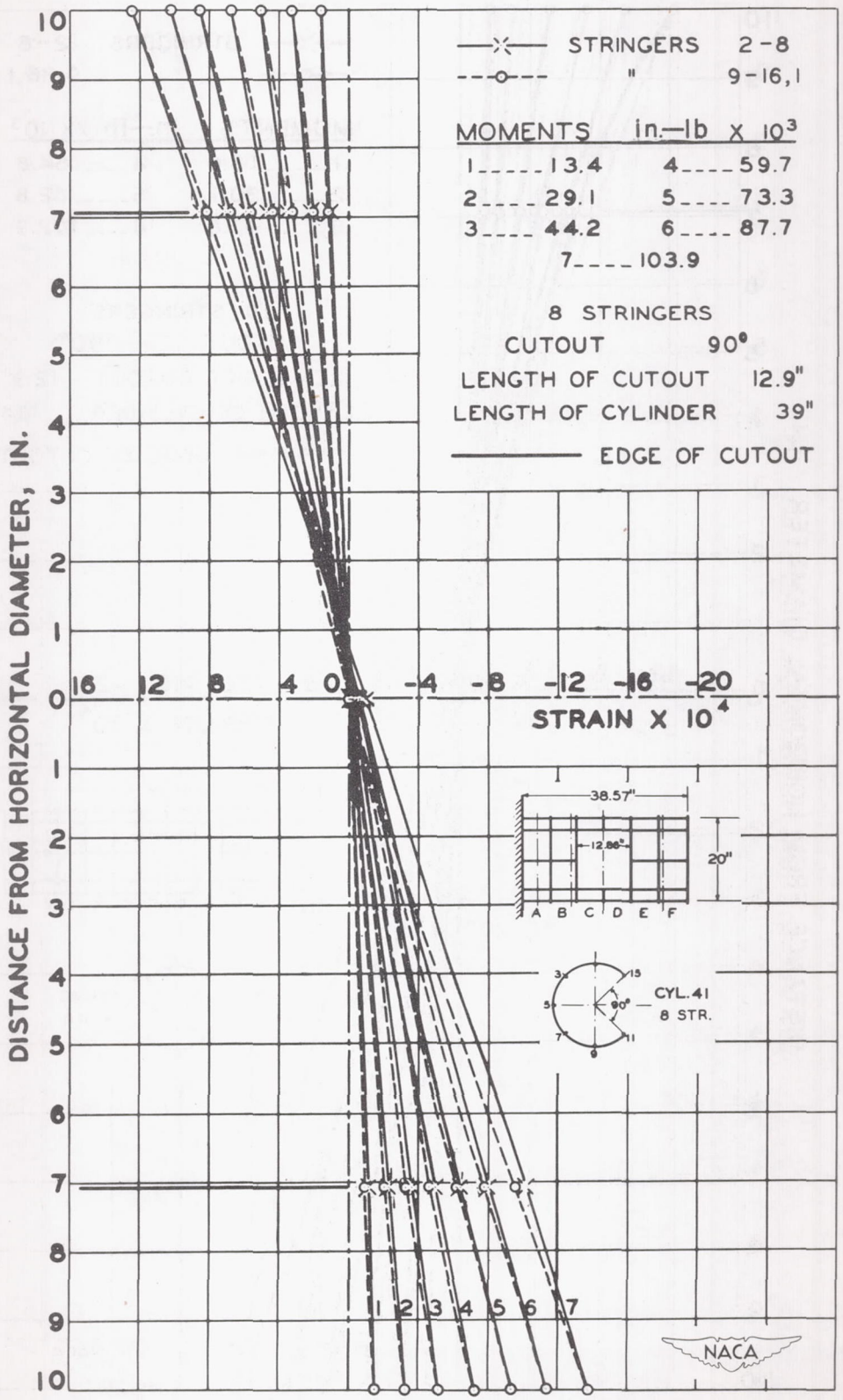

Figure 24.- Strain diagram of cylinder 41. Band F.

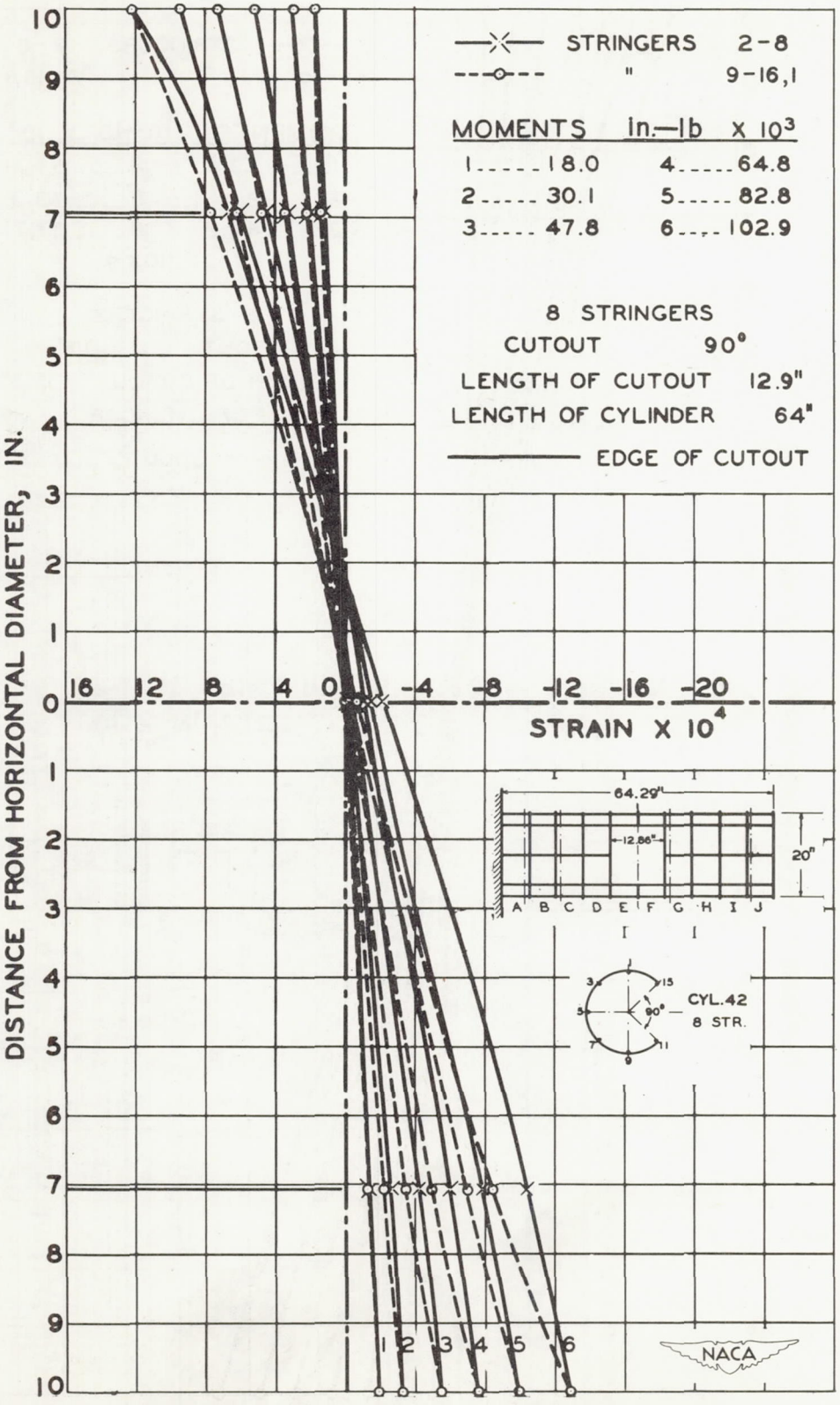

Figure 25.- Strain diagram of cylinder 42. Band A.

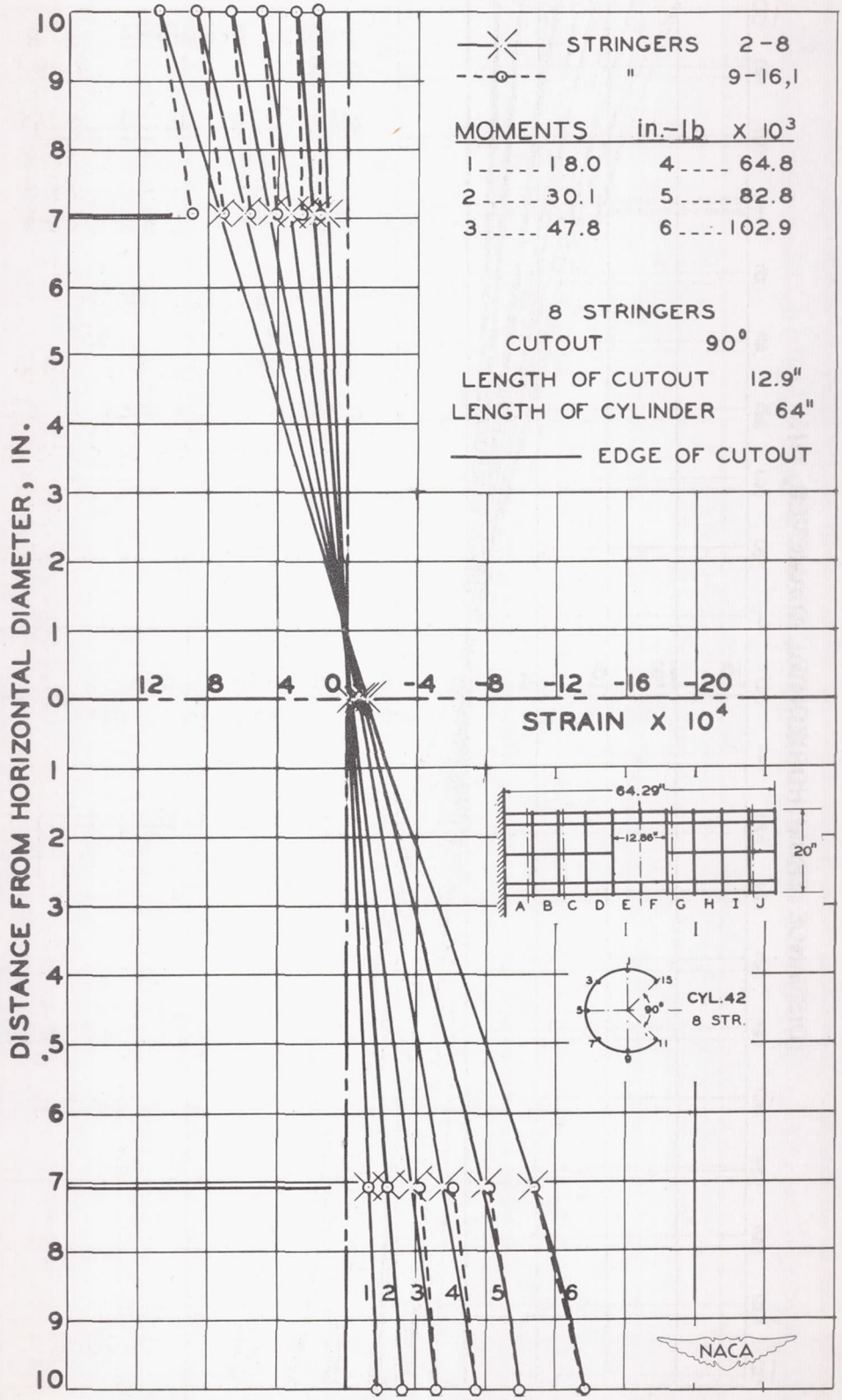

Figure 26.- Strain diagram of cylinder 42. Band F.

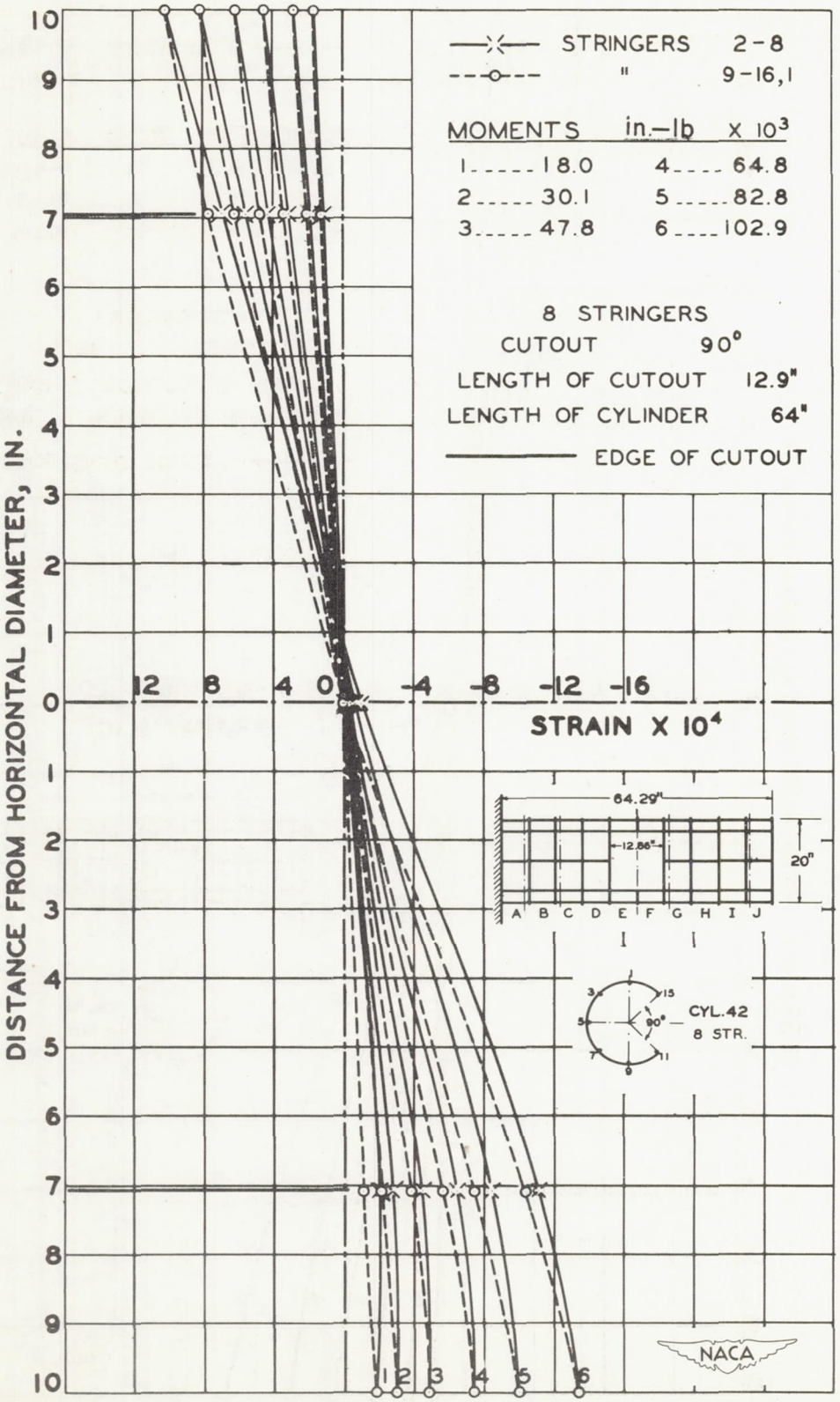

Figure 27.- Strain diagram of cylinder 42. Band G.

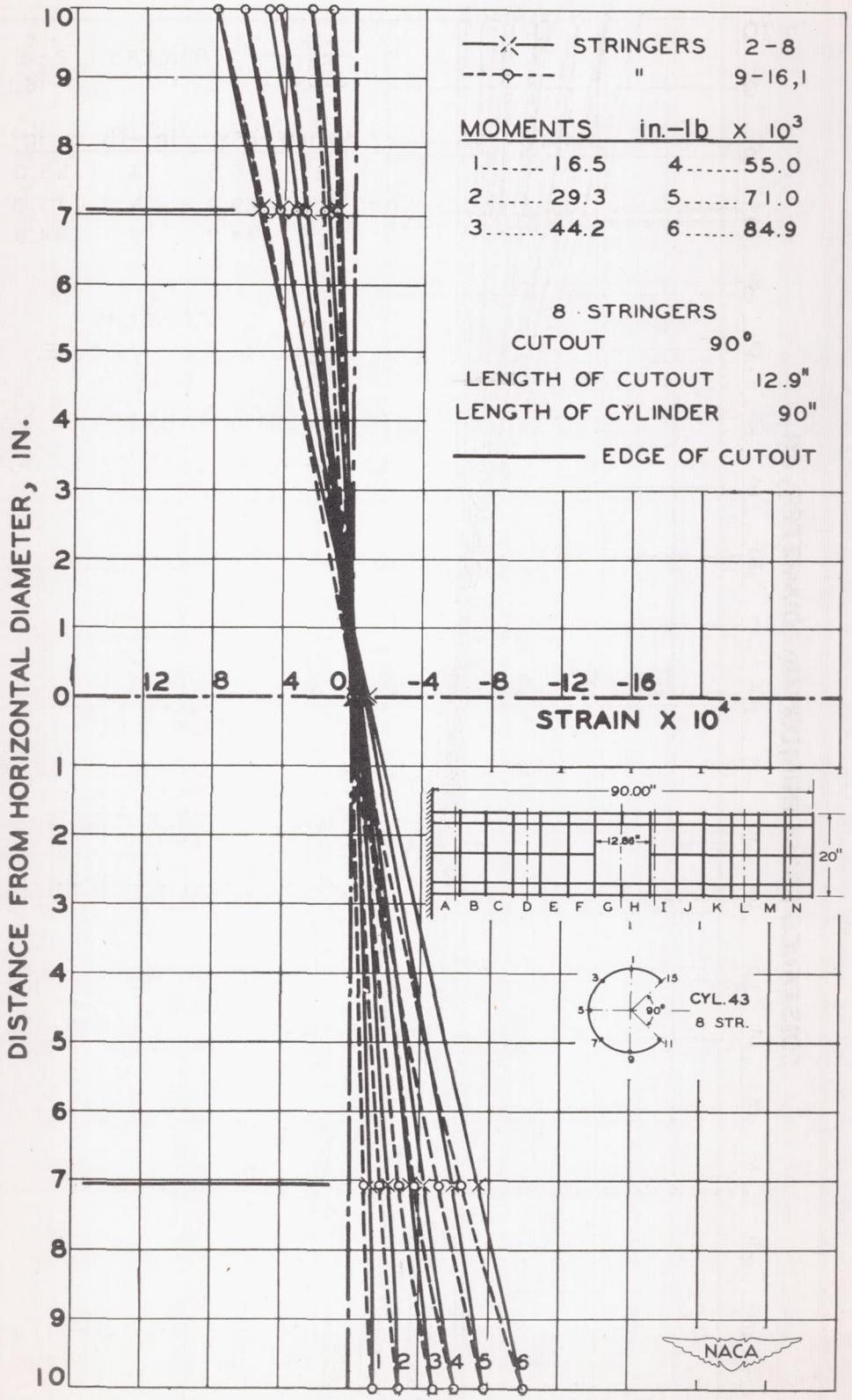

Figure 28.- Strain diagram of cylinder 43. Band D.

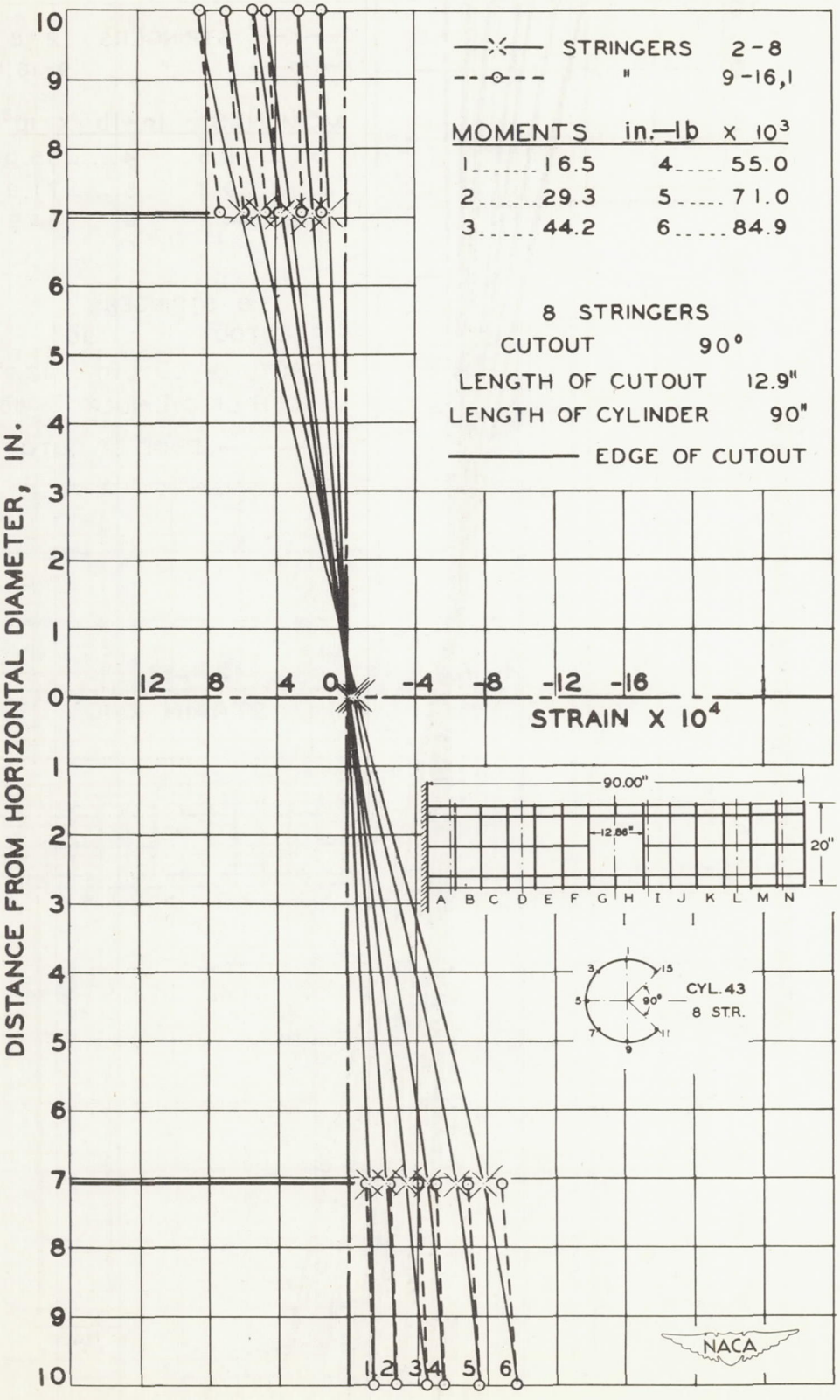

Figure 29.- Strain diagram of cylinder 43. Bands G and H.

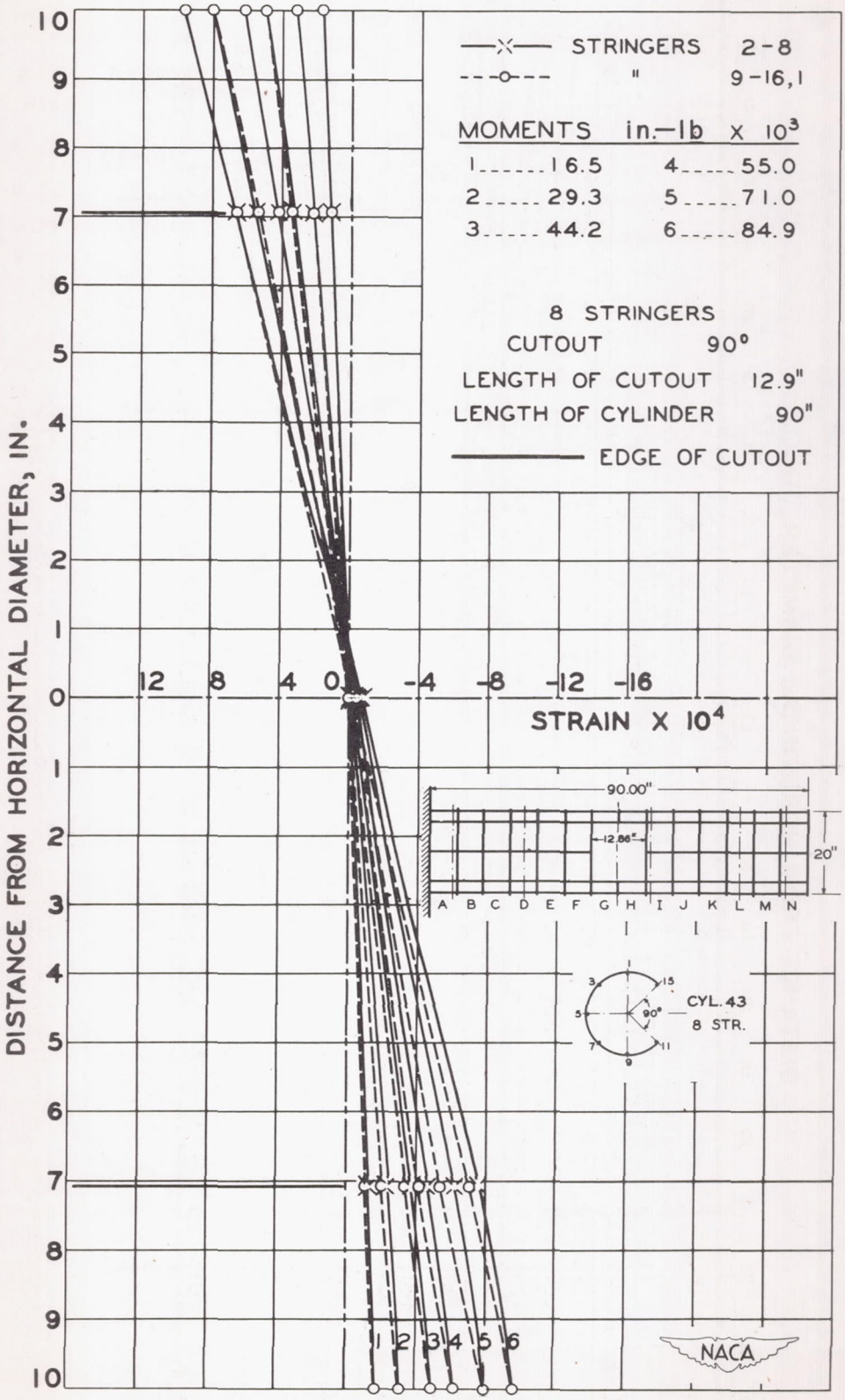

Figure 30.- Strain diagram of cylinder 43. Band N.

BANDS

		C			D			E			F			G			
		ϵ_x	ϵ_c	γ	ϵ_x	ϵ_c	γ	ϵ_x	ϵ_c	γ	ϵ_x	ϵ_c	γ	ϵ_x	ϵ_c	γ	
STR. 16	(A)	118	−29	15	111	−33	−17	–	–	−45	118	−28	−31	125	−36	−32	(A) STR. 16
	(B)	370	−102	50	352	−102	−45	–	–	−29	381	−126	−38	401	−121	−90	(B)
	(C)	719	−215	98	676	−200	−29	–	–	−14	648	−214	−9	673	−214	−141	(C)
STR. 2	(D)	860	−260	99	814	−242	−24	–	–	−2	762	−244	−14	785	−251	−159	(D) STR. 2
	(A)	13	−4	−2										13	−3	3	(A)
	(B)	42	−16	−9										35	−13	−9	(B)
	(C)	59	−30	−39										64	−26	30	(C)
STR. 4	(D)	59	−34	71										75	−34	42	(D) STR. 4
	(A)	−1	0.4	3													(A)
	(B)	−7	−0.4	8													(B)
	(C)	−13	−3	6													(C)
STR. 6	(D)	−20	−7	−12													(D) STR. 6

ROWS (A) $M = 11{,}300$ in.-lb
ROWS (B) $M = 36{,}000$ in.-lb
ROWS (C) $M = 63{,}300$ in.-lb
ROWS (D) $M = 76{,}100$ in.-lb
ALL STRAINS TO BE MULTIPLIED BY 10^{-6}

NACA

Figure 31.- Strains calculated from rosette data. Cylinder 40.

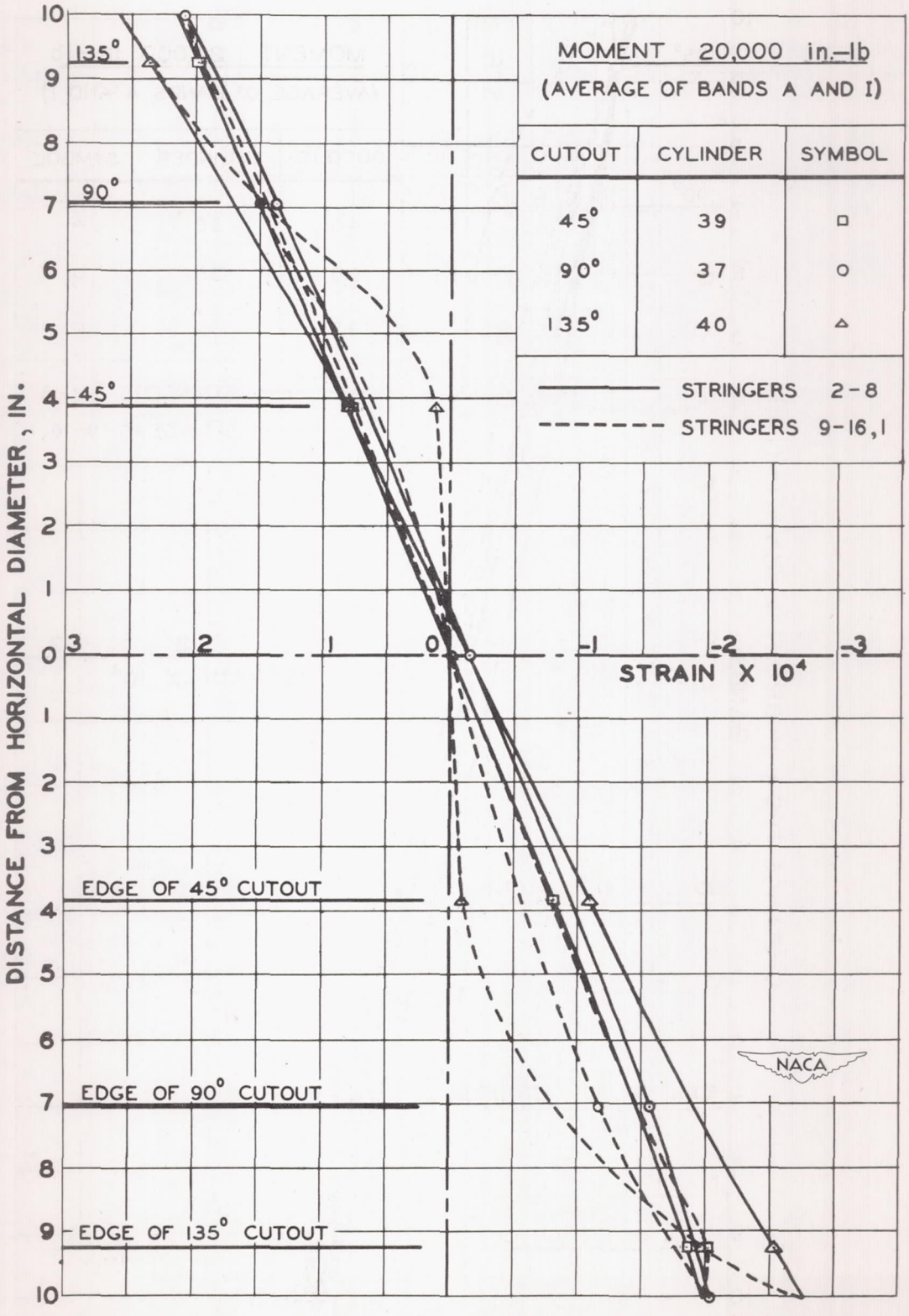

Figure 32.- Effect of size of cutout on strain distribution. 8 stringers. End bands.

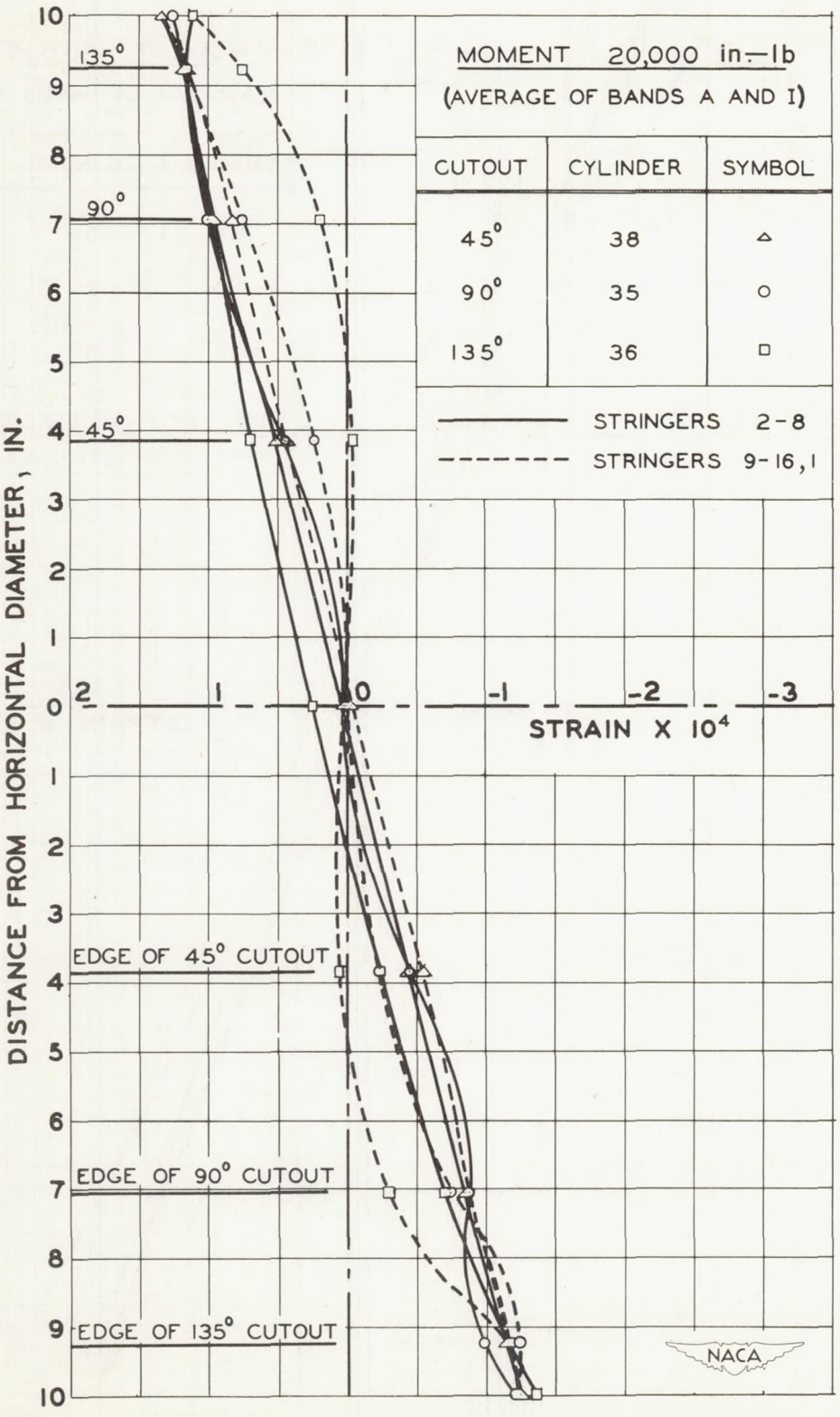

Figure 33.- Effect of size of cutout on strain distribution. 16 stringers. End bands.

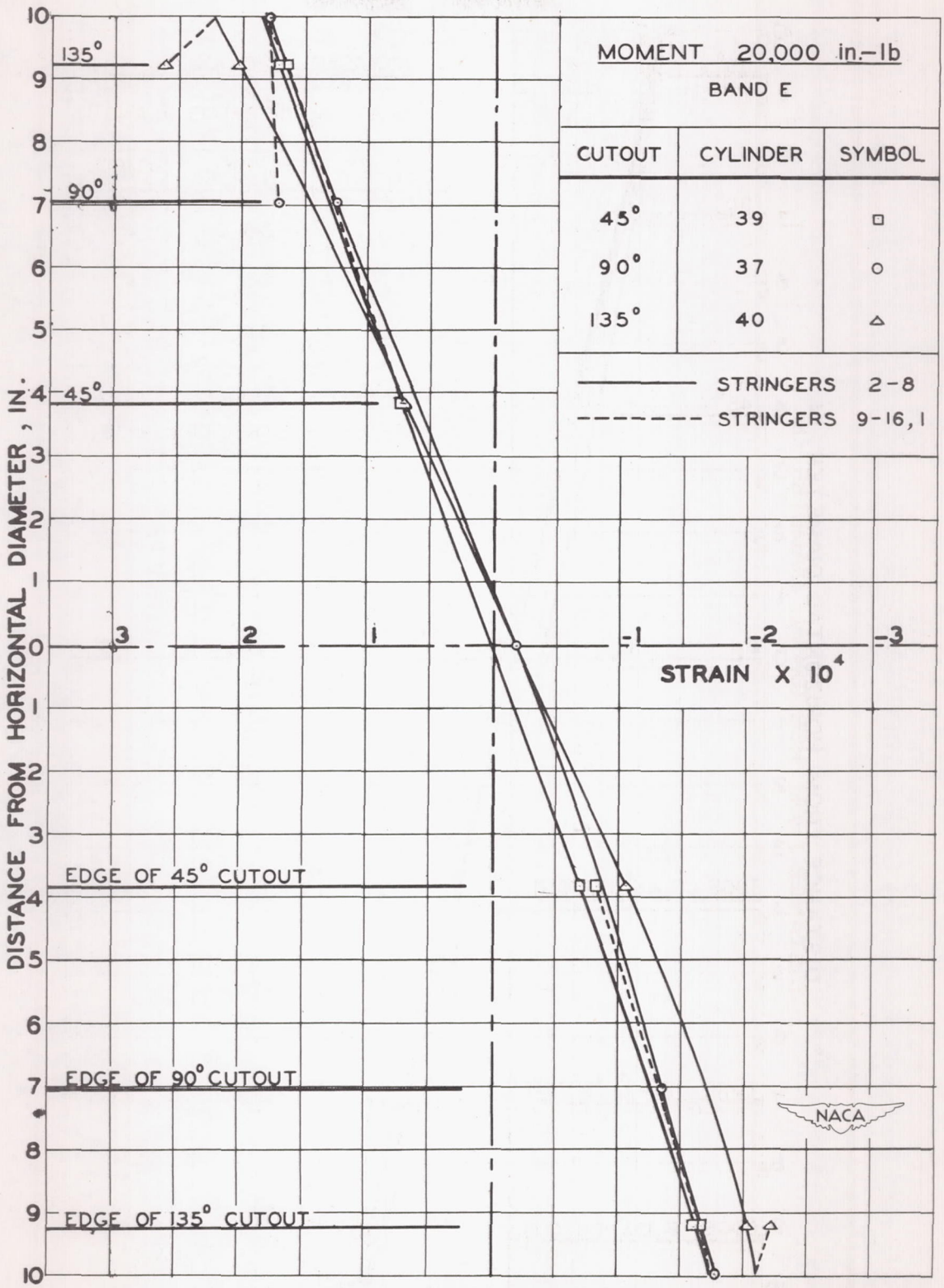

Figure 34.- Effect of size of cutout on strain distribution. 8 stringers. Middle bands.

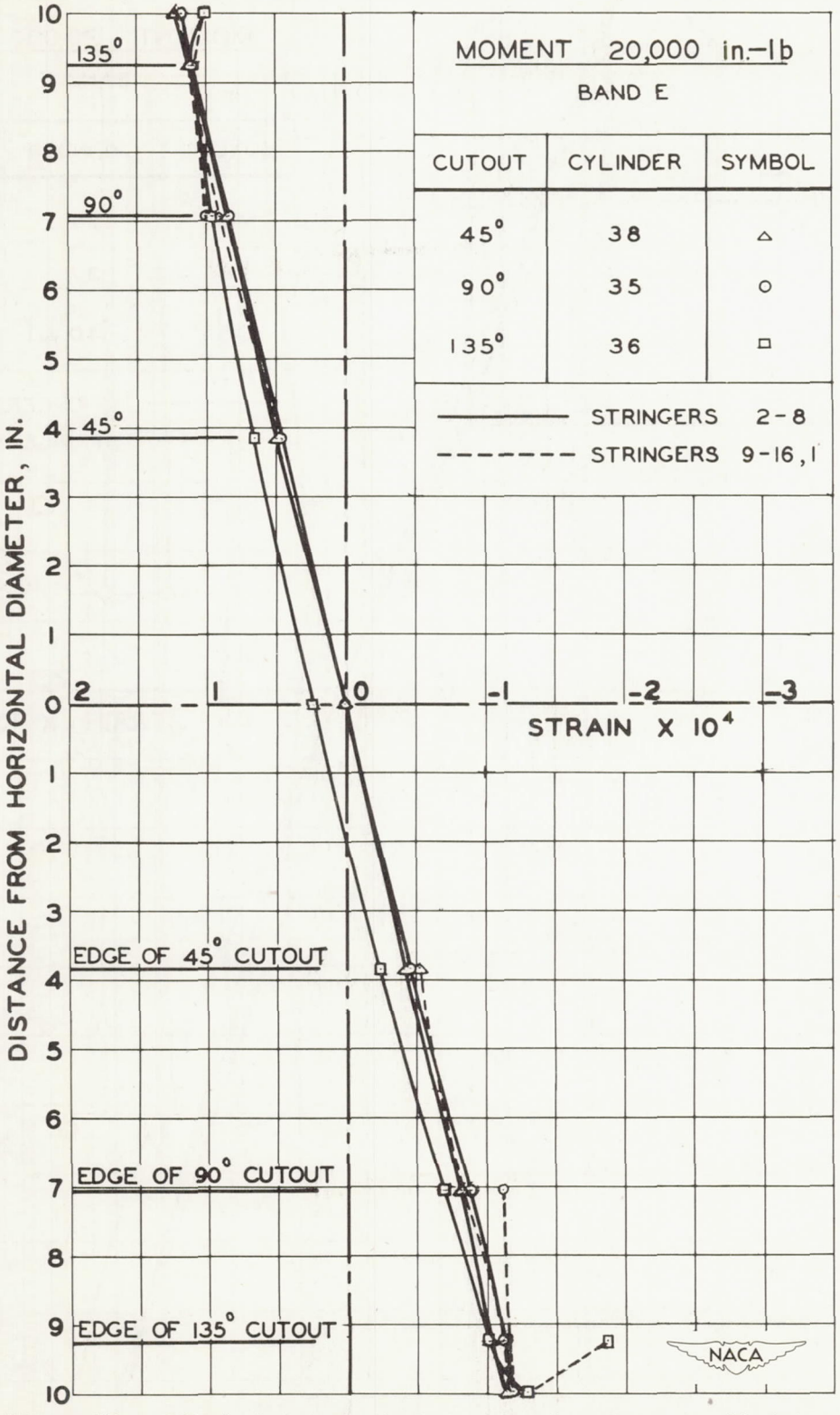

Figure 35.- Effect of size of cutout on strain distribution. 16 stringers. Middle bands.

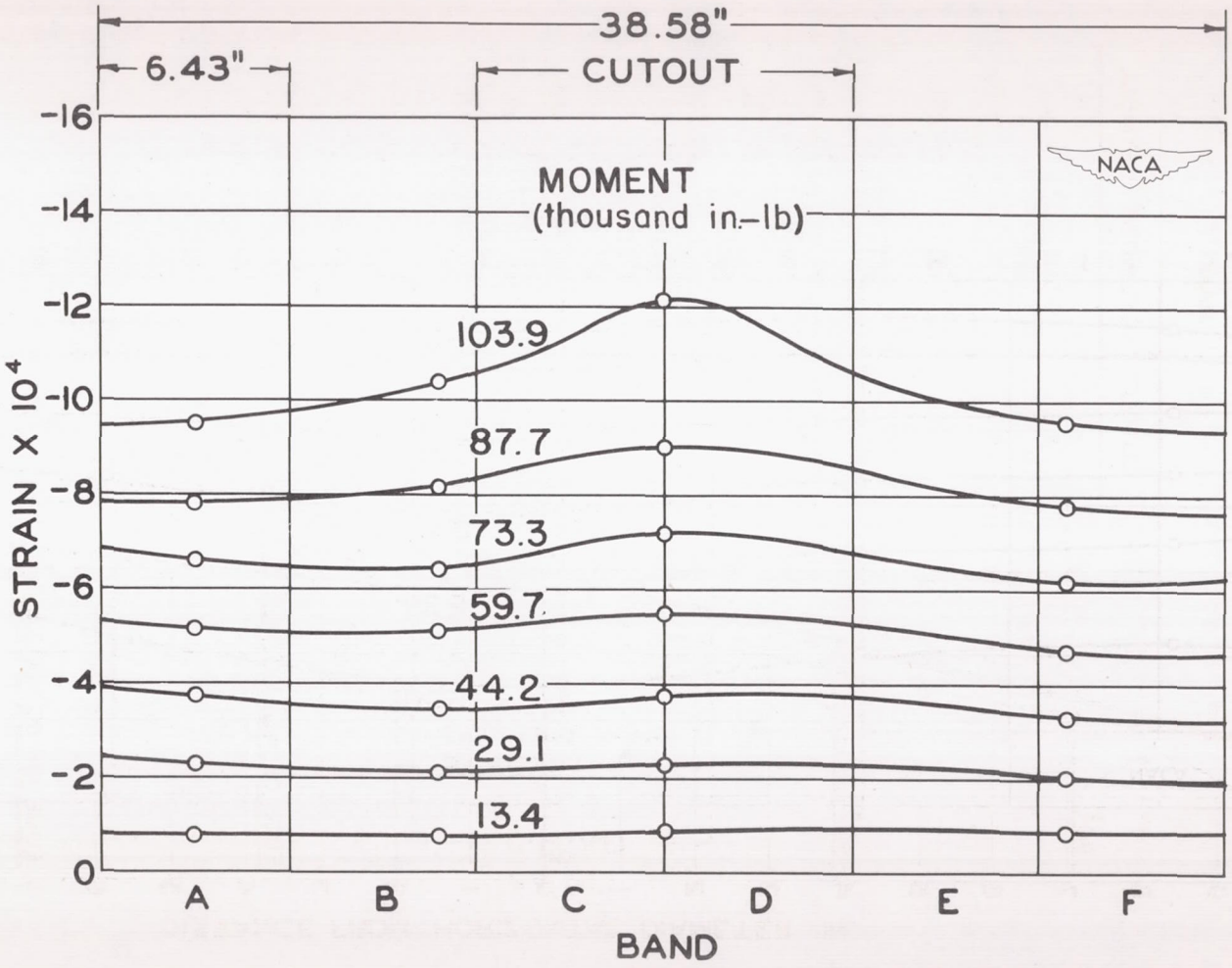

Figure 36.- Strain variation along stringer 11. Cylinder 41.

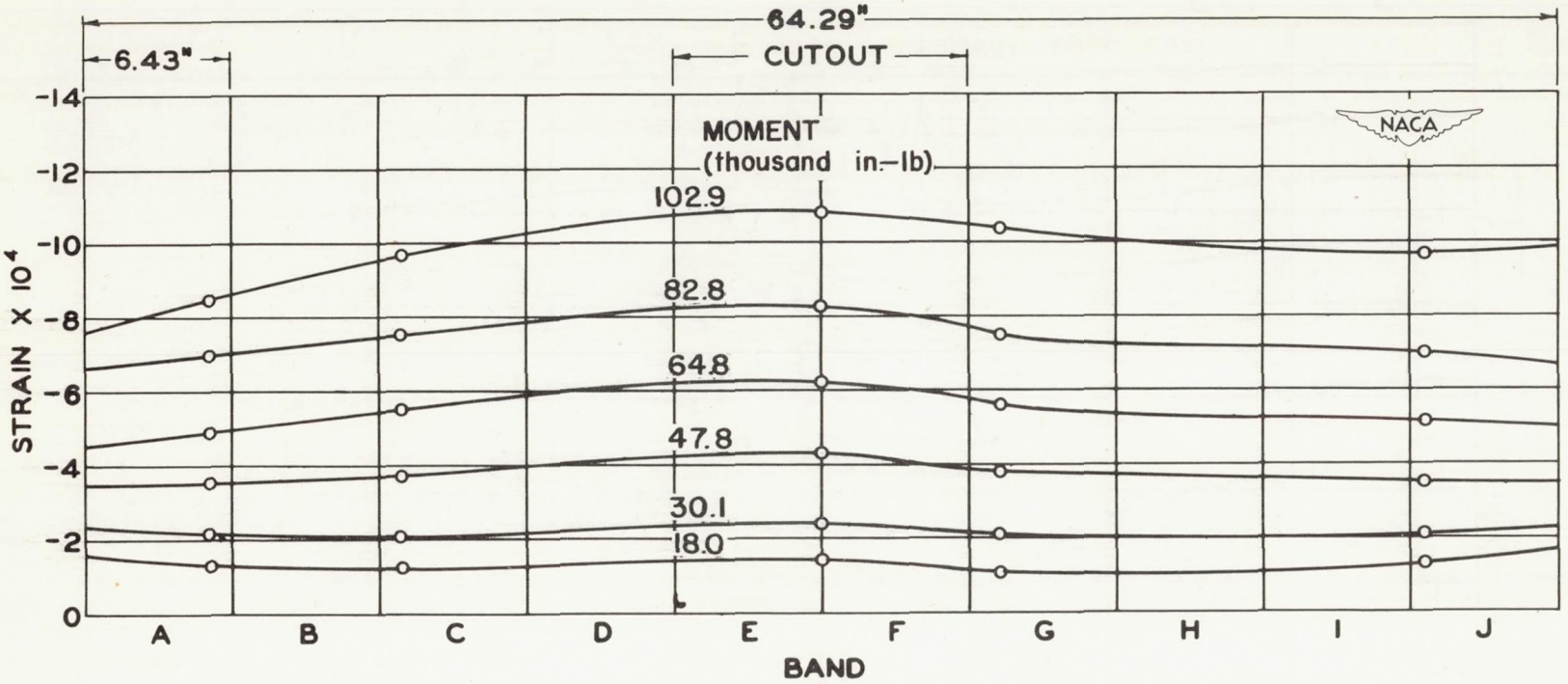

Figure 37.- Strain variation along stringer 11. Cylinder 42.

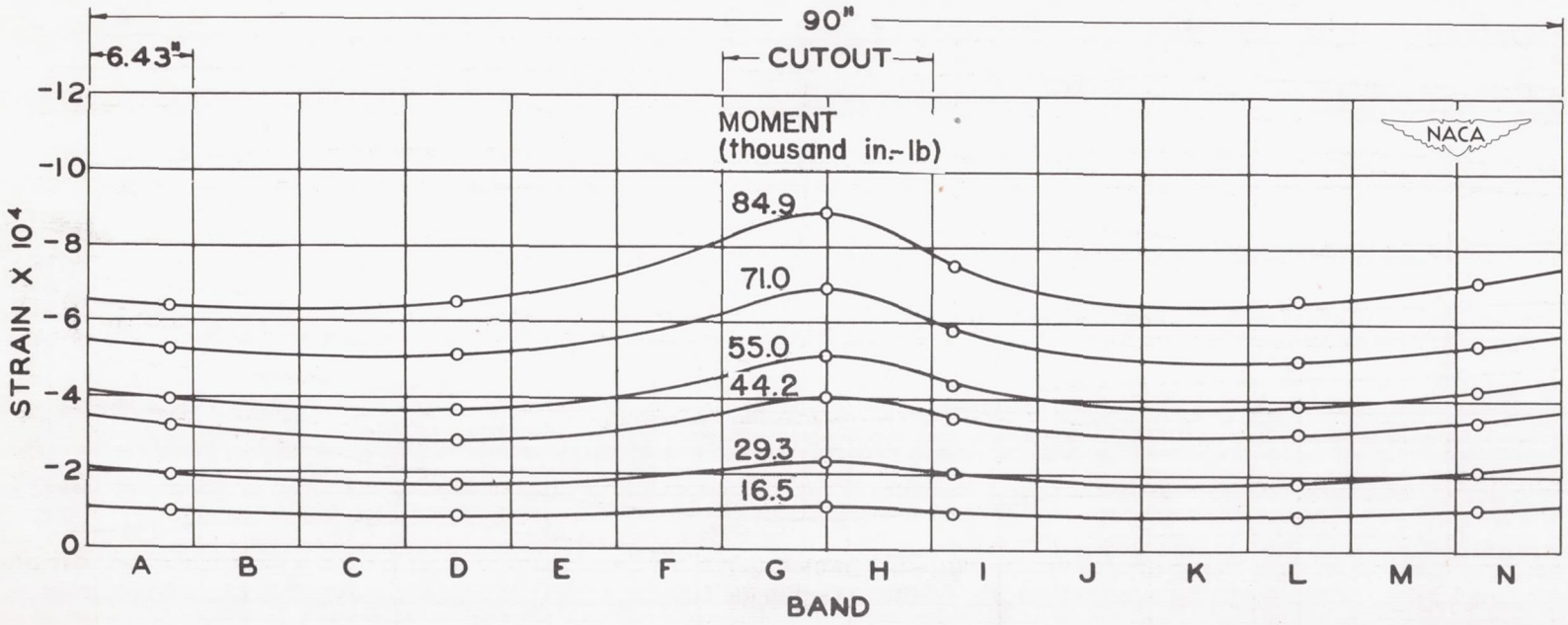

Figure 38.- Strain variation along stringer 11. Cylinder 43.

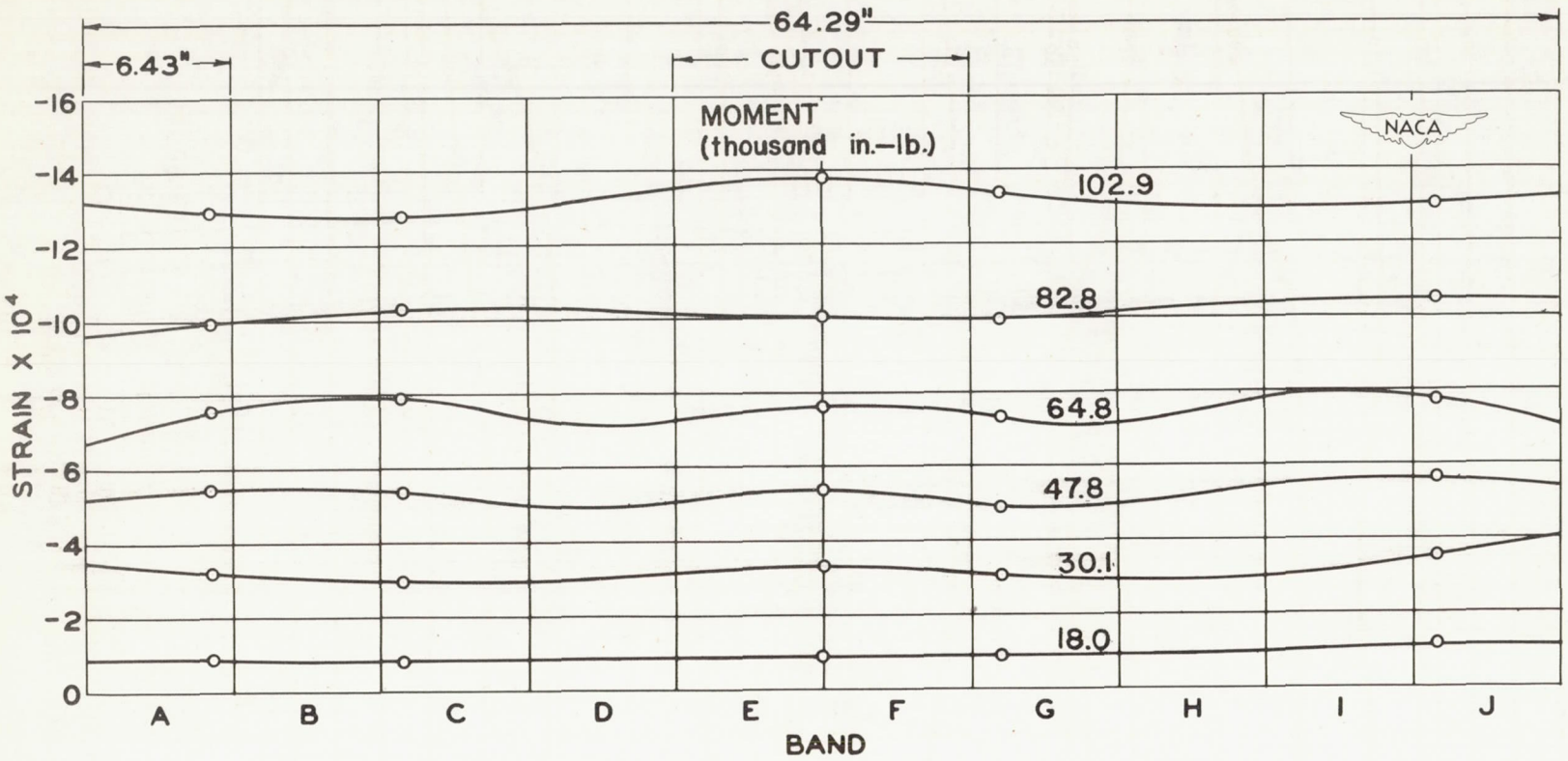

Figure 39.- Strain variation along stringer 9. Cylinder 42.

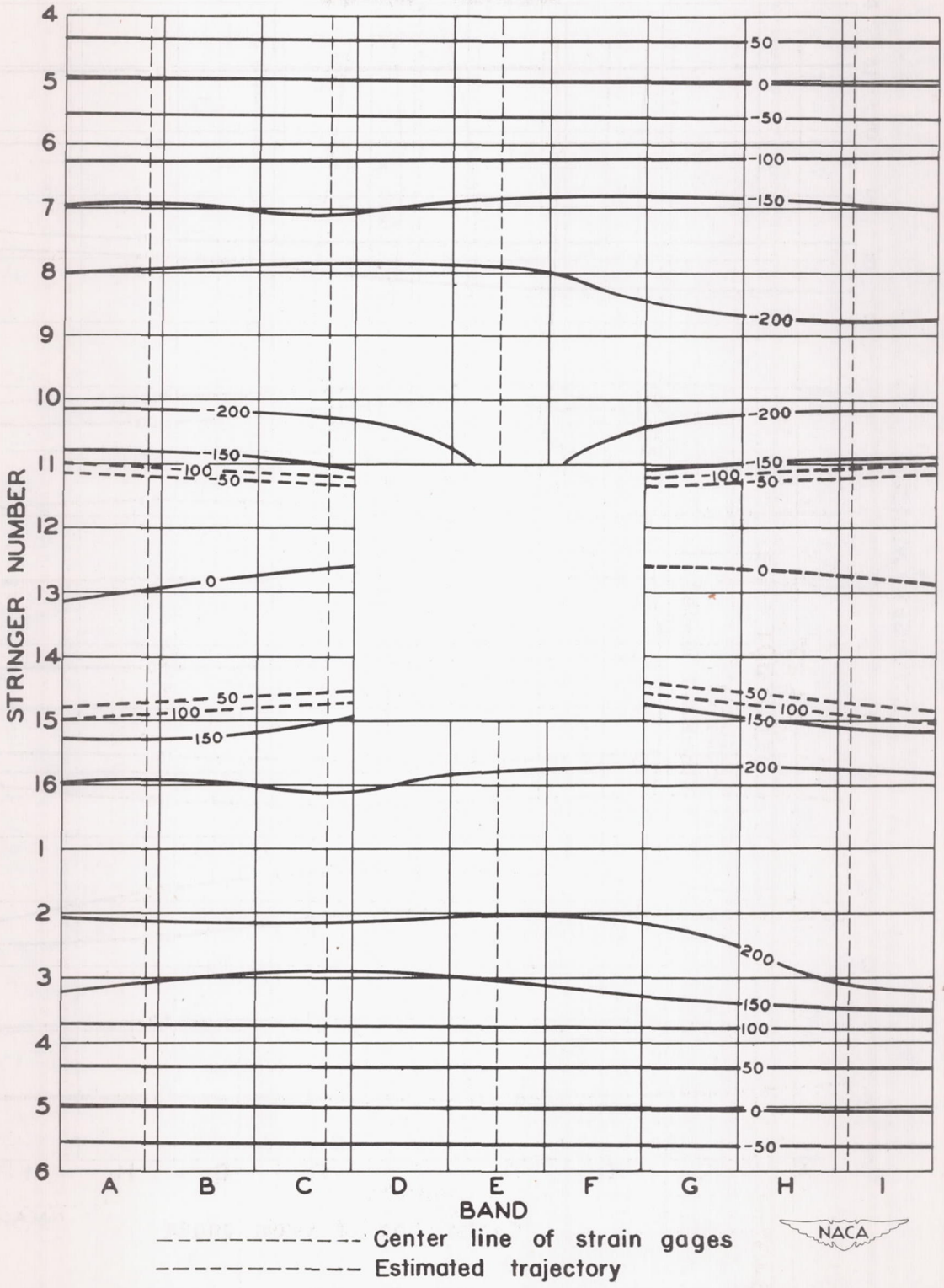

Figure 40.- Strain trajectories for cylinder 35. Moment, 36,200 inch-pounds. Values of strain to be multiplied by 10^{-6}.

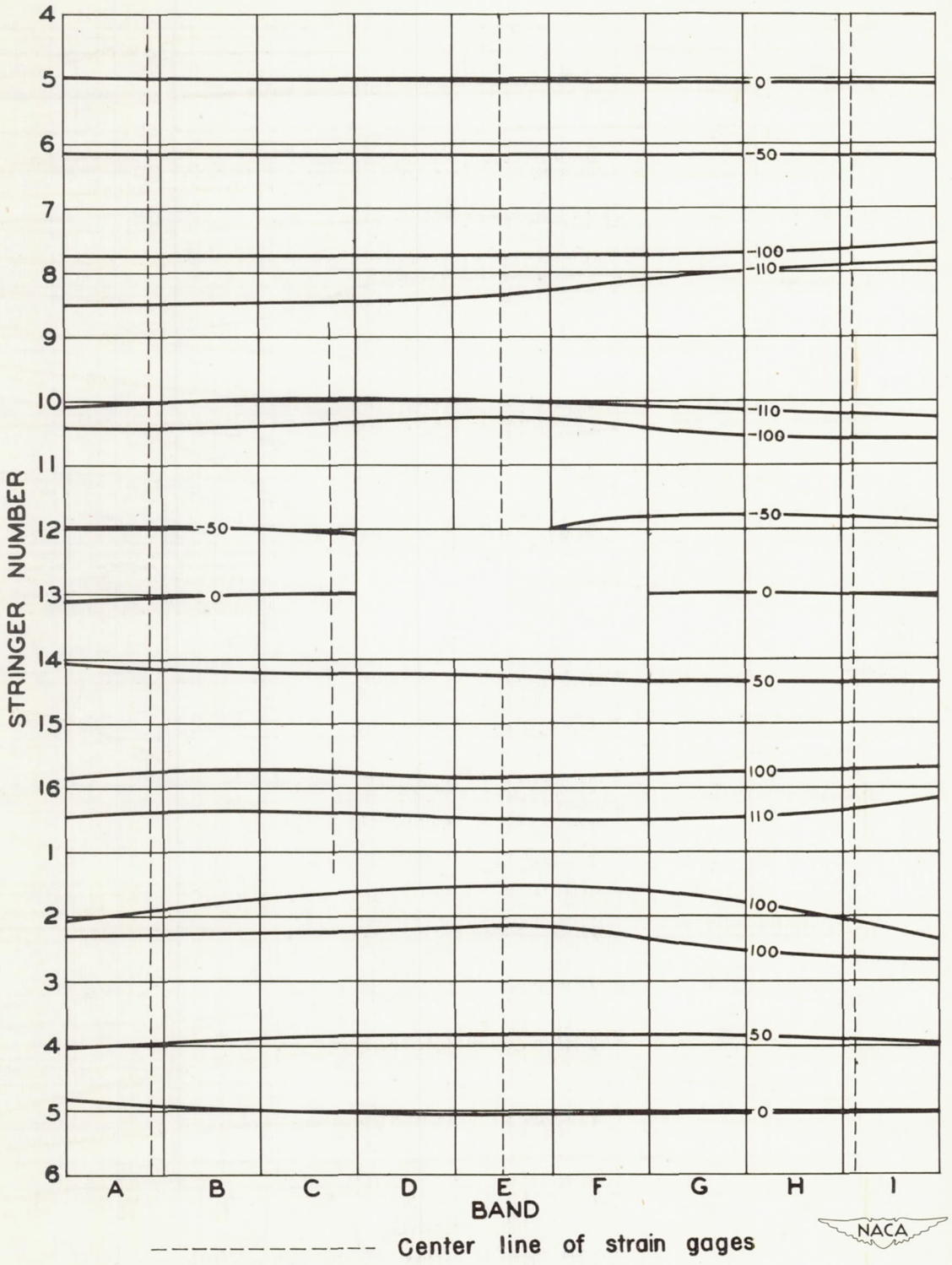

Figure 41.- Strain trajectories for cylinder 38. Moment, 20,000 inch-pounds. Values of strain to be multiplied by 10^{-6}.

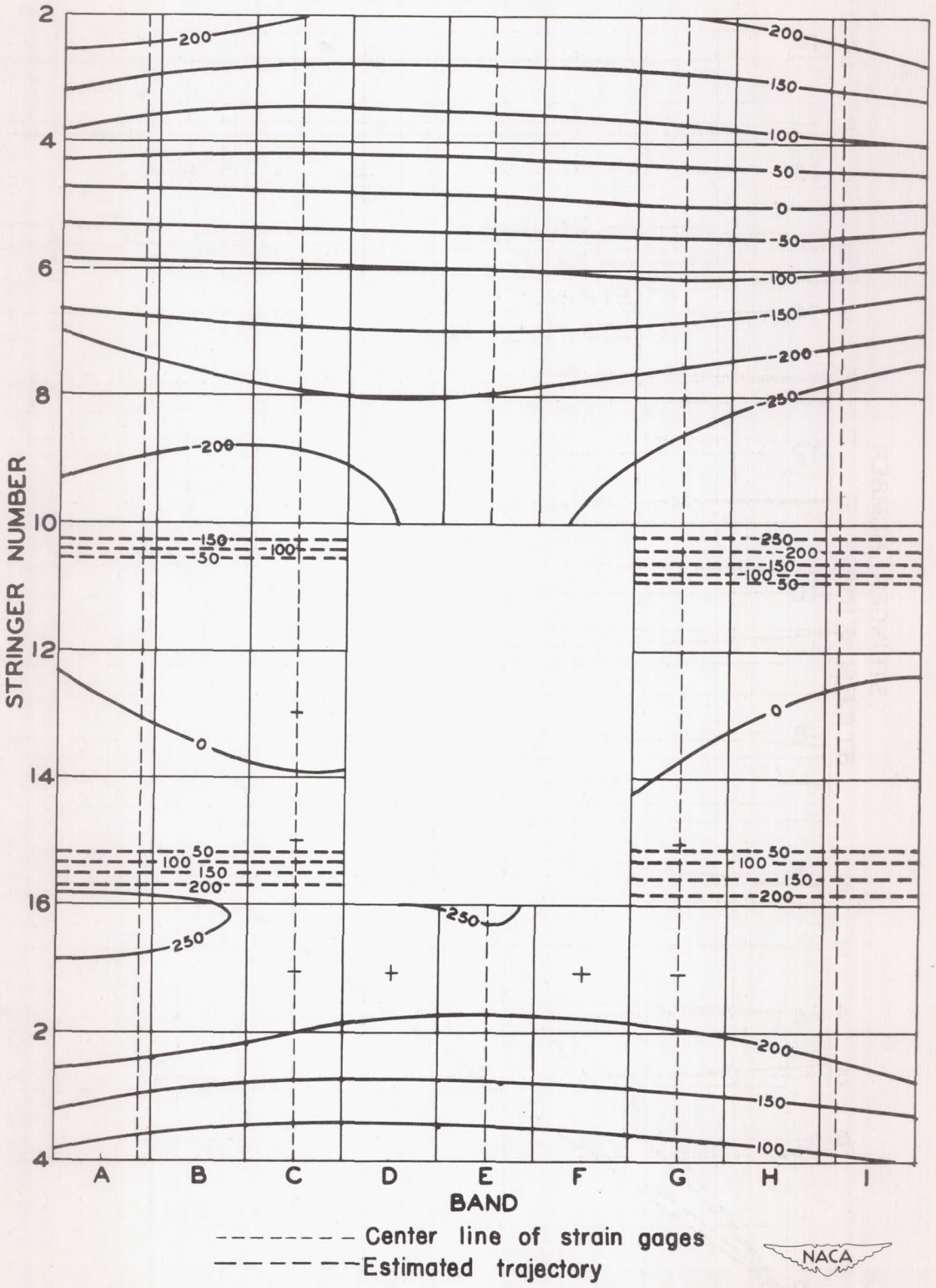

Figure 42.- Strain trajectories for cylinder 40. Moment, 20,000 inch-pounds. Values of strain to be multiplied by 10^{-6}.

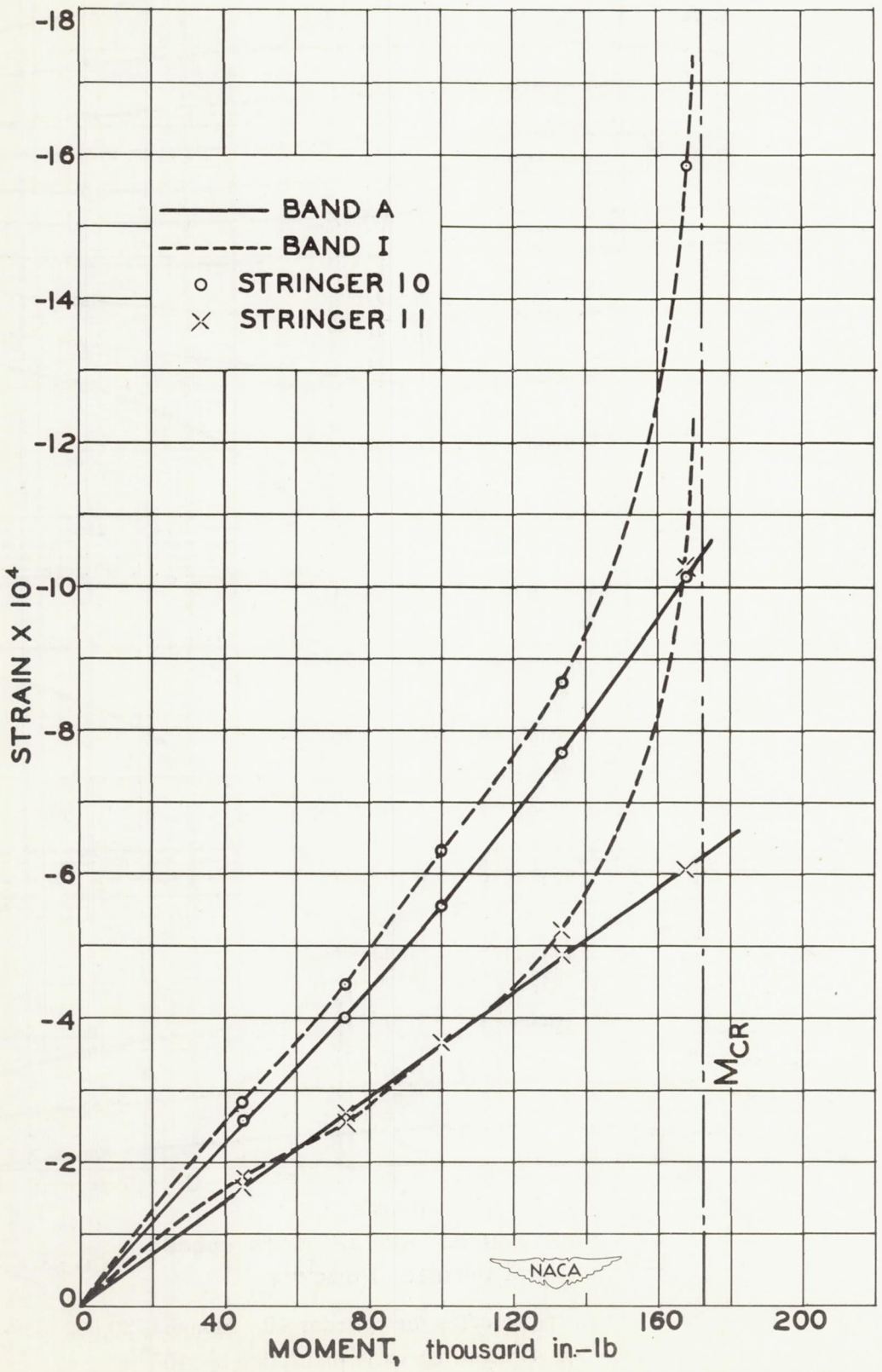

Figure 43.- Stringer strain variation with moment. Cylinder 35. End bands.

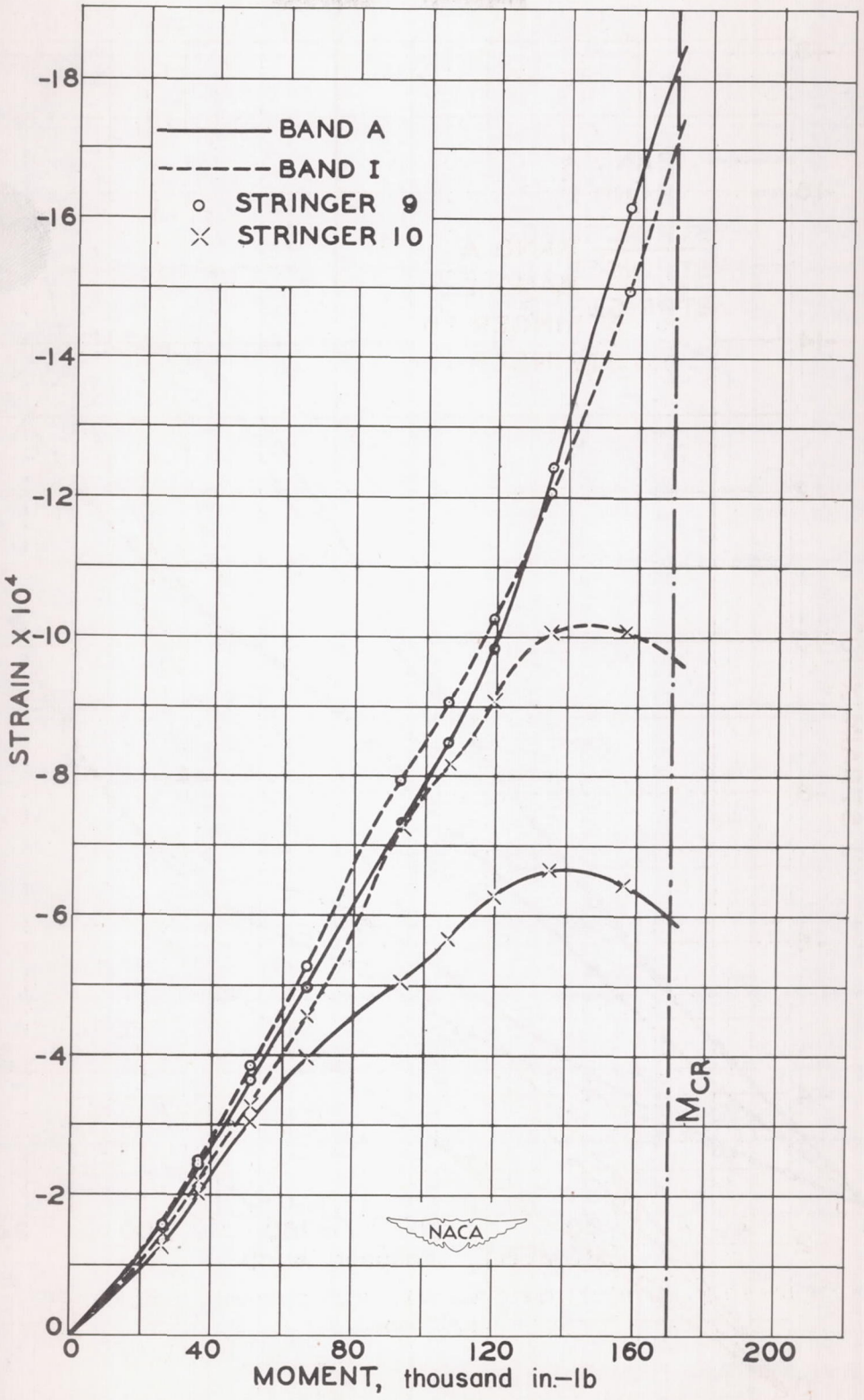

Figure 44.- Stringer strain variation with moment. Cylinder 36. End bands.

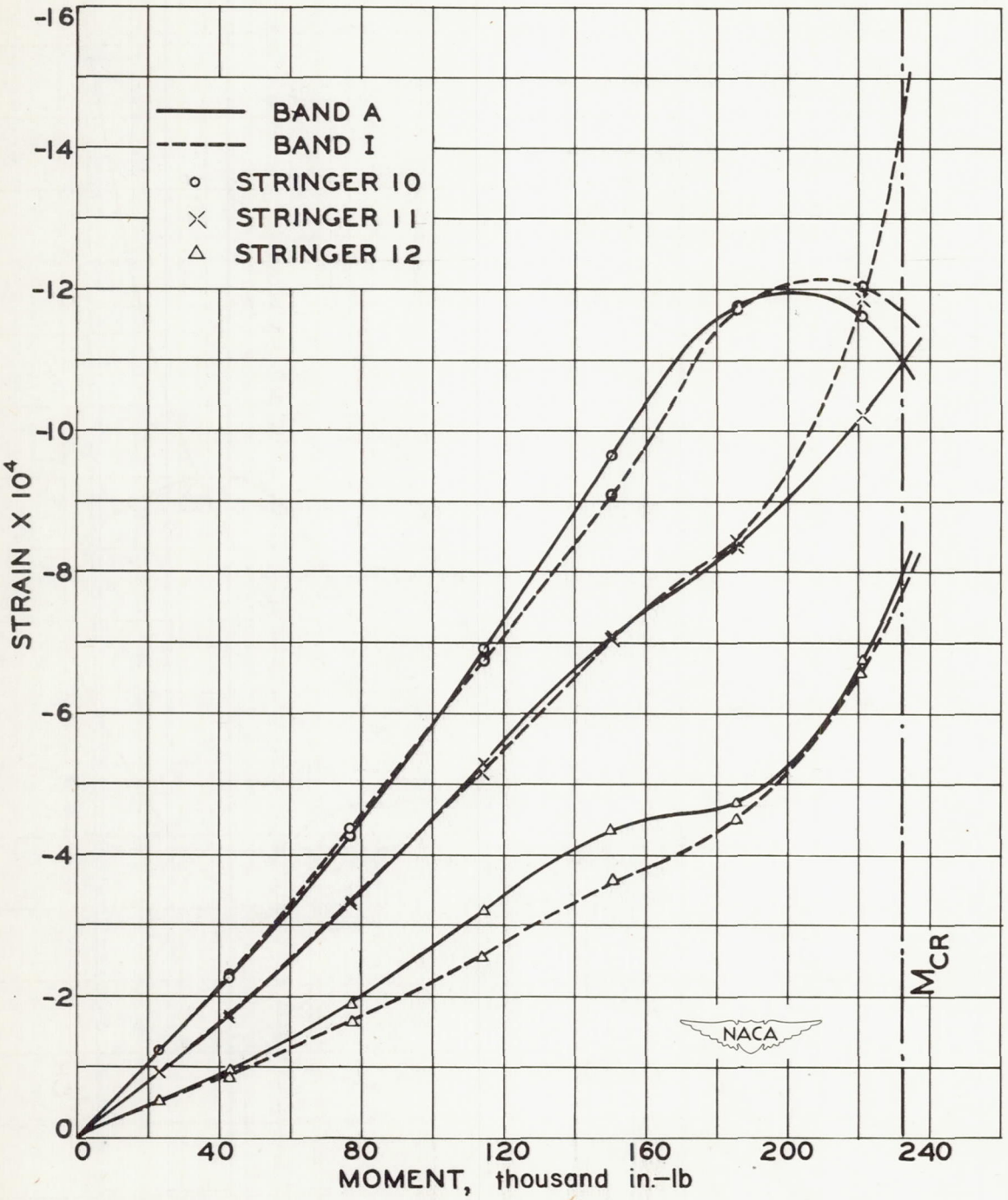

Figure 45.- Stringer strain variation with moment. Cylinder 38. End bands.

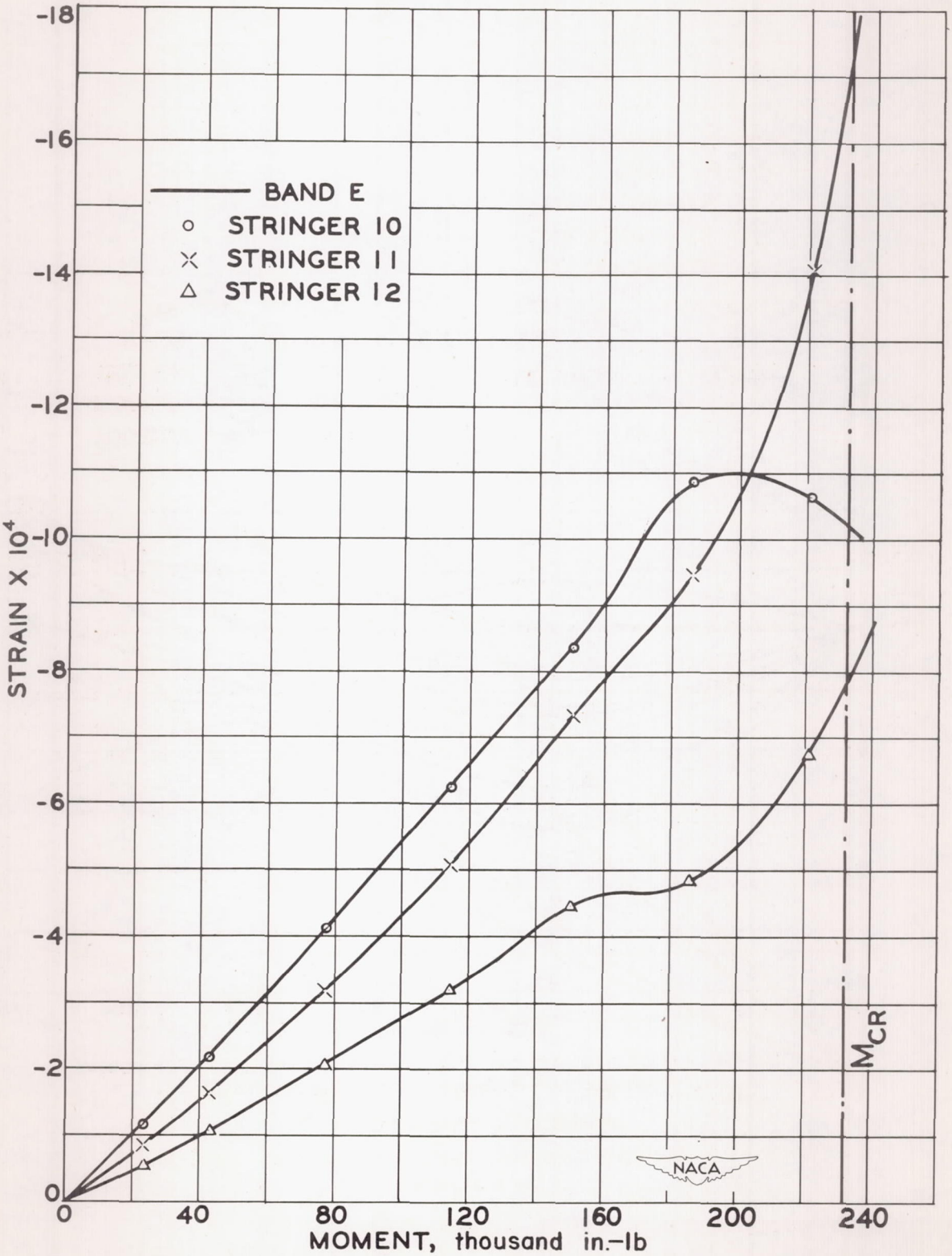

Figure 46.- Stringer strain variation with moment. Cylinder 38. Middle band.

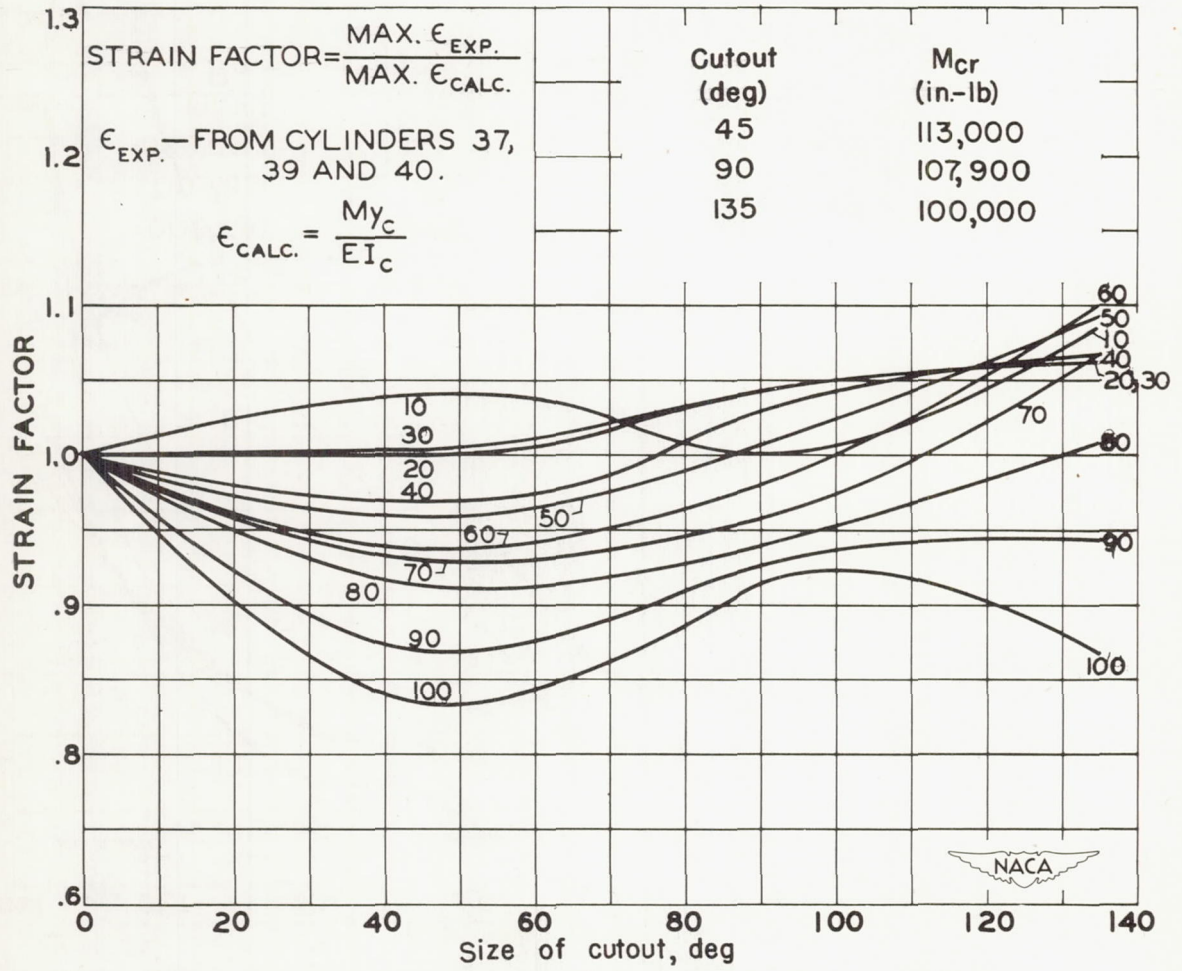

Figure 47.- Strain factors for cylinders with 8 stringers. Percentage of maximum moment indicated on curves.

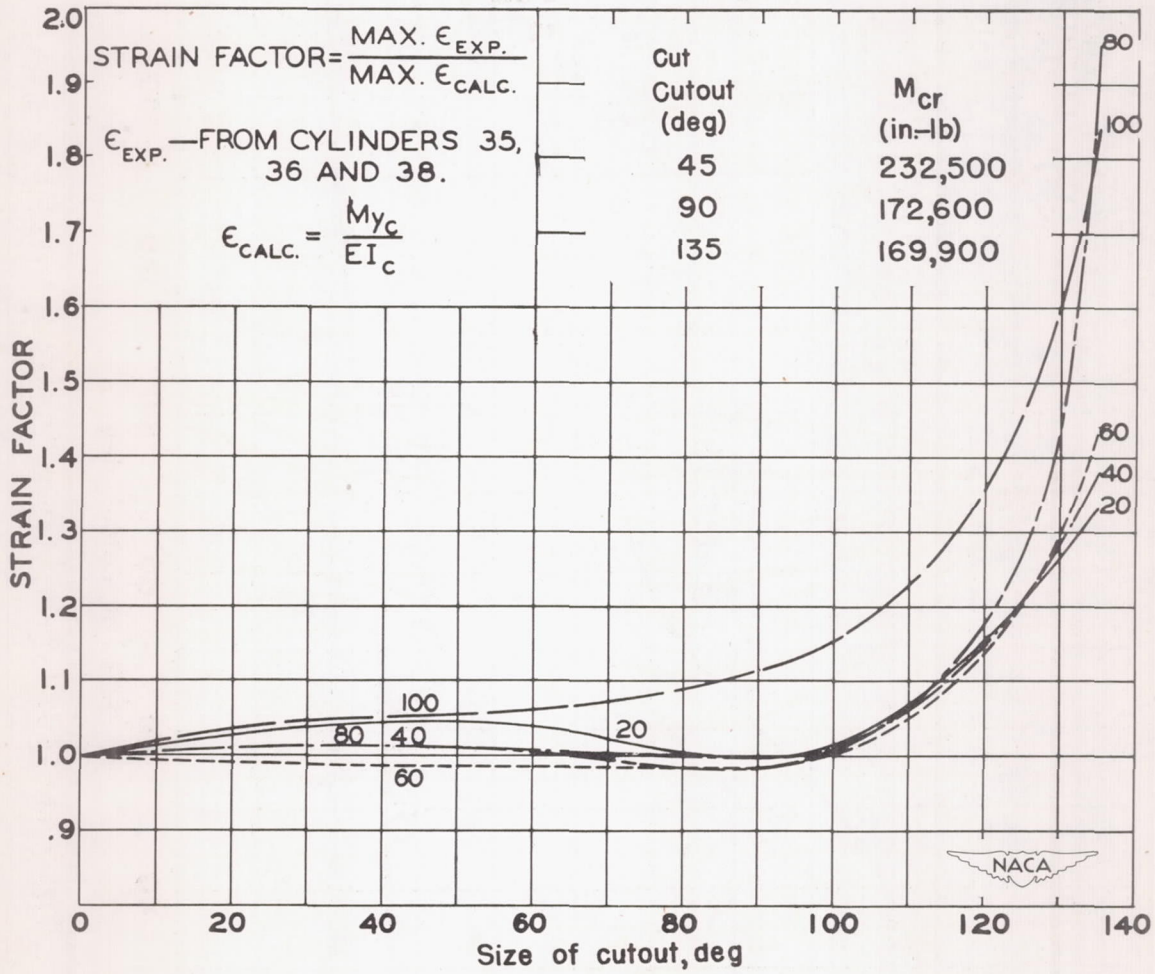

Figure 48.- Strain factors for cylinders with 16 stringers. Percentage of maximum moment indicated on curves.

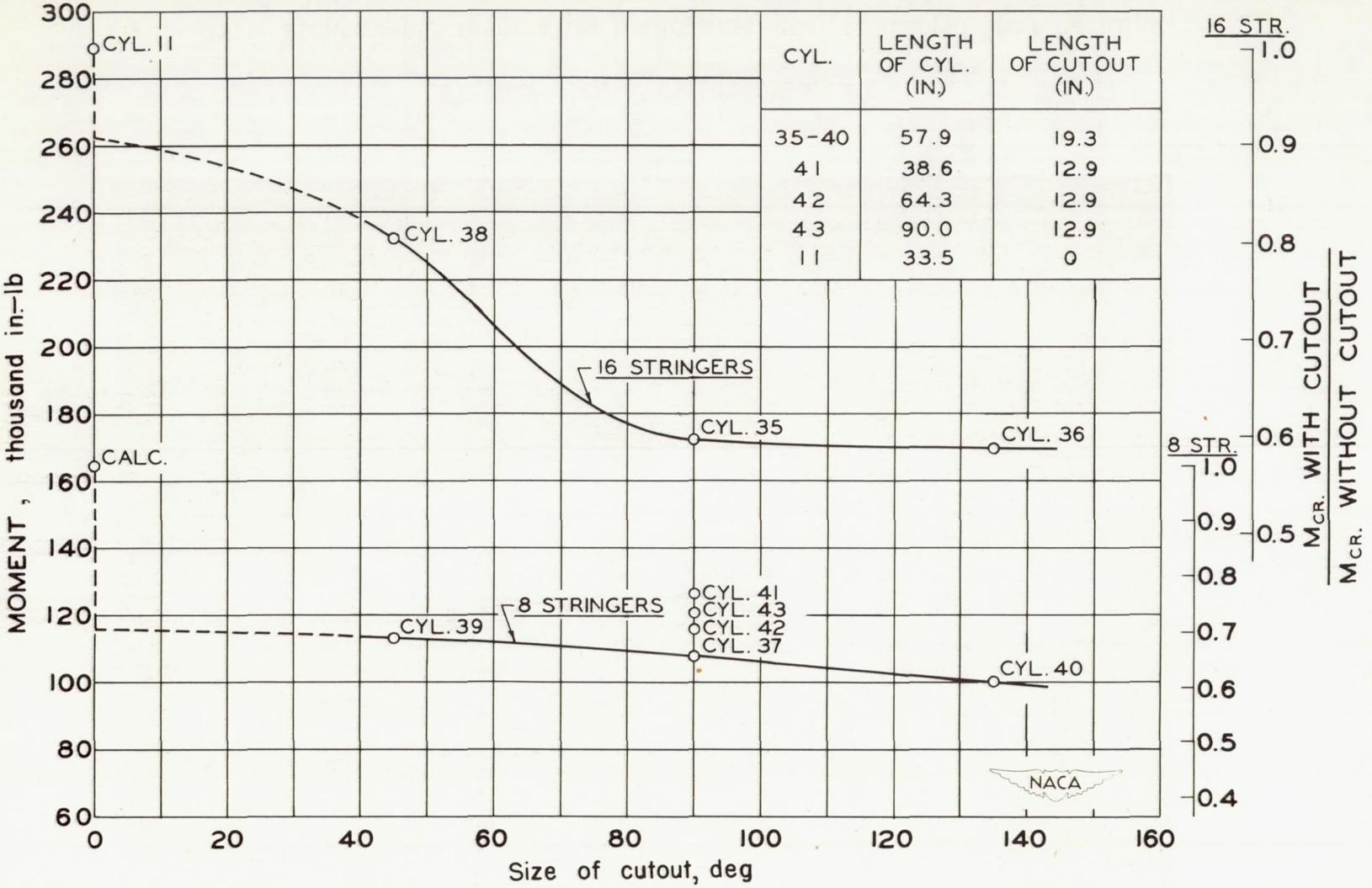

Figure 49.- Effect of size of cutout on critical moment.

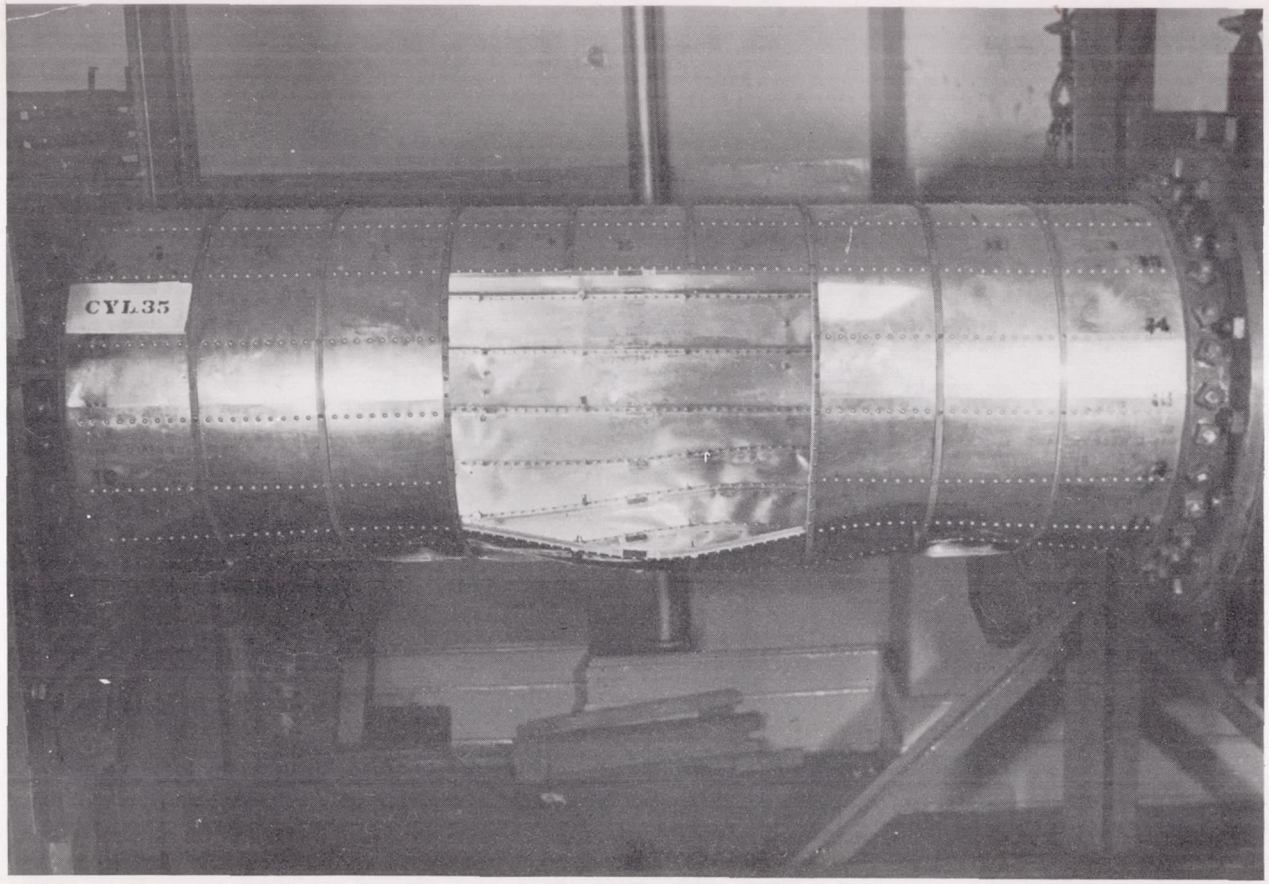

(a) Side view of cylinder 35.

Figure 50.- Photographs taken after loading had been continued after buckling.

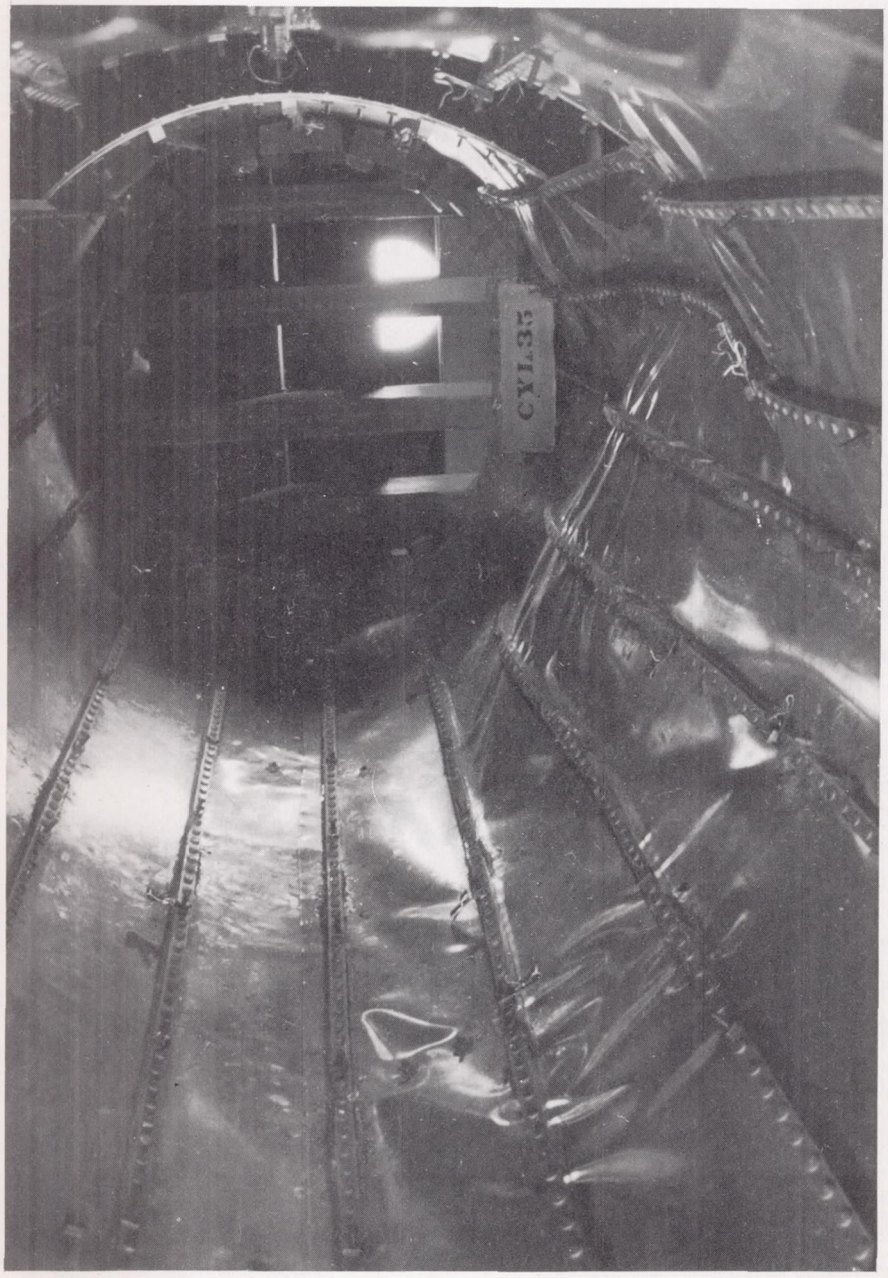

(b) Inside view of cylinder 35.

Figure 50.- Continued.

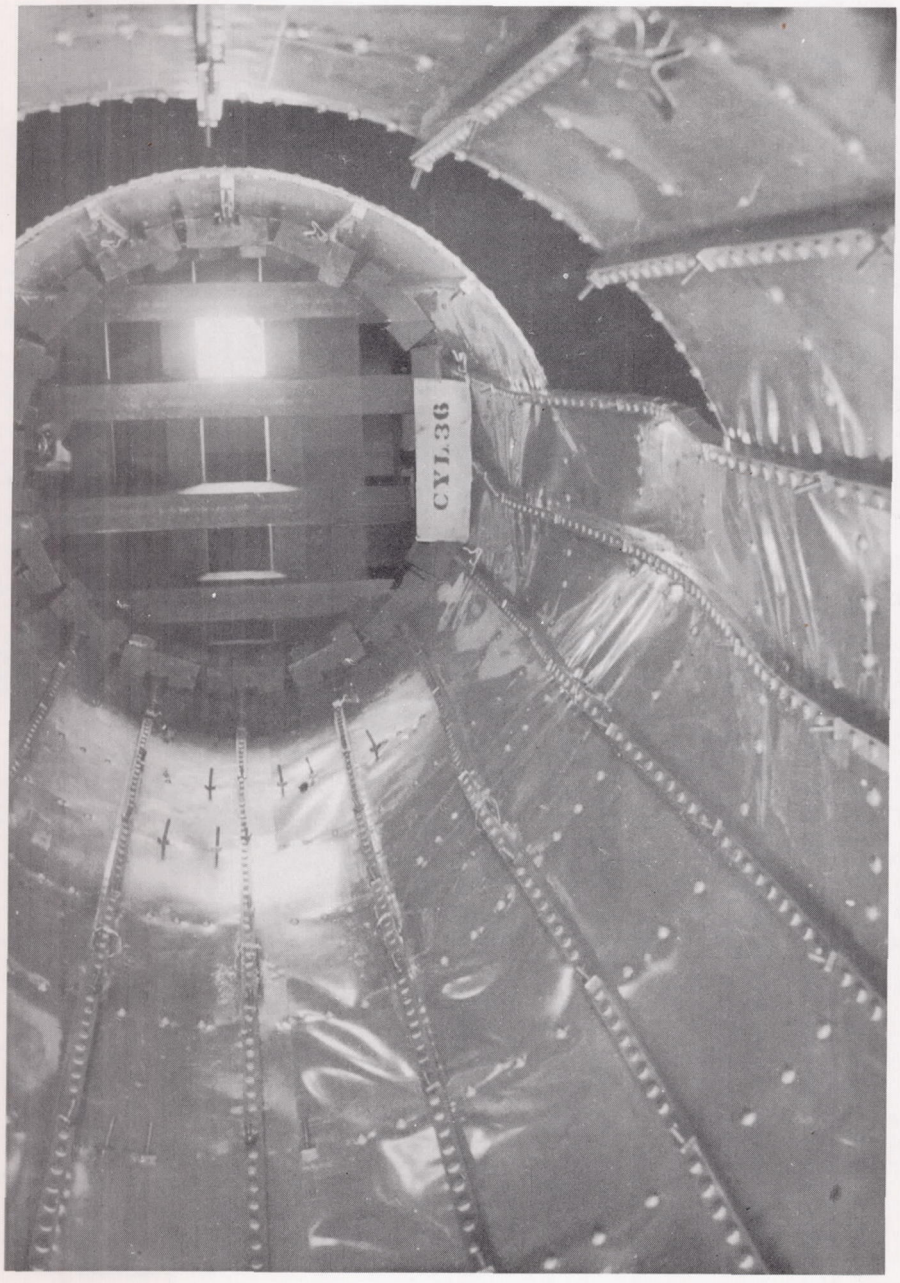

(c) Inside view of cylinder 36.

Figure 50.- Continued.

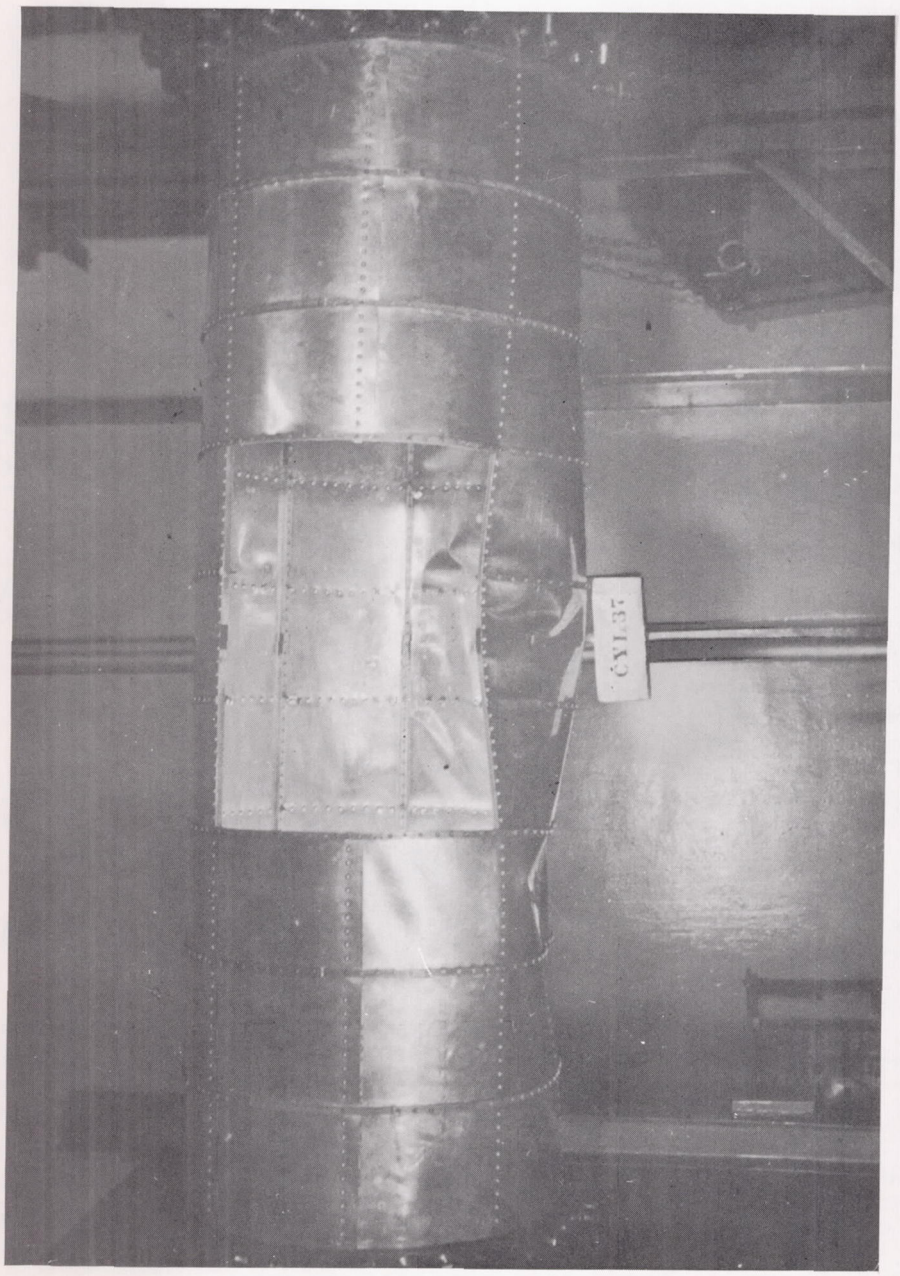

(d) Side view of cylinder 37.

Figure 50.- Continued.

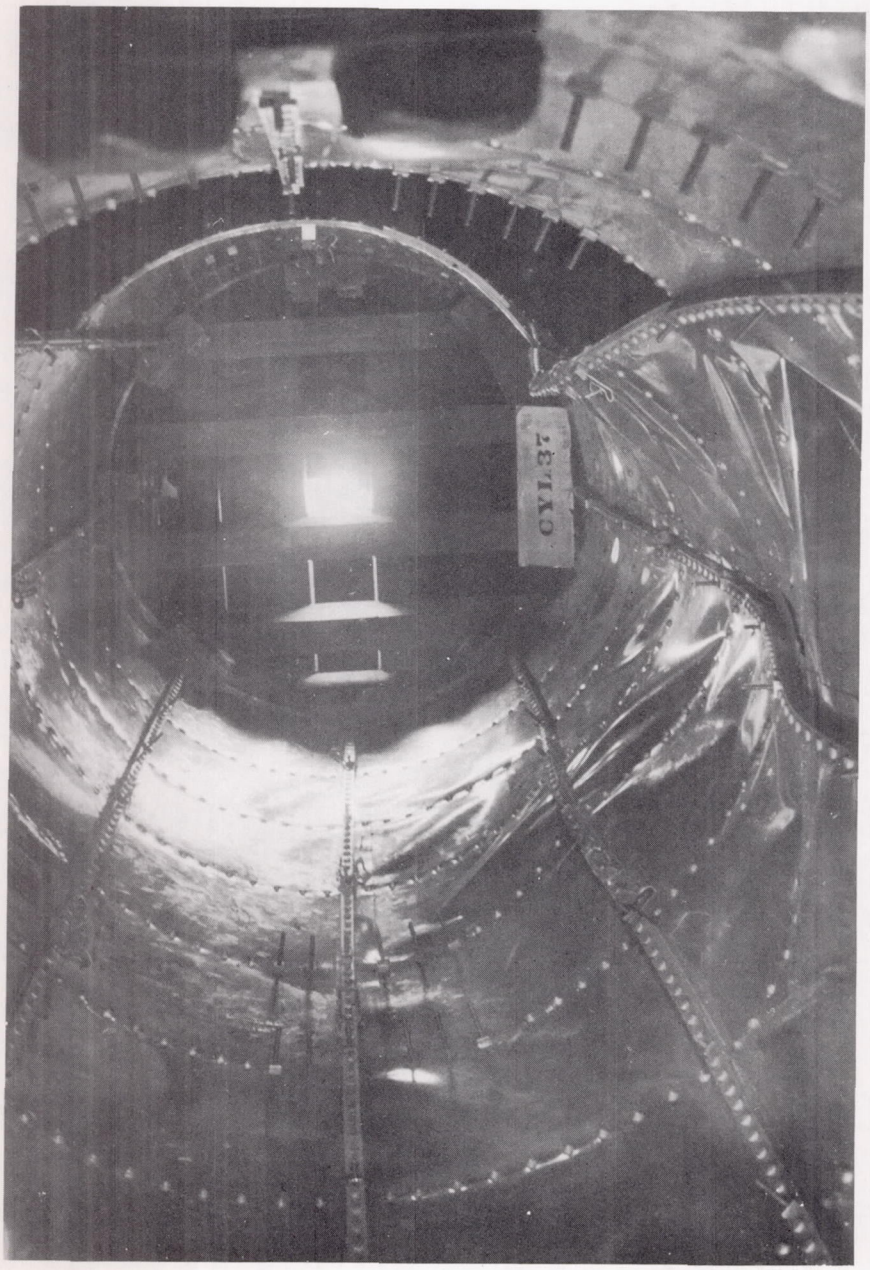

(e) Inside view of cylinder 37.

Figure 50.- Continued.

(f) Inside view of cylinder 38.

Figure 50.- Concluded.

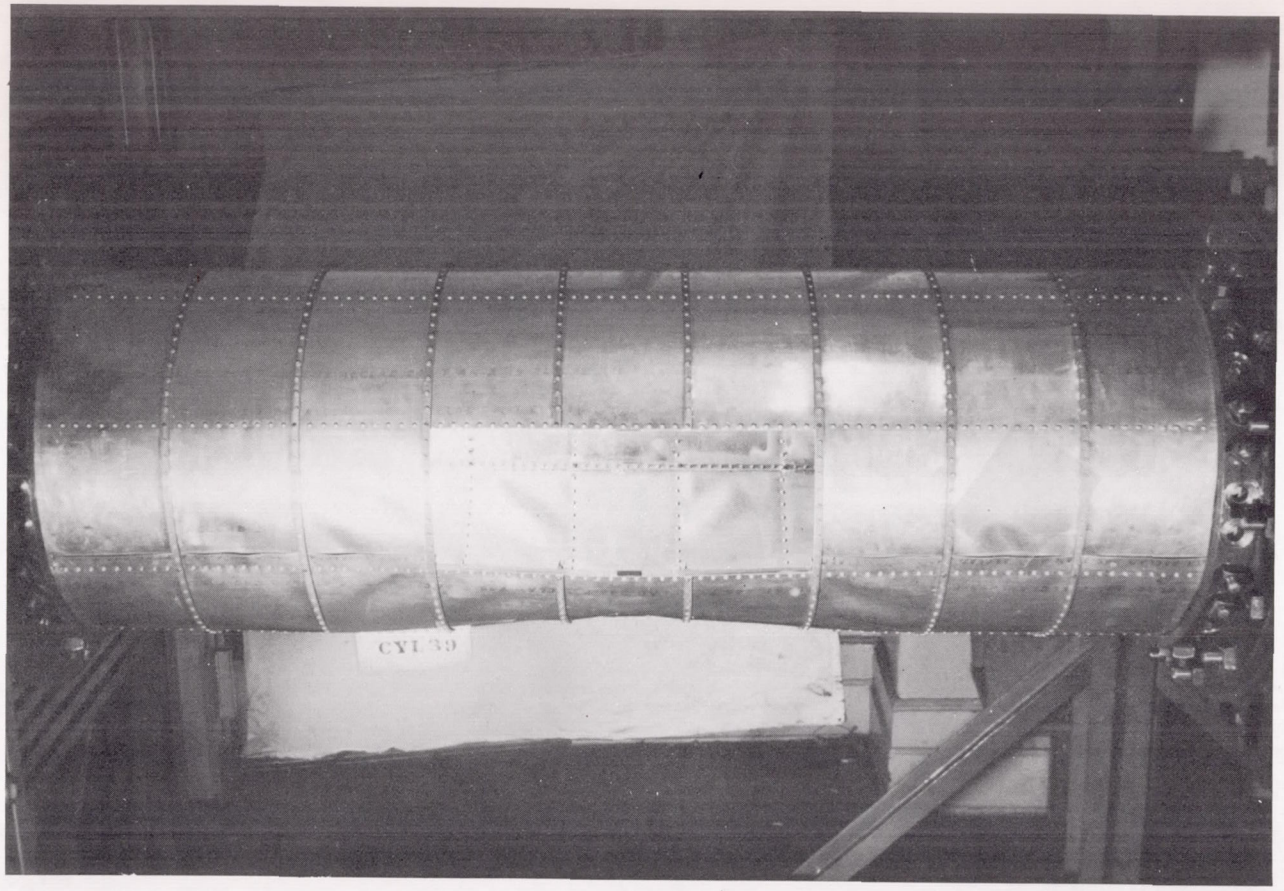

(a) Side view of cylinder 39.

Figure 51.- Photograph taken immediately after buckling.

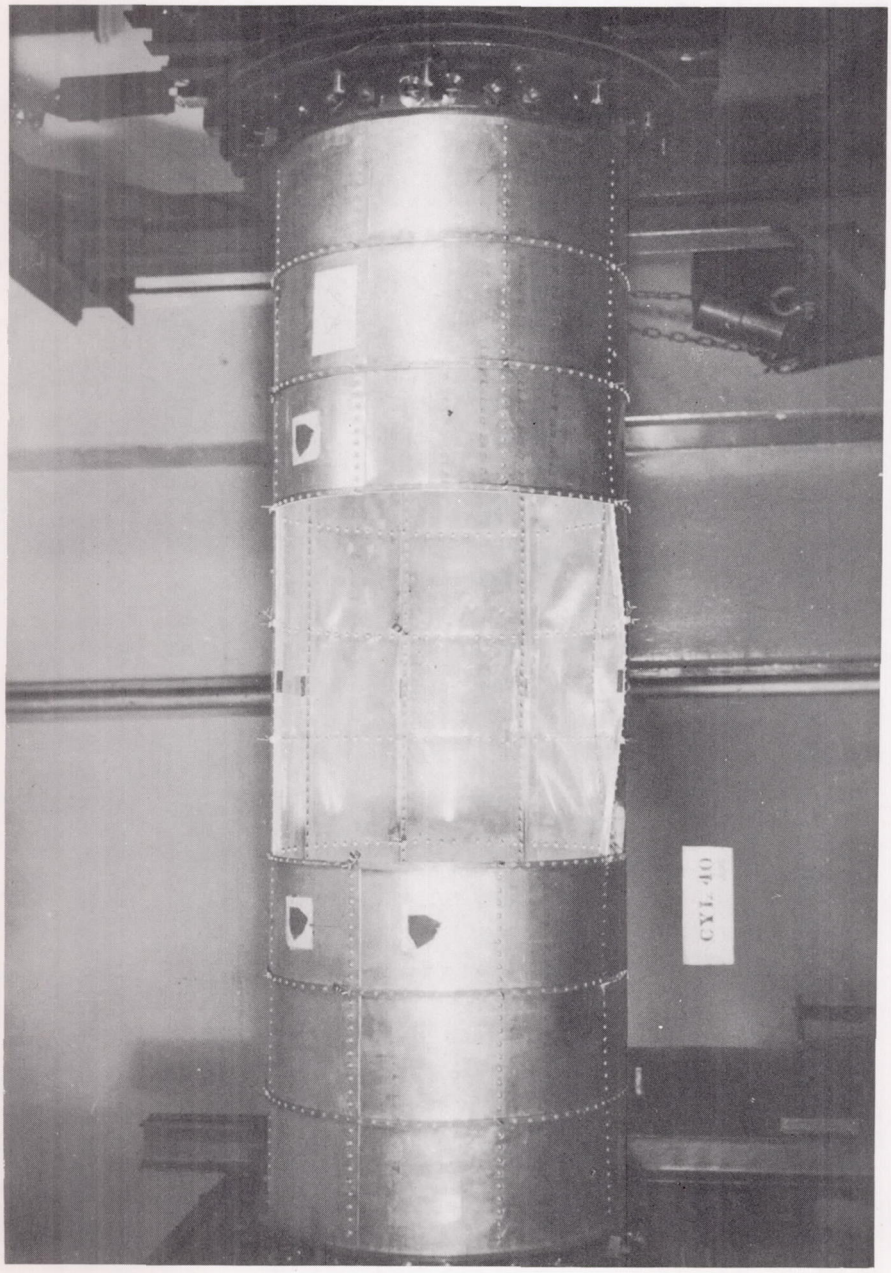

(b) Side view of cylinder 40.

Figure 51.- Continued.

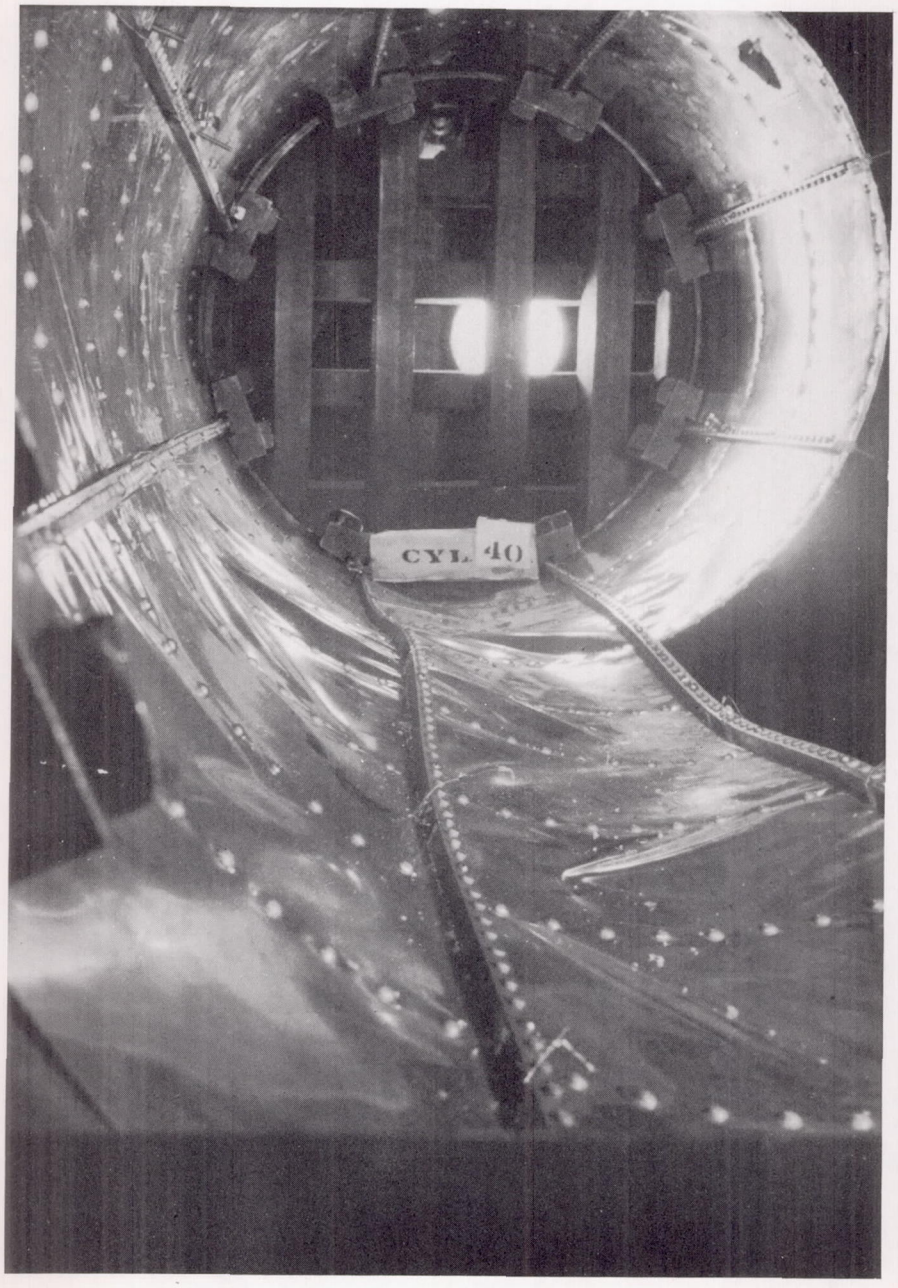

(c) Inside view of cylinder 40.

Figure 51.- Continued.

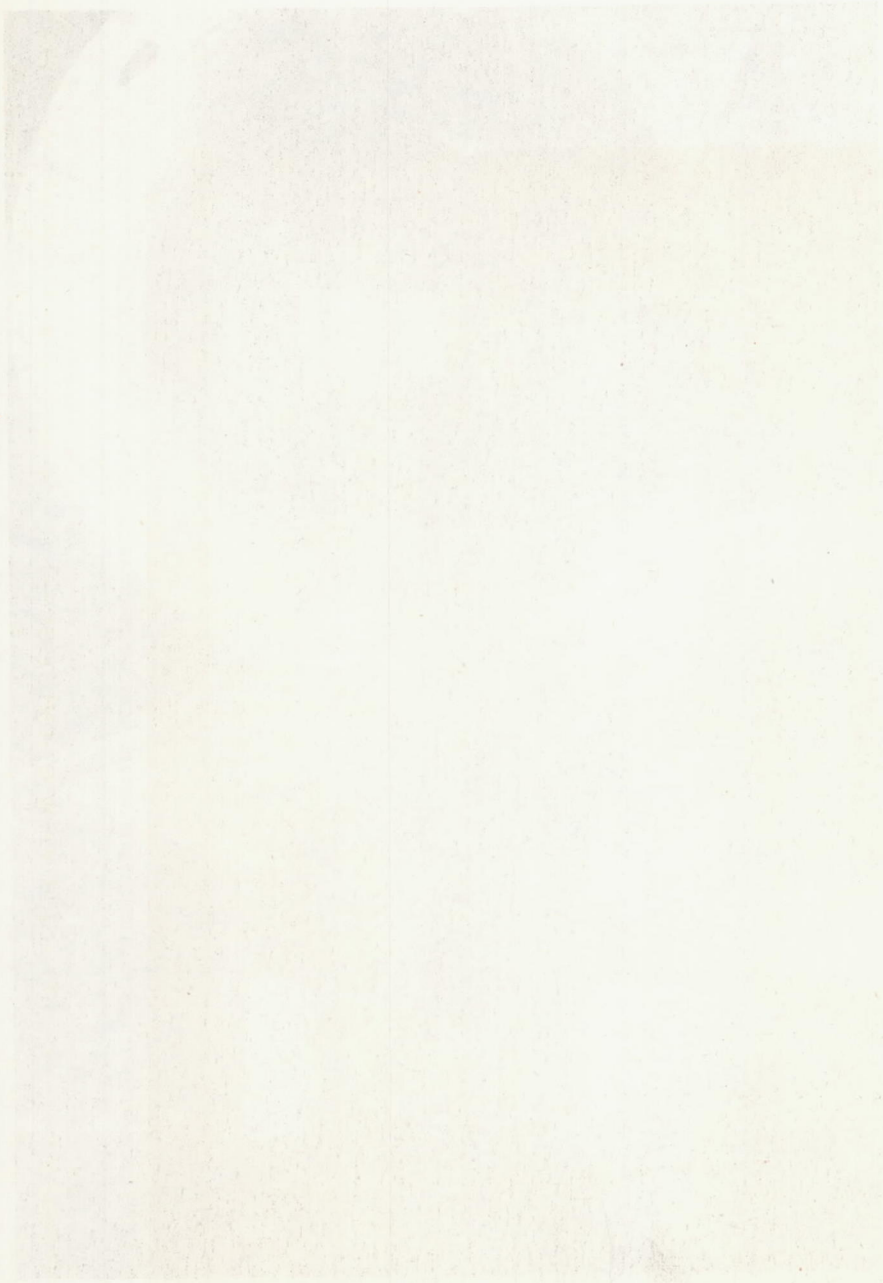

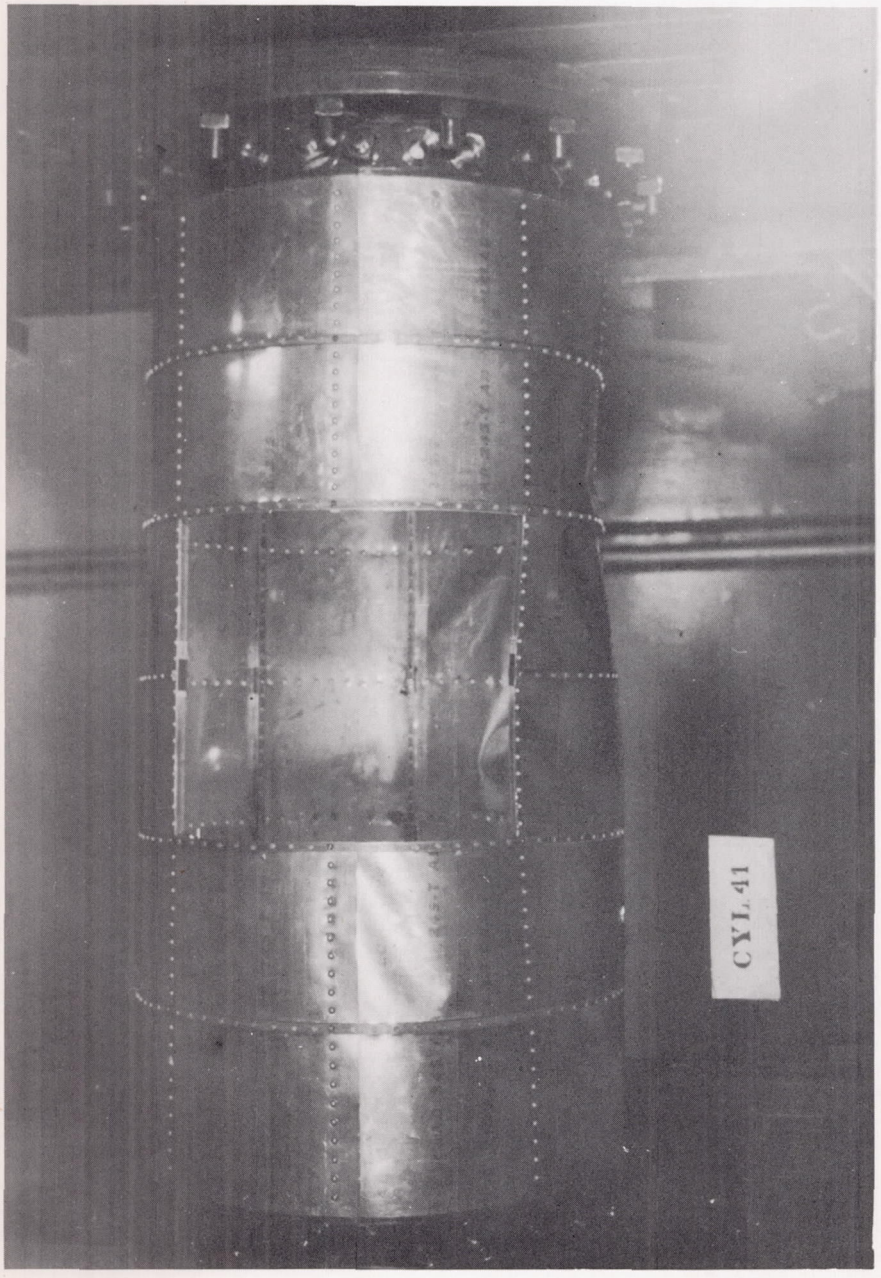

(d) Side view of cylinder 41.

Figure 51.- Continued.

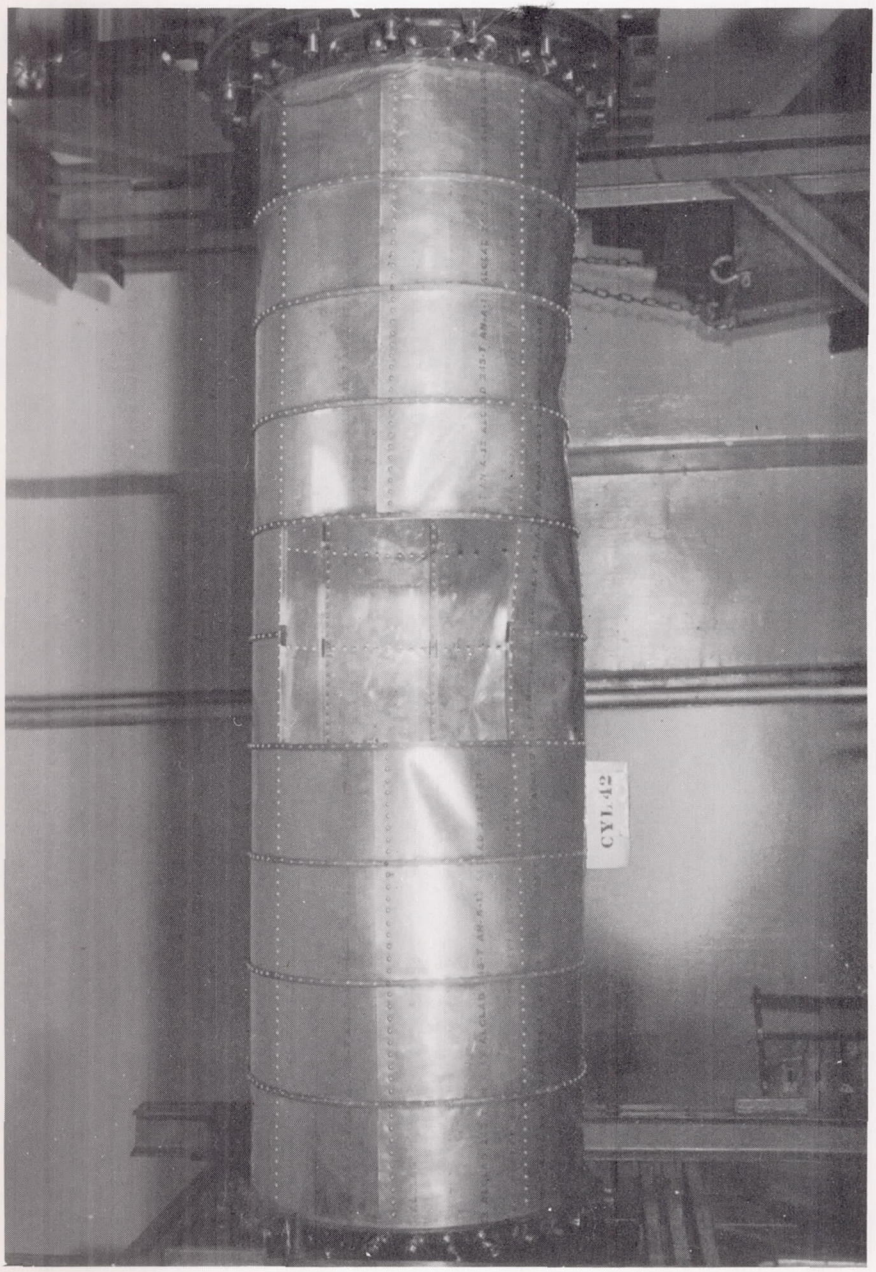

(e) Side view of cylinder 42.

Figure 51.- Continued.

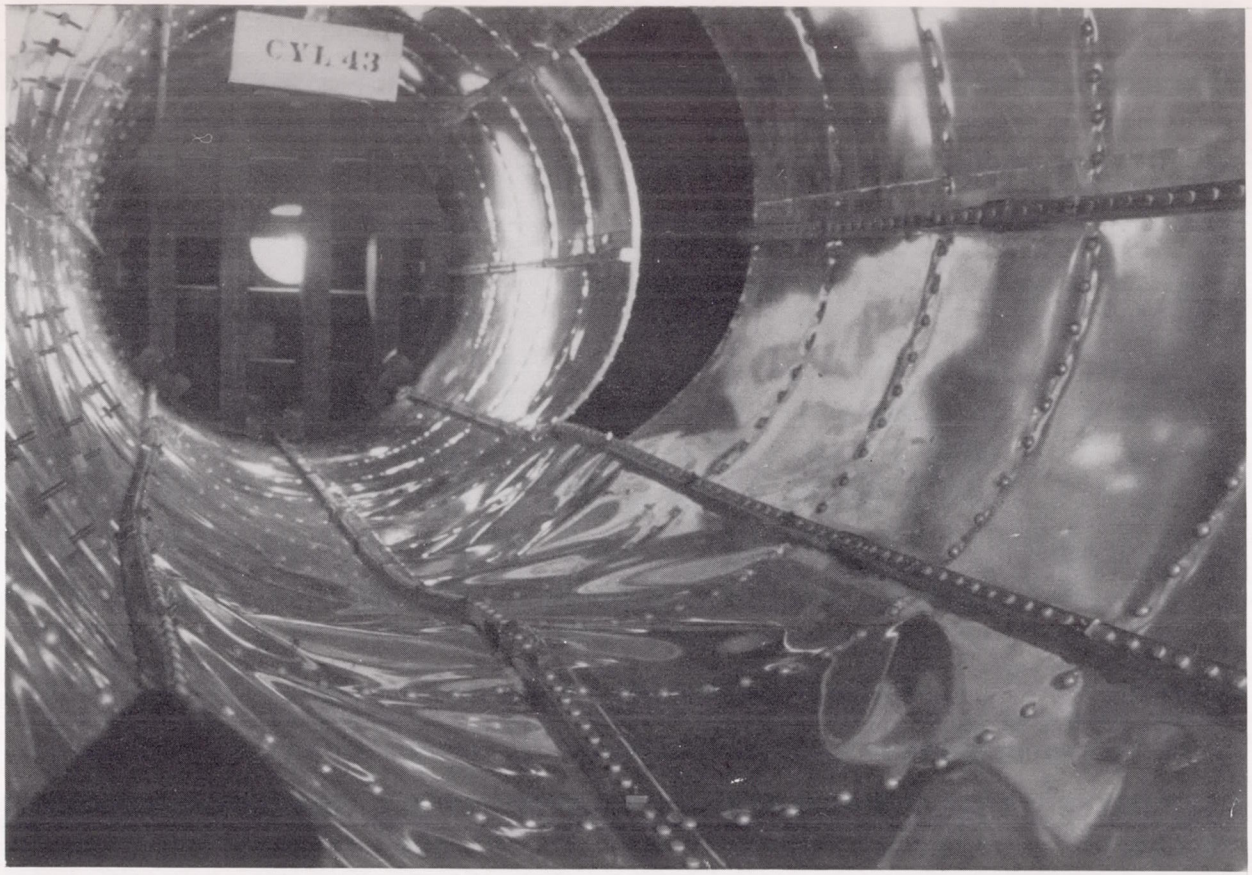

(f) Inside view of cylinder 43.

Figure 51.- Concluded.